

**SEPARATION PROCESSES TO IMPROVE UTILIZATION OF
BIO-OIL FROM SWITCHGRASS PYROLYSIS**

A Dissertation
Presented to
The Academic Faculty

by

Lydia Kyoung-Eun Park

In Partial Fulfillment
of the Requirements for the Degree
Doctor of Philosophy in the
School of Civil and Environmental Engineering

Georgia Institute of Technology
May 2017

COPYRIGHT © 2017 BY LYDIA KYOUNG-EUN PARK

SEPARATION PROCESSES TO IMPROVE UTILIZATION OF BIO-OIL FROM SWITCHGRASS PYROLYSIS

Approved by:

Dr. Sotira Yiacoumi, Advisor
School of Civil and Environmental
Engineering
Georgia Institute of Technology

Dr. Facundo M. Fernández
School of Chemistry and Biochemistry
Georgia Institute of Technology

Dr. Costas Tsouris
School of Civil and Environmental
Engineering
Georgia Institute of Technology
Energy and Transportation Science
Division
Oak Ridge National Laboratory

Dr. Abhijeet P. Borole
Biosciences Division
Oak Ridge National Laboratory
Bredesen Center for Interdisciplinary
Research and Education
The University of Tennessee

Dr. Spyros G. Pavlostathis
School of Civil and Environmental
Engineering
Georgia Institute of Technology

Date Approved: March 27, 2017

*To my dear and loving husband,
my beloved parents, who sacrificed so much,
and my precious children.*

ACKNOWLEDGMENTS

I am deeply thankful to my advisor, Dr. Sotira Yiacoumi, for her guidance, support, advice, understanding, and encouragement, and for giving me the opportunity to continue my PhD studies. I also want to sincerely thank Dr. Costas Tsouris for his knowledge, mentorship, and support in carrying out this research. I truly respect his passion for science and research. Without the mentorship of Dr. Yiacoumi and Dr. Tsouris, I would not be able to complete this study.

I would like to thank my committee members, Dr. Spyros G. Pavlostathis, Dr. Facundo M. Fernández, and Dr. Abhijeet P. Borole for their valuable time, guidance, and support. Their insightful comments and advice allowed me to tackle the challenges of working with bio-oil.

I am very fortunate to work with my lab mates, Dr. Yong-ha Kim, Austin Ladshaw, and Alex Wiechert. Special thanks are also given to Dr. Guangxuan Zhu for making sure our laboratories are functional and safe, Dr. Shoujie Ren for assistance with chemical analysis and providing bio-oil, Dr. Xiaofei (Sophie) Zeng for her assistance with high-performance liquid chromatography analysis, Jiaojun Liu and Stephanie Field for their assistance with the total acid number analysis, and David Bostwick at the Georgia Institute of Technology Bioanalytical Mass Spectrometry Facility for his help with chemical analysis.

I would like to acknowledge the financial support by the U.S. Department of Energy, BioEnergy Technologies Office, under the Carbon, Hydrogen, and Separation Efficiencies (CHASE) program. I thank all the members of the CHASE project from the

Georgia Institute of Technology, University of Tennessee, and Oak Ridge National Laboratory.

I especially thank Samuel Hong, my best friend and loving husband, for his endless support and love. He encouraged me in every way to complete my PhD study.

Last but not least, I deeply thank my parents who sacrificed so much for me. They gave up their life in South Korea to enable me to pursue better education and opportunities in the United States. Without their indubitable sacrifice and hard work, I would not be here. I also want to thank my family in Korea and friends in Atlanta for their prayers and support.

TABLE OF CONTENTS

ACKNOWLEDGMENTS	v
LIST OF TABLES	xi
LIST OF FIGURES	xiii
LIST OF ABBREVIATIONS	xviii
LIST OF SYMBOLS	xxi
SUMMARY	xxii
CHAPTER 1. Introduction	1
1.1 Statement of the Problem	1
1.2 Scope and Objectives	4
1.2.1 Significance of this Research	5
1.3 Organization of Dissertation	6
CHAPTER 2. Background	10
2.1 Upgrading Technologies	10
2.1.1 Physical Upgrading Technologies	10
2.1.2 Chemical Upgrading Technologies	12
2.2 Acidity Measurement–Total Acid Number	14
2.2.1 Standard Method (ASTM D664)	14
2.3 Process Intensification	18
2.3.1 Definitions	18
2.3.2 Examples of Process Intensification – Static Mixer and Centrifugal Contactor	19

2.4	Capacitive Deionization	22
2.4.1	Theory: Electrosorption and Regeneration (Discharging)	22
2.4.2	Factors	25
2.5	Acknowledgments	25
 CHAPTER 3. Separation of Switchgrass Bio-oil by Water/Organic Solvent		
Addition and pH Adjustment		26
3.1	Introduction	27
3.2	Materials and Methods	31
3.2.1	Production of Bio-oil	31
3.2.2	Physical Properties of Bio-oil	31
3.2.3	Liquid-Liquid Extraction	32
3.2.4	pH Adjustment of Bio-oil	33
3.2.5	GC-MS Analysis	34
3.2.6	High-Performance Liquid Chromatography (HPLC) Analysis	34
3.3	Results and Discussion	37
3.3.1	Water Addition	37
3.3.2	Organic Solvent Addition: Hexadecane vs. Octane	42
3.3.3	Combined Extraction vs. Sequential Extraction	43
3.3.4	pH Adjustment of Aqueous Bio-oil	53
3.4	Conclusions	59
3.5	Acknowledgments	59
 CHAPTER 4. Contribution of Acidic Components to the Total Acid Number		
(TAN) of Bio-Oil		60

4.1	Introduction	61
4.2	Materials and Methods	70
4.2.1	Materials	70
4.2.2	Methods	70
4.3	Results and Discussion	74
4.3.1	Chemical Composition and TAN Analysis of Switchgrass Bio-oil	74
4.3.2	Comparison between Measured and Theoretical TAN Values	74
4.3.3	TAN Analysis of Standard Solutions	79
4.3.4	Influence of Titration Solvent on TAN Analysis - MINEQL+ Modeling of Aqueous TAN Analysis	90
4.3.5	Recovery Test on Acetic Acid in Bio-oil Samples	95
4.3.6	Limitations of the Bio-oil TAN Analysis	103
4.4	Conclusions	104
4.5	Acknowledgments	105
 CHAPTER 5. pH Neutralization of Bio-Oil from Switchgrass Intermediate Pyrolysis Using Process Intensification Devices		
		106
5.1	Introduction	107
5.2	Materials and Methods	109
5.2.1	Production of Bio-oil	109
5.2.2	Analysis of Bio-oil Samples	109
5.2.3	pH Neutralization of Bio-oil	111
5.2.4	Bio-oil Heating Experiments	112
5.3	Results and Discussion	114

5.3.1	Batch Systems	114
5.3.2	Continuous-Flow Systems with NaOH Solution	129
5.3.3	Bio-oil Heating Experiments	134
5.3.4	Discussion of increased TAN value of the system after pH neutralization	137
5.4	Conclusions	141
5.5	Acknowledgments	142
CHAPTER 6. Electrosorption of Acids From Bio-Oil for Hydrogen Production via Microbial Electrolysis		143
6.1	Introduction	143
6.2	Materials and Methods	145
6.2.1	Extraction of Acids from Neutralized Bio-oil Organic Phase using Water	145
6.2.2	CDI Experiments	146
6.2.3	Characterization of Carbon Aerogel	147
6.2.4	Physical and Chemical Analyses of Solutions	147
6.3	Results and Discussion	150
6.3.1	Water Extraction	150
6.3.2	Characteristics of Carbon Aerogels	154
6.3.3	CDI Results	156
6.4	Conclusions	163
CHAPTER 7. Conclusions and Recommendations		164
APPENDIX A. Supporting Information		172
REFERENCES		184
VITA		203

LIST OF TABLES

Table 2.1. Recommended size of test portion from ASTM D664 ⁶²	17
Table 3.1. Physical properties of switchgrass crude bio-oil.....	35
Table 3.2. Concentration of acetic acid, relative percentages of types of chemical species present in the samples of each phase, and relative percentages of chemical categories excluding alkanes from solvents	45
Table 3.3. Changes in the amount of each phase after combined and sequential extraction.....	46
Table 4.1. Standard methods of acidity analysis	65
Table 4.2. Modifications of total acid number analysis of biofuels	67
Table 4.3. Modifications of total acid number analysis of biofuels (continued)	68
Table 4.4. The chemical compositions of crude bio-oil, aqueous (centrifuged) bio-oil, and organic bio-oil.	76
Table 4.5. Theoretical and measured TAN values of acetic and propionic acids standard solutions.	77
Table 4.6. Slopes of the linear relationships between TAN value and the molar concentration of various chemicals found in bio-oil with their chemical structure and pK_a values obtained from the literature for HMF ¹²⁰ and online chemical calculations from Chemicalize provided by ChemAxon ¹¹⁹ for other chemicals.	89
Table 4.7. Summary of TAN values from MINEQL+ modeling and experimental TAN analysis in aqueous system and the titration solvent from ATSM D664.....	94
Table 5.1. Mass and TAN balances of pH neutralization of AqBO.....	121

Table 5.2. Total acid numbers, water contents, and chemical composition of bio-oil samples before and after pH neutralization.	122
Table 5.3. Experimental conditions and results of the static mixer and centrifugal contactor experiments.	131
Table 5.4. Changes in amounts of chemicals in bio-oil phases after pH neutralization for the batch NaOH(aq) addition experiment and the mean difference and deviations over all pH neutralization experiments.	140
Table 6.1. TAN values and chemical compositions of initial aqueous and organic bio-oil and neutralized aqueous and organic phases from NaOH(aq) addition to AqBO.	152
Table 6.2. Summary of results from CDI experiments	159

LIST OF FIGURES

Figure 1.1. A flow chart showing production of switchgrass bio-oil, phase separation using the centrifugal contactor, and hydrogen production in a MEC using the acid-rich aqueous phase. (NBOOP: neutralized bio-oil organic phase, NBOAP: neutralized bio-oil aqueous phase). [Switchgrass photo: https://www.gardenia.net/rendition.slider_detail/uploads/plant/1433256670-603d263a69fa7639a/Panicum_virgatum_Cloud_Nine_2009_09.jpg]	9
Figure 2.1. The centrifugal contactor/reactor developed for liquid–liquid systems: (a) A schematic diagram and a photograph of the centrifugal contactor/reactor; ⁸¹ (b) stationary operation, organic and aqueous fluids colored red and blue, respectively, and continuous operation. ⁸³	21
Figure 2.2. (A) Electrosorption and (B) regeneration or discharging of the CDI system.	24
Figure 3.1. Flow charts for sequential and combined extractions.	36
Figure 3.2. Mass-balance diagram for the water addition experiment (1:4 wt. ratio of AqBO to water; the mass of water is shown in parentheses).....	39
Figure 3.3. Chromatograms of (A) octane phase (SolvB-C8), (B) organic bio-oil phase (SBoop), and (C) water phase (SBoap) from combined extraction.	41
Figure 3.4. Mass-balance diagram for combined extraction with octane (the mass of water is shown in parentheses)	47
Figure 3.5. Mass-balance diagram for sequential extraction with octane (the mass of water is shown in parentheses)	48

Figure 3.6. (A) Chromatogram of the hexadecane phase (SolvB-C16) from the sequential extraction of AqBO. (B) Chromatogram of the organic bio-oil phase (SBoop) after contact with hexadecane from sequential extraction. (C) Chromatogram of the octane phase (Solv-C8) from the sequential extraction of aqueous bio-oil. (D) Chromatogram of the organic bio-oil phase (SBoop) from sequential extraction with octane.....	52
Figure 3.7. Mass-balance diagram for pH adjustment (the mass of water is shown in parentheses).....	55
Figure 3.8. An organic phase (NBOOP) precipitated out of aqueous bio-oil as the pH was increased through the addition of NaOH (50%) solution. The conductivity of the aqueous phase (NBOAP) also increased with pH due to the addition of NaOH and precipitation of organic species.	56
Figure 3.9. The amount of total acetate and acetic acid in the aqueous phase (NBOAP) of bio-oil as a function of pH measured by HPLC. The total concentration agrees with the addition of the calculated acetate and acetic acid concentrations. Changes in the pH value of the aqueous phase (NBOAP) as a function of NaOH (50 %) solution added to 10 g of AqBO.	57
Figure 3.10. Representative GC-MS analysis of (A) organic phase (NBOOP) precipitated and (B) aqueous phase (NBOAP) after pH adjustment (pH 5.8).....	58
Figure 4.1. Relationship between measured TAN values of acetic acid and propionic acid solutions (2, 4, 6 wt%) and their theoretical TAN values obtained from Equation (4.1). 78	
Figure 4.2. The same relationship is found when the TAN value is plotted vs. molar concentrations of formic and acetic acid (data obtained from Figure 5 in Oasmaa et al. ⁴⁶).	80

Figure 4.3. Different linear relationships between TAN values and weight percent concentrations of standard solutions of acetic acid, propionic acid, vanillic acid, and phenol.....	82
Figure 4.4. Relationship between TAN and molar concentrations of various bio-oil components. The TAN value of acetic, propionic, and hydroxybenzoic acids shows the same linear relationship vs. molar concentrations, represented by a solid trendline. The TAN vs. molar concentration line for vanillic acid shows a higher slope because of the release of 2 protons during titration to pH 11. Phenol and HMF show zero contribution to the TAN value.....	88
Figure 4.5. Titration curves of acetic acid (2 wt%) solution from MINEQL+ modeling, aqueous titration, and standard titration (ASTM D664).	93
Figure 4.6. Measured TAN values of aqueous bio-oil (90% of the value) and aqueous bio-oil samples with known amounts of acetic acid added, calculated TAN of aqueous bio-oil samples using the measured TAN values of aqueous bio-oil (90%) and acetic acid standard solutions (2, 4, and 6 wt%) through Equation (4.7) (broken line), and measured molar concentrations of acetic acid from HPLC analysis vs. overall concentration of added acetic acid.	97
Figure 4.7. (A) HPLC chromatographs of aqueous bio-oil, (B) aqueous bio-oil with added acetic acid (overall 6 wt% in aqueous bio-oil), and (C) zoomed-in view for acetic acid peaks from aqueous bio-oil (dotted line) and aqueous bio-oil with added acetic acid (solid line).	100
Figure 4.8. Carboxylic acids and other chemical components that contribute to the TAN value of the aqueous bio-oil. The molar concentration equivalent to others (20%) is	

overestimated in the graph because chemical species other than acetic and propionic acids (e.g., vanillic acid) have a stronger effect on the TAN value than monoprotic carboxylic acids.	102
Figure 5.1. Schematics of the pH neutralization experiment using (A) a static mixer, (B) a centrifugal contactor, and (C) both a static mixer and a centrifugal contactor in series.	113
Figure 5.2. Schematic of pH neutralization of AqBO from switchgrass crude bio-oil..	117
Figure 5.3. Chromatograms of (A) AqBO, (B) NBOAP, and (C) NBOOP from the GC-MS analysis.	119
Figure 5.4. Mass and TAN balances over pH neutralization with NaOH(aq) in a batch system.	120
Figure 5.5. Measured pH values of bio-oil after adding Ca(OH) ₂ powder.	125
Figure 5.6. TAN (mgKOH/g) values of AqBO heated at 70 °C for 0, 1, 4, and 8 hours.	136
Figure 6.1. CDI cell with two half cells, each of which contains (1) a Plexiglas cover, (2) a viton gasket, (3) a titanium plate (current collector) with a carbon sheet, (4) a plastic mesh, and (5) a hollow middle viton gasket with syringe needles for input/output. Right: a picture of a carbon sheet taped to a current collector plate made of titanium.	149
Figure 6.2. Flow chart of pH neutralization of AqBO followed by water extraction of NBOOP.	153
Figure 6.3. (A) Nitrogen sorption isotherms of the carbon aerogel material used in this study. (B) The BJH pore size distribution for carbon aerogel used in this study.	155

Figure 6.4. Relative concentrations of acetate ions in the initial phase, CDI-treated phase, and rinsing water phase for the CDI experiments 1, 3, and 8. <i>Note:</i> The experiment numbers correspond to the numbers found in Table 6.2	160
Figure 6.5. Relative concentrations of propionate ions in the initial phase, CDI-treated phase, and rinsing water phase for the CDI experiments 1, 3, and 8. <i>Note:</i> The experiment numbers correspond to the numbers found in Table 6.2	161
Figure 6.6. Relative percent of chemical oxygen demand (COD) levels in the initial phase, CDI-treated phase, and rinsing water phase for Experiments 1, 3, and 8.....	162
Figure 7.1. Overall flow diagram from pyrolysis to hydrogen production with weights and organic contents of phases.	168

LIST OF ABBREVIATIONS

AOCS	American Oil Chemists' Society
AqBO	aqueous bio-oil; water-like, less viscous supernatant liquid obtained from centrifuging crude bio-oil
ASTM	American Society for Testing and Materials
BET	Brunauer-Emmet-Teller
BJH	Barrett-Joyner-Halenda
Boap	water phase; water-like liquid phase formed by adding water to aqueous bio-oil
Boop	organic bio-oil phase; paste-like precipitate formed by adding water to aqueous bio-oil
CDI	capacitive deionization
CE	capillary electrophoresis
CHASE	Carbon, Hydrogen, and Separation Efficiencies
COD	chemical oxygen demand
DC	direct current
EDL	electrical double layer
EIA	Energy Information Agency
GC-FID	gas chromatography–flame ionization detector
GC-MS	gas chromatography–mass spectrometry
GIT	Georgia Institute of Technology

HDO	hydrodeoxygenation
H/N	high number ($\gg 1$)
HPLC	high-performance liquid chromatography
IC	ion chromatography
IEO	International Energy Outlook
MEC	microbial electrolysis cell
MINEQL+	chemical equilibrium modeling system that can be used to perform calculations on low temperature (0-50 °C), low to moderate ionic strength (< 0.5 M) aqueous systems
N/A	not available
N/D	not detected
N/M	not measurable
NBOAP	neutralized bio-oil aqueous phase; aqueous phase separated after adjusting pH of aqueous bio-oil
NBOOP	neutralized bio-oil organic phase; organic phase separated after adjusting pH of aqueous bio-oil
OECD	Organization for Economic Co-operation and Development
OrgBO	organic bio-oil; paste-like, more viscous precipitate or pellet obtained from centrifuging crude bio-oil
ORNL	Oak Ridge National Laboratory
RI	refractive index
SBoap	aqueous bio-oil phase; organic solvent contacted aqueous bio-oil from organic solvent and combined extractions
SBoop	organic bio-oil phase; organic solvent contacted organic bio-oil from organic combined and sequential extractions
SD	standard deviation.

SolvB solvent phase; organic solvent phase after contact with aqueous bio-oil and/or water

TAN total acid number

UT The University of Tennessee

Chemicals

AA acetic acid

C16 Hexadecane

C8 Octane

CH₃COO⁻ Acetate

CH₃COOH acetic acid

CoMo cobalt-molybdenum

H₂SO₄ sulfuric acid

HBA hydroxybenzoic acid

HMF Hydroxymethylfurfural

K⁺ potassium ion

KCl potassium chloride

KOH potassium hydroxide

NaCl sodium chloride

NaOH sodium hydroxide

NiMO nickel-molybdenum

LIST OF SYMBOLS

A	ampere; the unit of electrical current
Å	angstrom; the unit of length ($1 \text{ Å} = 10^{-10} \text{ m} = 0.1 \text{ nm}$)
BTU	the British thermal unit; the amount of heat required to raise the temperature of one pound of water by one degree Fahrenheit
cSt	centistokes, cSt; the unit of kinetic viscosity ($1 \text{ cSt} = 1 \text{ mm}^2 \cdot \text{s}^{-1} = 10^{-6} \text{ m}^2 \cdot \text{s}^{-1}$)
M	molar concentration (mol/L)
mM	milimolar (10^{-3} mol/L)
mS	millisiemens; the unit of electric conductance ($1 \text{ S} = 1 \text{ kg}^{-1} \cdot \text{m}^{-2} \cdot \text{s}^3 \cdot \text{A}^2$)
wt%	weight percent

SUMMARY

The increase in energy demand and limited unsustainable fossil fuel reservoirs lead us to seek an alternative energy source. One potential renewable energy source is bio-oil produced from pyrolysis, a thermal decomposition process of biomass. Bio-oil has benefits and potential as biorenewable energy that may supplement or even replace fossil fuels in the future. The challenging characteristics (e.g., high moisture content, high acidity, and variable chemical compositions) of bio-oil, however, hinder its applications today. To expand the utilization of bio-oil in the real world, the quality of bio-oil needs to be improved through upgrading technologies.

The main objective of the work presented in this dissertation is to separate components of switchgrass pyrolysis bio-oil through various processes to improve its utilization. The research targets the acidity of bio-oil and explores separation processes such as solvent extraction, water addition, pH neutralization, and capacitive deionization (CDI). Moreover, to better understand the change in acidity after treatment of bio-oil, the relationship between the total acid number (TAN) and the amount of acid in the system has been investigated.

The addition of water results in phase separation of bio-oil. The combined extraction (adding water and organic solvents together) of bio-oil could extract effectively more chemical species from bio-oil than sequential extraction (adding water and organic solvents sequentially). The alkali addition of bio-oil resulted in the optimal phase separation at pH 6.0, and the quality of bio-oil improved with approximately 37% less oxygen and 100% increased heating value than the initial aqueous bio-oil (AqBO).

For pH neutralization of bio-oil, sodium hydroxide and potassium hydroxide, instead of calcium hydroxide, were found to be appropriate. The overall TAN values of the system increased after pH neutralization of bio-oil. The TAN analysis of standard solutions demonstrated that acids (e.g., vanillic acid) that act as polyprotic acids have a stronger influence on the TAN values than acids (e.g., acetic acid) that act as monoprotic acids. The TAN values from the aqueous system matched well with those from the MINEQL+ model. These results were significantly different from those obtained from the American Society for Testing and Materials (ASTM) standard method. Different titration solvents (i.e., the mixture of toluene, 2-propanol, and water for the ASTM method and water for the modeling and aqueous system) potentially lead to changes in acid-base reactions of acids during the TAN analysis.

Furthermore, this study expands the fields of process intensification and CDI to biorenewable energy. The results from the continuous-flow systems of pH neutralization using a static mixer and a centrifugal contactor were comparable with those from batch systems. The process intensification experiments using the static mixer and centrifugal contactor demonstrated a potential to scale up pH neutralization of bio-oil. After pH neutralization, acids were present as conjugate ions in the aqueous phases, and some acids were still present in the organic phases. Acids in the organic phase were separated through water addition. Then, through CDI of the resulting water phase, acids were enriched in the rinsing stream. The CDI treatment would allow the microbial electrolysis cell (MEC) application produce hydrogen effectively, which is essential in hydrodeoxygenation of bio-oil and would lead the entire pyrolysis process to become a carbon-neutral process.

Overall, this research on separation of bio-oil components is an intermediate step between biomass pyrolysis for bio-oil production and further processes of bio-oil, including the MEC application that can be used to produce hydrogen. Through this study, the carbon cycle of the overall bio-oil production and upgrading processes can be closed, leading bio-oil to be a carbon-neutral energy source.

CHAPTER 1. INTRODUCTION

1.1 Statement of the Problem

Energy consumption is increasing not only in the United States but also in other Organization for Economic Co-operation and Development (OECD) countries as well as non-OECD countries. According to International Energy Outlook 2016, total global energy consumption is projected to increase 48% from 2012 to 2040.¹ Energy consumption in non-OECD countries will increase by 71% between 2012 and 2040 compared with an increase of 18% in OECD nations.¹

The increase in energy consumption will also increase the dependence on fossil fuels. Higher dependence on fossil fuels not only increases pollution in the environment but also increases threats in social, economic, and international relation aspects. Oil Change International reported that between one-quarter and one-half of all interstate wars since 1973 were estimated to be linked to oil, and that civil wars are 50% more likely to occur in countries with oil.² Professor Colgan from Brown University, the author of “Petro-Aggression: When Oil Causes War,” reported that fossil fuel is a leading cause of war as stated in various reports and peer-reviewed journals.³⁻⁵

Today’s primary energy source is undoubtedly fossil fuel.⁶ However, fossil fuels are considered unsustainable, and the amount of fossil fuels in reservoirs is limited, which is calculated as 1,500 gigatonnes of carbon.⁶ According to the modeling work published by Shafiee and Topal,⁷ depletion times for oil, coal, and gas were approximately 35, 107, and 37 years, respectively. These estimations indicate that coal—the only fossil fuel remaining after 2042—will be available up to 2112.⁷ In addition, the

use of fossil fuels is known to cause various problems. The increase in fossil fuel consumption leads to pollution in the air that results in global warming and other climate changes.⁸ The use of fossil fuel is reported to be responsible for more than two-thirds of the greenhouse gas emissions addressed by the Kyoto Protocol.⁶ The changes in the climate and environment due to the use of fossil fuels even affect the ecosystem. For example, the number of polar bears in the arctic is decreasing due to changes in their habitat because of ice melting.^{9, 10}

The increase in energy consumption, unsustainable and limited fossil fuels, and negative environmental impacts call for alternative energy sources. Renewable energy is a potential solution for environmental problems (e.g., acid rain, ozone depletion, and greenhouse effect), the increase in energy demand, and the depletion of nonrenewable energy sources.¹¹ Unlike nonrenewable energy sources, renewable energy is sustainable and environmentally friendly. Various types of renewable energy include solar, wind, hydropower, geothermal, hydrogen, and biomass.¹ The cost of producing renewable energy has continued to decrease due to technological developments.^{12, 13} For example, the cost of photovoltaics' manufacturing dropped 20 to 25 percent for each doubling of production volume.¹³

Among various renewable energy sources, biomass energy has benefits and potential. The use of biomass energy or biofuels would improve energy security, diminish greenhouse gas and pollutant emissions, enhance vehicle performance, improve rural economic development, and protect ecosystems.¹⁴ Some different types of biofuels include raw biomass (e.g., wood burning for cooking in underdeveloped countries), bioethanol, biodiesel, and bio-oil (pyrolysis oil). The two most common biorenewable

energy sources that are currently applied are (bio)ethanol and biodiesel. These two biomass energy sources have been applied to substitute fossil fuels. Currently, it is easy to find signs in gas stations in the United States indicating that gasoline and diesel may contain up to 10% ethanol and 5% biodiesel, respectively. In some countries, bioethanol has supplemented and replaced some gasoline uses. In Brazil, bioethanol accounted for 30% of automobile fuels in the early 2000s,¹⁴ and 27 billion liters of bioethanol was produced in 2010.¹²

Another promising biorenewable energy is bio-oil, also known as pyrolysis oil. Bio-oil is one of three products from pyrolysis, which is a process that thermally decomposes biomass under oxygen-limited conditions. The other two products of pyrolysis are syngas and biochar. Depending on the residence time of the solid phase within the pyrolysis reactor, pyrolysis systems can be categorized into fast, intermediate, and slow. In general, fast pyrolysis systems produce more bio-oil, and slow pyrolysis systems produce more biochar. The proportions, characteristics, and properties of products from pyrolysis also depend on various factors, including the pyrolysis reactor design, carrier gases, flow rate of the gas, type of biomass, temperature, and rate of heating.¹⁵

One of the major benefits of pyrolysis is that it converts solid biomass energy to liquid bio-oil energy. Liquefaction of biomass energy allows biomass to be applied in various areas, including heating, transportation, biomaterials, and chemicals. Moreover, bio-oil can be considered as carbon-neutral energy with a combination of other technologies, such as a microbial electrolysis cell (MEC).¹⁶ The carbon neutrality of bio-oil will be further discussed in later chapters.

Despite the great potential of bio-oil, it has some application-hindering properties (e.g., 40 wt% of oxygen, pH 2–3, and 15–30 wt% water content¹⁵). Properties of switchgrass intermediate pyrolysis bio-oil used in this study are found in **Table 3.1** in **Chapter 3**. Bio-oil has a high water or oxygen content resulting in combustion inefficiency. High oxygen content causes bio-oil to be reactive and unstable. In addition, the chemical composition of bio-oil varies significantly with feedstocks and pyrolysis procedures, and its diverse composition interferes with typical treatment processes for various applications. One of the problematic chemical groups in bio-oil is acid. The presence of acids in bio-oil not only causes acidity and corrosivity problems during storage and transportation but also leads to instability and chemical aging issues. Furthermore, the high viscosity and heterogeneity of bio-oil cause problems in handling during processing and utilization. Thus, bio-oil must be treated properly to be utilized in further applications. Various research groups have attempted to improve bio-oil through physical and chemical upgrading technologies that are discussed in the next chapter.

1.2 Scope and Objectives

Bio-oil used in this study was produced with a semipilot-scaled auger pyrolysis reactor at the Center for Renewable Carbon of The University of Tennessee (UT). The biomass feedstock was air-dried switchgrass (*Panicum virgatum* L.) from eastern Tennessee.

The main goal of this research is to separate components of switchgrass intermediate pyrolysis bio-oil through various processes to improve its utilization. The research focuses on the acidity of bio-oil and explores separation processes such as

solvent extraction, water addition, pH neutralization, and capacitive deionization (CDI).

To achieve the main goal, the objectives of this research are as follows:

- Extract hydrophilic and hydrophobic chemicals from switchgrass bio-oil using water addition and solvent extraction
- Separate aqueous and organic phases from switchgrass bio-oil
- Reduce the acidity or increase the pH of bio-oil by adding alkali
- Understand the relationship between the total acid numbers (TAN) and the concentrations of chemical components in bio-oil
- Examine, using TAN analysis, the changes in the acidity of bio-oil after pH neutralization or alkali addition
- Collect acidic components from bio-oil to utilize in MEC applications
- Intensify the pH neutralization process of bio-oil using a static mixer and a centrifugal contactor
- Enrich acids in bio-oil via capacitive deionization (CDI)

1.2.1 Significance of this Research

Bio-oil is the result of liquefaction of biomass that allows utilization of biomass in various applications (e.g., transportation fuel) as liquid. Furthermore, bio-oil production and applications are carbon-neutral processes through combining various available technologies (e.g., CDI and MEC). Through this research, improving bio-oil quality and separating valuable chemicals from bio-oil are examined for broad applications. This study incorporates various innovative technologies that have not yet been applied in the field of bio-oil. The use of a centrifugal contactor for intensifying bio-oil treatment

processes promises to explore the potential to scale up the bio-oil pH-neutralization process. The use of a CDI cell, which separates ions in solution with an applied electric field between porous carbon electrodes, enriches ions of acids for further utilization of acidic bio-oil components.

Overall, this study connects several fields of research between bio-oil production and further processes of bio-oil, including microbial electrolysis as shown in **Figure 1.1**. The extracted organic acids can be utilized to produce another valuable energy source, namely hydrogen. Hydrogen is required to upgrade bio-oil via hydrodeoxygenation (HDO). Today, hydrogen in HDO is commonly supplied by natural gas.¹⁷ To find a replacement for natural gas, Lewis et al.¹⁶ has recently demonstrated hydrogen production via MEC using the aqueous phase of bio-oil, which contains organic acids. By separating organic acids, the acidity and corrosivity problem of bio-oil would be resolved.

1.3 Organization of Dissertation

This dissertation has a total of seven chapters. The first two chapters provide the introduction and background of the study. The next four chapters present the accomplishments of the aforementioned research objectives. Finally, the last chapter presents the conclusions and recommendations of the study.

This first chapter provides a statement of the problem as well as the scope and objectives of the study. The following chapter, *Chapter 2*, provides background information needed for this research including discussion on upgrading technologies, acidity measurements, process intensification, and capacitive deionization.

Chapter 3 presents the research on separation of switchgrass bio-oil by water/organic solvent addition and pH adjustment. The combined and sequential extractions of bio-oil components by adding water and organic solvents are investigated. Phase separation after pH neutralization is also examined in this chapter.

In *Chapter 4*, the contribution of acidic components to the TAN of bio-oil is explored. Relationships between TAN values and concentrations of acids are presented. Comparisons among the standard TAN analysis, the experimental aqueous TAN analysis, and the results obtained from the MINEQL+ model are found in this chapter. The recovery test of acetic acid in bio-oil demonstrated that chemicals in aqueous bio-oil do not interfere with the TAN analysis.

Chapter 5 presents the research on pH neutralization of bio-oil from switchgrass intermediate pyrolysis using process intensification devices. pH neutralization of bio-oil in batch systems was performed using various alkali. Continuous-flow experiments were performed using a static mixer and a centrifugal contactor with the intention of process intensification. Furthermore, the change in the overall TAN values of the system after pH neutralization is examined.

In *Chapter 6*, water extraction of acidic components in neutralized bio-oil organic phases and the CDI treatment of aqueous phases are investigated. Acidic components, which are useful in microbial electrolysis to produce hydrogen, were enriched through water extraction and CDI.

This dissertation ends with *Chapter 7* that presents the conclusions and recommendations of the study. Additional figures and tables are found in *Appendix*. The

works cited in this dissertation are organized in *References* provided at the end of the thesis.

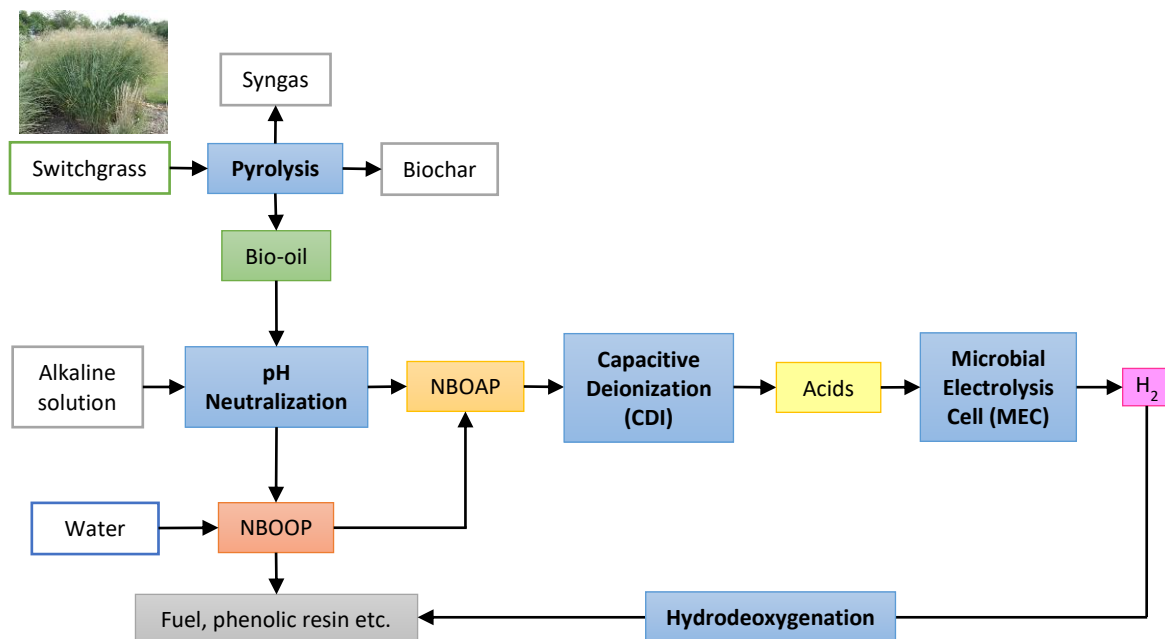


Figure 1.1. A flow chart showing production of switchgrass bio-oil, phase separation using the centrifugal contactor, and hydrogen production in a MEC using the acid-rich aqueous phase. (NBOOP: neutralized bio-oil organic phase, NBOAP: neutralized bio-oil aqueous phase). [Switchgrass photo: https://www.gardenia.net/rendition.slider_detail/uploads/plant/1433256670-603d263a69fa7639a/Panicum_virgatum_Cloud_Nine_2009_09.jpg]

CHAPTER 2. BACKGROUND

2.1 Upgrading Technologies

Various attempts have been made to improve the quality of bio-oil. There are two broad categories of upgrading approaches: physical and chemical upgrading technologies. Physical upgrading technologies discussed in this chapter include water addition, solvent extraction, and filtration. Chemical upgrading technologies described in this chapter include hydrodeoxygenation, catalytic reactive distillation, and esterification.

2.1.1 *Physical Upgrading Technologies*

2.1.1.1 Water Addition – Phase Separation

Among various physical and chemical upgrading treatments of bio-oil, phase separation has been critical for further processing of bio-oil. The addition of water to bio-oil is known to form two phases,¹⁸⁻²⁰ and has been commonly used to separate water-soluble components or the aqueous phase on top.²⁰⁻²⁴

The polarity and solubility of chemicals influence the extraction efficiency of chemicals in bio-oil during water addition. Levoglucosan and organic acids (e.g., acetic and propionic acids) have high distribution coefficients in water due to their high polarity and solubility.²⁵ Furans (e.g., furfural and furanone) have similar distribution coefficients to acetic acid.²⁰ Phenolics (e.g., syringol and guaiacol) have low polarity, however, due to their low initial concentration in crude bio-oil, a considerable amount of phenolics can be extracted by water.²⁵

In addition to water addition, Song et al.²⁶ examined the effect of aqueous salt solutions or solid salts on phase separation of bio-oil.

2.1.1.2 Solvent Extraction

Many research groups have attempted to separate different chemical groups using various organic solvents. Most recently, Ren et al.²⁵ were able to separate different chemicals using water and organic solvents (hexane, petroleum ether, chloroform, and ethyl acetate) sequentially. It was found that chloroform resulted in the highest extraction efficiency for furans, phenolics, and ketones, and ethyl acetate extracted organic acids.²⁵ At the same solvent-to-feed ratio, the number of chemicals extracted was lowest to highest in hexane, petroleum, chloroform, and ethyl acetate.²⁵

Previous research on the solvent extraction of bio-oil using cyclohexane, dichloromethane, ethyl acetate, and butyl acetate demonstrated that dichloromethane was the most effective solvent for extracting chemicals, especially alcohols and acids, from bio-oil.²⁷ Recently, liquid–liquid extraction of bio-oil was investigated using several solvents, namely hexane, petroleum ether, and chloroform.²² Among these three solvents, chloroform was the most effective in extracting phenols and guaiacols.²² With chloroform added to aqueous phase bio-oil (i.e., water phase separated after adding water to bio-oil at 1:1 volume ratio) at a volume ratio of 1:1, chloroform extracted 85.7 wt% of the total phenols and guaiacol in the water phase.^{22, 28} Furthermore, Ma et al. separated fractions of bio-oil by sequentially contacting with hexane, toluene, chloroform, and methanol in the order of increasing polarity.²⁸ It was found that as the polarity of the extraction solvent increased, the viscosity of fractions increased.²⁸ Consequently, liquid extraction has the potential to extract some valuable chemicals and improve the bio-oil quality.

2.1.1.3 Filtration

Hot-vapor filtration in pyrolysis can produce a high-quality product with lower char, ash, and alkali contents.²⁹ The viscosity and average molecular weight of bio-oil are decreased.³⁰ However, the yield of hot-filtered bio-oil is reduced by up to 20%.³⁰ Hot gas filtration substantially increases burning rate and lowers ignition delay of bio-oil during diesel engine test due to the lower average molecular weight.³¹

Removal of organic acids in bio-oil was attempted using nanofiltration and a reverse osmosis membrane.³² Teella et al.³² showed that separation of organic acids from the AqBO phase through nanofiltration and a reverse osmosis membrane is feasible. However, all membranes were irreversibly damaged due to phenolics.³²

2.1.2 *Chemical Upgrading Technologies*

2.1.2.1 Hydrodeoxygenation

Hydrodeoxygenation (HDO) is an oxygen removal process using catalysts. By reducing high oxygen content, the stability of bio-oil can be improved through HDO. The main pathway of HDO is $-(\text{CH}_2\text{O})- + \text{H}_2 \rightarrow -(\text{CH}_2)- + \text{H}_2\text{O}$.³³ Commonly used catalysts for HDO are transition metal sulfides catalysts such as nickel–molybdenum (NiMo) and cobalt–molybdenum (CoMo) supported on Al_2O_3 .³³ However, NiMo and CoMo may cause contamination during HDO by increasing sulfur content in bio-oil; reduced supported transition metal catalysts (e.g., iron, cobalt, nickel, copper) have been explored for HDO.³⁴ Recently, bimetallic catalysts (e.g., Pd–Fe, Ni–Cu/ ZrO_2 , Ni–Cu/ Al_2O_3) have shown great catalytic properties.^{35–39} Leng et al. was able to increase the heating value

and pH value of bio-oil through HDO using Ni–Fe bimetallic catalyst (i.e., Ni–Fe/Al₂O₃).³⁴

2.1.2.2 Catalytic Reactive Distillation

Bio-oil can be upgraded through catalytic reactive distillation by producing ethyl ester and removing water. Junming et al.⁴⁰ improved bio-oil quality using several solid acids (SO₄²⁻/M_xO_y) in reactive rectification. As a result, the upgraded bio-oil had a lower density, higher calorific value, and lower acidity.⁴⁰ Mahfud et al.⁴¹ improved bio-oil in its heating value, acidity, and water content through blending effects and esterification using an improved alcohol treatment method, which consisted of treating with a high-boiling alcohol like *n*-butanol in the presence of a solid acid catalyst at 323–353 K under reduced pressure (<10 kPa). Mahfud et al.⁴¹ found that *n*-butanol and the solid acid Nafion SAC13 have great potential.

2.1.2.3 Esterification

Esterification converts organic acids in bio-oil to esters. Esterification of organic acids in bio-oil has been achieved through catalysts (e.g., acidic ionic liquid catalysts C₆(mim)₂–HSO₄,⁴² and selected catalysts of 732- and NKC-9-type ion-exchange resins⁴³). Through esterification, the acidity and water content of bio-oil have been reduced. The heating values and stability of bio-oil have been increased. Esterification has also been included as an in-line reactive condensation process during pyrolysis.⁴⁴

2.2 Acidity Measurement–Total Acid Number

One of the challenging properties of bio-oil is high acidity (typically pH of 2–3⁴⁵⁻⁴⁷), which is especially problematic for storage and transportation. There have been various attempts to reduce the acidity of bio-oil, such as acetic acid extraction using long-chain tertiary amines.⁴⁸ To compare initial and upgraded bio-oils properly after acidity reduction, however, the acidity of bio-oil must be accurately quantifiable. Currently, various techniques are available for measuring the acidity of bio-oil, such as pH, ion chromatography (IC), high-performance liquid chromatography (HPLC), and gas chromatography–mass spectrometry (GC–MS), though each technique has some limitations.

The TAN analysis, which was originally developed for measuring the acidity of petroleum products, has been applied more recently to measure the acidity of various oil samples, including biodiesel and bio-oil.^{46, 49-61} TAN is the amount of potassium hydroxide (KOH, in milligram) required to titrate one gram of a sample. Compared with other analyses, one benefit of the TAN analysis is that it provides a single parameter that can be used for acidity comparisons regardless of differing characteristics between various bio-oil samples. The typical TAN value of switchgrass intermediate pyrolysis bio-oil is 137.4 ± 3.0 mgKOH/g.

2.2.1 Standard Method (ASTM D664)

Today, various standard methods are available to measure the TAN. Largely, there are potentiometric (ASTM D664⁶²) and colorimetric methods (ASTM D974,⁶³ ASTM D3339,⁶⁴ and American Oil Chemists' Society, AOCS Cd 3d 63⁶⁵). The

colorimetric methods are known to be simple, compatible for a colored sample, and better than potentiometric methods,^{50, 57} in which the dark brown (nearly black) color of bio-oil would most likely interfere with the endpoint determination during the analysis. Thus, for bio-oil analysis, the potentiometric method (ASTM D664⁶²) would be the appropriate option even though this method requires an electrode; the variability of the electrode dehydration may result in mediocre reproducibility and a lack of accuracy in the acidity analysis.^{50, 57}

Briefly, for each TAN analysis, a sample is placed in the titration solvent (125 mL), a mixture of toluene, anhydrous 2-propanol, and deionized water (100:99:1 v/v/v). The amount of the sample added is suggested by the ASTM D664 standard as shown in **Table 2.1**.⁶² The mixture of the sample and titration solvent is titrated to pH 11 using a titrant solution, 0.1 mol/L KOH in 2-propanol.⁴⁷ The modified electrode-cleaning procedure (spraying water for 1 min) was adapted from Baig et al.⁵¹ Samples were titrated to pH 11, and the TAN values were calculated by following ASTM D664 as shown in **Equation 2.1**.

The ASTM D664 method is known to have some challenges such as harmful environmental impacts, labor intensive, high cost, and errors in reproducibility.^{49, 51, 52, 58} To improve the currently available standard methods, many attempts have been made to modify standards. Some modifications are summarized in **Table 4.2** and **Table 4.3** in **Chapter 4** for reference. In this study, one minor modification of the electrode-cleaning procedure was included in the TAN analyses.⁵¹

$$\text{TAN, mgKOH/g} = (A - B) \times M \times 56.106/W \quad (2.1)$$

where:

A = volume of 0.100 M KOH solution used to titrate the sample to pH 11, mL,

B = volume corresponding to A for the blank titration, mL,

M = concentration of titrant solution, 0.100 mol/L,

W = mass of sample, g.

Table 2.1. Recommended size of test portion from ASTM D664.⁶²

Acid Number Range (mgKOH/g)	Mass of a sample (g)	Accuracy of weighing (g)
0.05 – < 1.0	20.0 ± 2.0	0.1
1.0 – < 5.0	5.0 ± 0.5	0.02
5 – < 20	1.0 ± 0.1	0.005
20 – < 100	0.25 ± 0.02	0.001
100 – < 260	0.1 ± 0.01	0.0005

2.3 Process Intensification

Process intensification improves energy and process efficiencies of chemical processes through improvement of mass and heat transfer, application of external force, enhancement of driving forces, and the combination of different unit operations in a single piece of equipment. Consequently, the benefits of process intensification are size reduction, energy saving, cost reduction, safety enhancement, environmental impacts reduction, and product quality improvement.

Process intensification has been applied in various areas, including biofuels, especially in biodiesel production. Process intensification has been applied to overcome challenges: (a) the production rate of biodiesel is often limited by mass transfer,^{66, 67} (b) reaction time is long,^{67, 68} and (c) commercial biodiesel production processes operate in batch reactors.⁶⁷ For example, McFarlane et al.⁶⁶ showed that the centrifugal contactor/reactor could eliminate mass-transfer limitations during transesterification of soybean oil. Although process intensification has not been applied much in pyrolysis and bio-oil applications yet, considering the tremendous benefits of process intensification, process intensification of bio-oil production and upgrading technologies has great potential.

2.3.1 Definitions

Though a universal definition of process intensification may not be obtained as Gerven and Stakiewicz⁶⁹ suggested, process intensification has been evolved and expanded in chemical engineering and various other fields.^{70, 71} Process intensification was first introduced by chemical engineers in the 1970s. Definitions in the early 1980s⁷²,

⁷³ focused primarily on reducing the size of chemical plants (e.g., “devising exceedingly compact plant which reduces both the ‘main plant item’ and the installations costs” by Ramshaw⁷²). Later, the definition was extended to include energy consumption, environmental impacts, and process efficiency: “any chemical engineering development that leads to a substantially smaller, cleaner, and more energy efficient technology.”⁷⁴ In addition to these benefits, Tsouris and Porcelli⁷⁵ and Reay⁷⁶ included multifunctionality and safety as follows: “technologies that replace large, expensive, energy-intensive equipment or process with ones that are smaller, less costly, more efficient or that combine multiple operations into fewer devices (or a single apparatus).”⁷⁵ Because previous definitions focused on unit operations, single devices, and individual methods, recent attempts were made to define process intensification at the macroscopic scale, where intensified modular processes can interact with one another.^{77, 78}

2.3.2 *Examples of Process Intensification – Static Mixer and Centrifugal Contactor*

A static mixer is an intensified equipment for process intensification. The static mixer was considered as core equipment in approximately 2,000 US patents in 2003.⁷⁹ Static mixers normally refer to tubes, columns, or pipelines equipped with stationary barriers that can split, stretch, reorder, and recombine fluids without additional energy sources.⁸⁰ Such stationary barriers are often called motionless inserts, elements, blades, or baffles. Because of these stationary inserts, miscible fluids are effectively mixed, and small bubbles and droplets can be formed when immiscible phases of fluids come into contact in a static mixer. Compared with typical mixing devices, such as mechanically agitated vessels, static mixers are of lower equipment cost, due to compactness, and

because additional energy sources for mixing are unnecessary, they can operate with less energy, in a smaller space, and with a shorter residence time.⁷⁹

A centrifugal contactor is another system that allows process intensification. The centrifugal contactor is a high-gravity field system that integrates liquid–liquid mixing, reaction, and phase separation within the same unit.^{66, 81-83} The centrifugal contactor/reactor developed at national laboratories under the United States Department of Energy consists mainly of two zones: a mixing zone and a separation zone (**Figure 2.1**). Reactions occur primarily in the mixing zone, where intensive shear mixing takes place. A high-gravity field in the separation zone subsequently forces the separation of the two phases. Thus, the centrifugal contactor/reactor is effective for mass transfer, chemical reaction, and phase separation. Biodiesel production has taken advantage of these features.⁶⁶ Owing to the high shear force and turbulent flow created in the mixing zone, mass-transfer effects were minimized, and thus the biodiesel production rate was assumed to be limited only by the reaction kinetics. The residence time of fluids in a conventional centrifugal contactor/reactor is relatively short. For a slow reactive system, such as biodiesel synthesis using esterification reactions, a modified centrifugal contactor was introduced to control the residence time in the mixing zone. This centrifugal contactor/reactor can be used for liquid–liquid systems at temperatures higher than 100°C and gas–liquid systems.

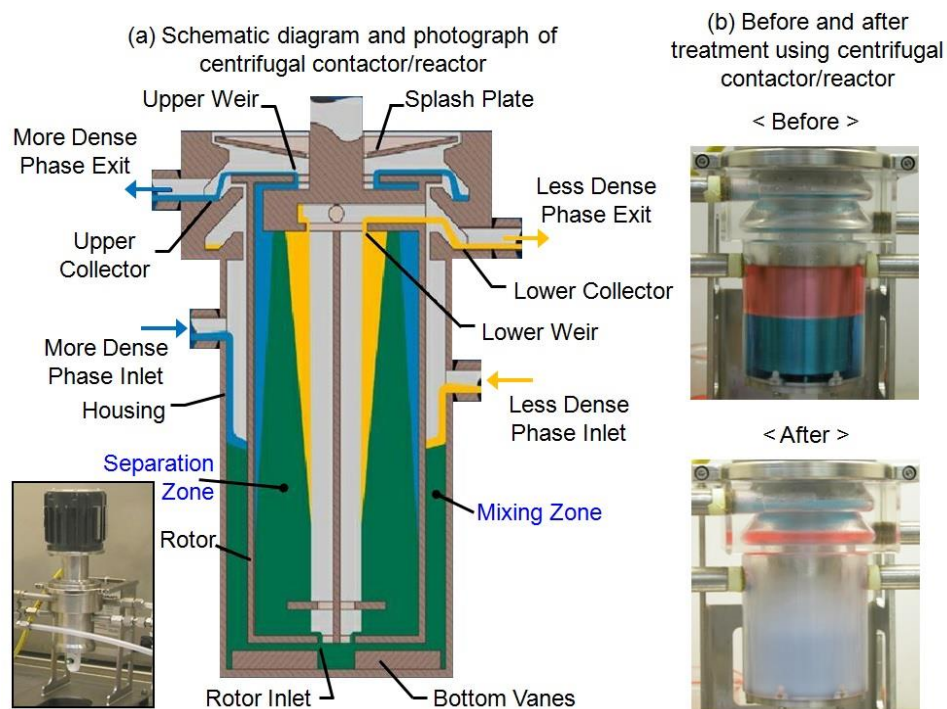


Figure 2.1. The centrifugal contactor/reactor developed for liquid–liquid systems: (a) A schematic diagram and a photograph of the centrifugal contactor/reactor;⁸¹ (b) stationary operation, organic and aqueous fluids colored red and blue, respectively, and continuous operation.⁸³

2.4 Capacitive Deionization

CDI is a technology developed in the mid-1960s and early 1970s that removes ions from solution by applying an electric field. CDI is a low-pressure, nonmembrane electrosorption process. CDI has been mainly applied in seawater desalination and brackish wastewater treatment. In CDI, an electric field is applied to force ions toward oppositely charged electrodes. On the surface of the electrodes, ions are held by forming an electrical double layer (EDL). After the treated water is removed from the CDI system and a rinsing stream is introduced into the CDI cell, ions that were held near the electrodes are released to the rinsing stream by turning off or changing the applied electric field. Therefore, ions can be removed from the initial water and can be collected in the rinsing stream. The ion-removal capacity of CDI depends on various factors, including electrical resistivity and surface area of electrodes. Thus, there have been various studies on the materials of electrodes. Some of the advantages of CDI are reversibility, no chemicals, no high-pressure pumps unlike reverse osmosis, low energy consumption (low voltage), and reduction of secondary wastes.

2.4.1 *Theory: Electrosorption and Regeneration (Discharging)*

In CDI technology, the solution flows between two electrodes (typically made with sponge-like porous carbon materials) connected to a power source. When the electric field is on, the two electrodes become differently charged—positive and negative—resulting in cathode and anode, respectively [**Figure 2.2 (A)**].

When salts are present in the solution, they are separated into the positively charged ions (cations) and the negatively charged ions (anions). Cations are attracted to

the negatively charged electrode, the anode. Likewise, anions are attracted to the positively charged electrode, the cathode. When cations cover the surface of the anode [the top electrode in **Figure 2.2 (A)**] as a first layer, these cations in the first layer attract anions and form a double layer. This double layer of cations and anions is known as the EDL. An EDL also forms near the cathode [the bottom electrode in **Figure 2.2 (A)**]. The process of ions being attached to the electrodes in the CDI technology is called “electrosorption.” Through electrosorption, ions are held near the electrode. Then, the solution, with fewer ions, can exit the CDI system as the treated solution.

After the treated solution exits the CDI system, the electrodes need to be regenerated or prepared for the next solution stream. To collect the ions near the electrodes and regenerate the electrodes in the CDI system, a second water stream or rinsing water enters the CDI system while the electric field is still on. When the electric field is turned off, the electrodes lose their positive or negative charge. Thus, the electrodes cannot hold the ions anymore. Then, the ions are released back into the rinsing water stream and can be collected as ion-enriched water. This process of recollecting ions with rinsing water by stopping the electric field and regenerating the electrodes is known as “discharging” or “regeneration” [**Figure 2.2 (B)**].

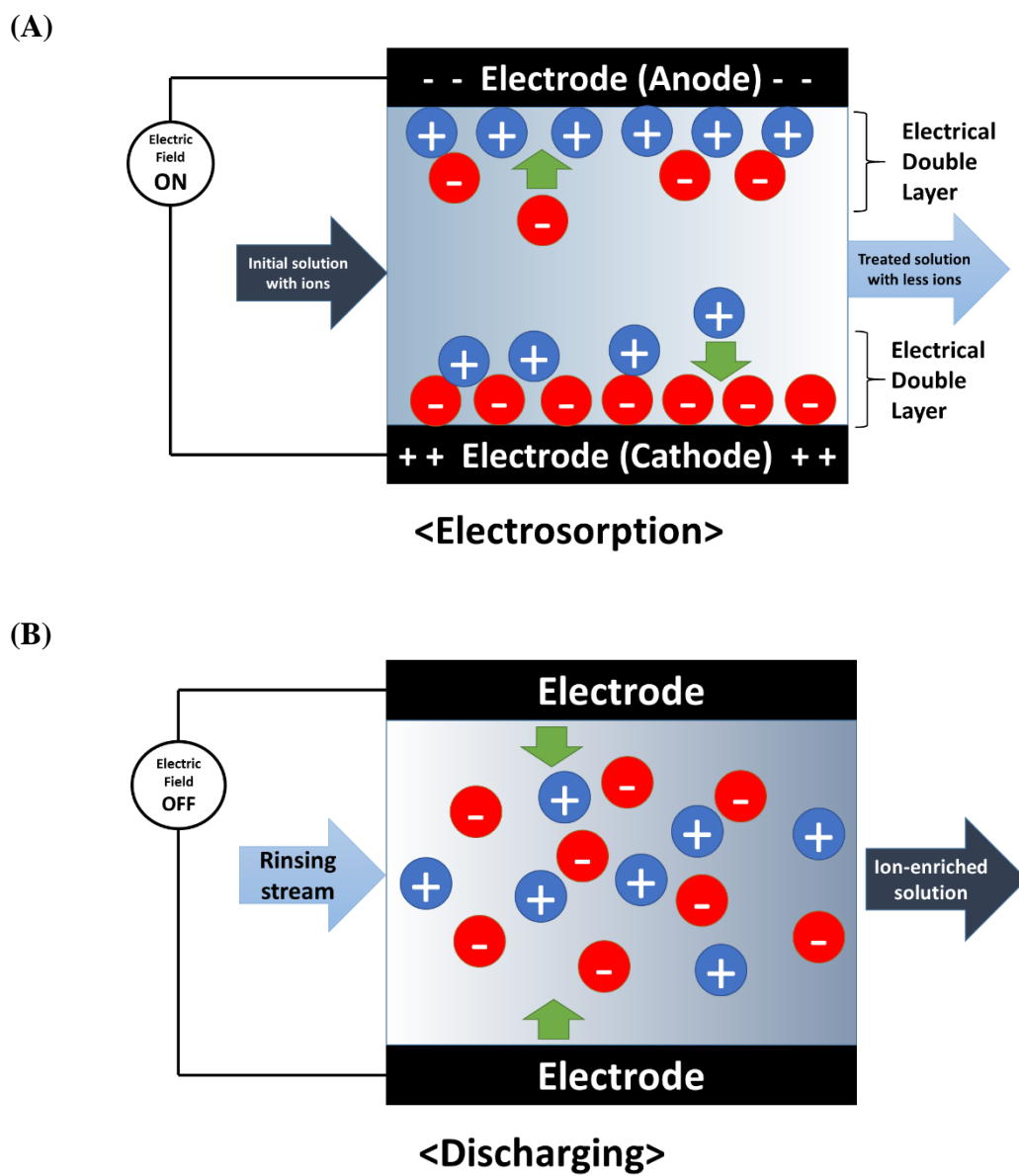


Figure 2.2. (A) Electrosorption and (B) regeneration or discharging of the CDI system.

2.4.2 Factors

The factors that influence electrosorption include types of potential (e.g., DC potential with or without pulsed potential), kinds of electrodes (e.g., porosity, resistivity, and materials), and temperature. The ion-removal efficiency increased at higher temperature. For example, Tsouris et al.⁸⁴ demonstrated that the capacity of electrosorption increased by 10.5% at 40 °C compared with the capacity at room temperature. To achieve a high capacity in CDI, high specific area, electrical conductivity, and stability in materials of electrodes are required.⁸⁴ Mesoporosity of CDI materials results in higher electrosorption capacity than microporosity, which limits mass transport rates.⁸⁴ New types of electrodes, such as flow-electrodes, also proved useful in enhancing the performance of CDI and membrane CDI.⁸⁵

2.5 Acknowledgments

This chapter involved contributions from coauthors: Kim, Y.-H.; Park, L. K.-E.; Yiacoumi, S.; Tsouris, C. 2017. “Modular Chemical Process Intensification: A Review.” In press, *Annual Review of Chemical and Biomolecular Engineering* **8**, DOI: 10.1146/annurev-chembioeng-060816-101354.⁸⁶

CHAPTER 3. SEPARATION OF SWITCHGRASS BIO-OIL BY WATER/ORGANIC SOLVENT ADDITION AND PH ADJUSTMENT

Applications of bio-oil are limited by its challenging properties including high moisture content, low pH, high viscosity, high oxygen content, and low heating value. Separation of switchgrass bio-oil components by adding water, organic solvents (hexadecane and octane), and sodium hydroxide may help to overcome these issues. Acetic acid and phenolic compounds were extracted in aqueous and organic phases, respectively. Polar chemicals, such as acetic acid, did not partition in the organic solvent phase. Acetic acid in the aqueous phase after extraction is beneficial for a microbial-electrolysis-cell application to produce hydrogen as an energy source for further hydrodeoxygenation of bio-oil. Organic solvents extracted more chemicals from bio-oil in combined than in sequential extraction; however, organic solvents partitioned into the aqueous phase in combined extraction. When sodium hydroxide was added to adjust the pH of aqueous bio-oil, organic-phase precipitation occurred. As the pH was increased, a biphasic aqueous/organic dispersion was formed, and phase separation was optimized at approximately pH 6. The neutralized organic bio-oil had approximately 37% less oxygen and 100% increased heating value compared to the initial centrifuged bio-oil or aqueous bio-oil, separated from the crude bio-oil. The less oxygen content and increased heating value indicated a significant improvement in the bio-oil quality through neutralization.

3.1 Introduction

The U.S. Energy Information Administration forecasts that by 2040 the world energy consumption will increase 56%.⁸⁷ While the energy consumption is expected to increase, use of fossil fuels, currently the main energy source, is expected to decrease because of their suspected contribution to global warming. One of the candidates to substitute fossil fuels is biofuels utilizing biomass.⁸⁸ There is enough biomass from available land resources to accomplish the goal of replacing 30% of fossil fuels with biofuels by 2030 according to a joint report by the U.S. Departments of Agriculture and Energy.⁸⁹ Biomass products are currently used as fuel additives such as biodiesel and ethanol.

Another type of biofuel, bio-oil or pyrolysis oil is a liquid condensate of vapors from biomass pyrolysis, a process of heating biomass in oxygen-limited conditions. Some products of pyrolysis include char, syngas, bio-oil, CO₂ and C₁-C₄ hydrocarbons (e.g. CH₄, C₂H₆, C₃H₈, C₄H₁₀). Depending on the biomass materials, reactor designs, and reaction conditions including heating rates and reaction temperature, the chemical and physical properties of bio-oil can vary. Although bio-oil has a significant potential as an energy source, challenging properties of bio-oil such as non-homogeneity, high moisture content, high viscosity, high density, high oxygen content and high acidity can limit its applications. High acidity is especially problematic in transportation and storage of bio-oil. Moreover, due to high moisture content, bio-oil has a low calorific value. Thus, bio-oil needs to be upgraded before it can be efficiently used as an energy source.

Many research groups have previously investigated various approaches to improving bio-oil quality. Some proposed upgrading technologies are

hydrodeoxygenation,³⁴ supercritical fluid extraction,⁹⁰ reactive distillation,^{40, 91} catalysis,⁴ esterification,⁴³ and water addition.¹⁸⁻²⁰ Among various physical and chemical upgrading treatments of bio-oil, phase separation has been critical for further processing of bio-oil. The addition of water to bio-oil is known to form two phases,¹⁸⁻²⁰ and has been commonly used to separate water-soluble components or aqueous phase on top. Song et al.²⁶ examined the effect of aqueous salt solutions or solid salts on phase separation of bio-oil. Previous research on the solvent extraction of bio-oil using cyclohexane, dichloromethane, ethyl acetate, and butyl acetate demonstrated that dichloromethane was the most effective solvent for extracting chemicals, especially alcohols and acids from bio-oil.²⁷ Recently, liquid-liquid extraction of bio-oil was investigated using several solvents including hexane, petroleum ether, and chloroform.²² Among these three solvents, chloroform was the most effective in extracting phenols and guaiacols.²² With chloroform added to aqueous phase bio-oil (i.e., water phase separated after adding water to bio-oil at 1:1 volume ratio) at a volume ratio of 1:1, chloroform extracted 85.7 wt% of the total phenols and guaiacol in the water-phase.^{22, 28} Furthermore, Ma et al. separated fractions of bio-oil by sequentially contacting with hexane, toluene, chloroform, and methanol in the order of increasing polarity.²⁸ It was found that as the polarity of extraction solvent increased, the viscosity of fractions increased.²⁸ Consequently, liquid extraction has the potential to extract some valuable chemicals and improve the bio-oil quality.

In addition to phase separation, separating organic acids (e.g., acetic acid) that cause high acidity and corrosivity of bio-oil is important in upgrading bio-oil. Reactive extraction using long-chain tertiary amines,⁴⁸ nanofiltration, and reverse osmosis

membrane³² recovered acetic acid from bio-oil. The extracted organic acids can be utilized to produce another valuable energy source, hydrogen. Hydrogen is also required to upgrade bio-oil via hydrodeoxygenation. Today, hydrogen in hydrodeoxygenation is commonly supplied by natural gas.¹⁷ To find a replacement for natural gas, Lewis et al.¹⁶ recently demonstrated hydrogen production via microbial electrolysis cell (MEC) using the aqueous phase of bio-oil, which contains organic acids. By separating organic acids, the acidity and corrosivity problem of bio-oil would be resolved.

Here, for separating organic acids, liquid-liquid extraction using water and/or organic solvents is investigated. Different extraction methods, such as combined and sequential aqueous/organic extractions, are compared. For combined extraction, both water and organic solvents are contacted with the aqueous bio-oil (AqBO) – centrifuged bio-oil – at the same time. In sequential extraction, water is added first with the AqBO. Then, the separated organic phase is contacted with organic solvent sequentially. The motivation behind extraction experiments using organic solvents, octane and hexadecane, is to utilize some chemical components in the bio-oil as fuel additives. Octane and hexadecane were used as model molecules representative of gasoline and diesel, respectively. Although liquid extraction may not efficiently separate chemicals from bio-oil, it can selectively separate certain groups of chemicals from bio-oil.

Along with many other organic compounds present in the bio-oil, phenolics contribute to high oxygen content. The oxygen content can be lowered, and the stability of bio-oil can be increased by removing phenolics from bio-oil. Phenolics, usually produced from fossil fuels, are valuable chemicals in producing phenolic resins, fine chemicals, pharmaceuticals, and food processing.⁹² Approaches to producing phenolic

resins from bio-oil are described in a review article.⁹³ Currently, chemical conversion through hydrodeoxygenation and physical removal through extraction are the two main ways to lower the content of phenolics in bio-oil. Hydrodeoxygenation of phenol to cycloalkane using metal catalysts in the presence of acids can overcome the phenolics-associated problems.⁹⁴ Alternatively, Guo et al.⁹⁵ converted phenolic compounds into alcohols using Ru/SBA-15 catalyst. Furthermore, Zilnik and Jazbinšek⁹⁶ extracted phenolics by adding sodium hydroxide (NaOH) solution, followed by butyl acetate. Wang et al.⁹⁷ changed the pH by using NaOH and hydrochloric acid in multiple steps to extract neutral and phenolic fractions from an organic phase. In this study, instead of using the organic phase, we used AqBO to further remove phenolics so the precipitated organic phase (NBOOP: for neutralized bio-oil phase) may be treated further to produce phenolic resins, fuel additives, or replacement of fossil fuels. To find optimal conditions for phenolic separation from the AqBO, the AqBO was adjusted to various pH values using NaOH.

The objectives of this research are to find optimal conditions for phase separation of bio-oil: an aqueous bio-oil phase for producing hydrogen by microbial electrolysis and an organic phase for obtaining valuable chemicals and fuel additives. Phase separation is crucial for separating acids from the bio-oil to lower its acidity, and for removing phenolics from the aqueous phase to lower the oxygen content and produce valuable chemicals. Due to the heterogeneity of bio-oil, all the experiments use the AqBO after centrifuging crude bio-oil produced from intermediate pyrolysis of switchgrass via an auger reactor.

3.2 Materials and Methods

3.2.1 Production of Bio-oil

Switchgrass intermediate pyrolysis for bio-oil production was conducted with a semi pilot-scaled auger pyrolysis system (Proton Power, Inc., Lenoir City, TN, USA) at the Center for Renewable Carbon of The University of Tennessee (UT). The auger pyrolysis system was composed of a feeding system with hopper and single auger, a rectangular auger reactor (10 W×10 H×250 L cm) with dual augers, a pyrolysis vapor condensation section, a particle precipitating chamber, and a biochar collector (**Figure A1 in Appendix**). Air-dried switchgrass (*Panicum virgatum L.*) obtained from a local producer in eastern Tennessee was used as biomass feedstock for bio-oil production. The details of switchgrass compositions were described in a previous report.⁹⁸ Briefly, the contents of cellulose, hemicellulose, and lignin were approximately 34%, 26%, and 19%, respectively, based on dry biomass. Before pyrolysis, switchgrass was ground to less than 2-mm particle size. Switchgrass pyrolysis was conducted at 500 °C with a residence time of 90 s and feeding rate of 10 kg h⁻¹ in the presence of N₂. In this study, a mass of 20 kg switchgrass was pyrolyzed for bio-oil production. The water content of switchgrass was about 7-8 wt%.

3.2.2 Physical Properties of Bio-oil

Physical properties such as density, pH range, viscosity, water content, solid content, ash content, total acid number (TAN), oxygen content, and heating value were first determined for bio-oil (**Table 3.1**). Each measurement was conducted in triplicate. The bio-oil density was measured according to the standard ASTM D1217 method with a

pycnometer.⁹⁹ The pH was measured with an Extech pH meter. The water content was measured with a Schott TitroLine Karl Fischer volumetric titrator according to the ASTM D4377 standard.¹⁰⁰ The viscosity was measured at 40 °C with serialized Schott Ubbelohde capillary viscometers according to the ASTM D445 standard.¹⁰¹ The ash content was measured according to the ASTM D482 standard at 575 °C.¹⁰² The methanol-insoluble materials in bio-oil were measured to determine the solid content according to Boucher et al.¹⁰³ The TAN was measured by titrating bio-oil in the solvent of isopropyl alcohol and toluene with 0.1M KOH isopropyl alcohol solution to an endpoint of pH 11 according to the ASTM D664 standard.⁶² The oxygen content and heating value were analyzed by ALS Environmental (Tucson, Arizona) following the ASTM D5373 M - Pyrolysis / IR detection method and the ASTM D4809 method, respectively.

3.2.3 *Liquid-Liquid Extraction*

Deionized water was used for preparing all aqueous solutions used in the experiments of this study. Hexadecane (C16) and octane (C8) obtained from Sigma-Aldrich were used as representative species for diesel and gasoline, respectively. Crude bio-oil obtained from UT was centrifuged to obtain aqueous bio-oil (AqBO) and organic bio-oil (OrgBO). The nomenclature of bio-oil and phases is summarized in Abbreviation. The AqBO refers to the supernatant after centrifuging crude bio-oil. The OrgBO refers to the precipitate or particles collected at the bottom after centrifugation. After centrifugation of crude bio-oil, the AqBO was 82 wt%, and the OrgBO was 18 wt%. Only the AqBO was used in the experiments described here. In general, the mixture of AqBO and solvents was put in a centrifuge tube and placed in a shaker overnight to reach

equilibrium. After reaching equilibrium, the mixture was centrifuged at 3000 rpm for 30 minutes for phase separation. The different phases were separated to measure the weight using a balance (Ohaus Analytical plus).

3.2.3.1 Combined Extraction

As shown in **Figure 3.1**, the AqBO was mixed with deionized water and C16 or C8 at an arbitrary ratio of 1:2:2 by weight. For phase separation, the mixture was centrifuged after shaking for several hours overnight. The separated phases were analyzed individually using gas chromatography / mass spectrometry (GC-MS). Solvent phases were analyzed without any treatment while the aqueous and bio-oil phases were diluted twenty times with methanol prior to GC-MS analysis.

3.2.3.2 Sequential Extraction

Deionized water was added to the AqBO at 1:2 weight ratio of AqBO to water. The mixture was shaken overnight. On the next day, the phases were separated after centrifugation. Then, C16 or C8, at the same weight as the initial water, was added to the separated Boop (see **Figure 3.1**) for further extraction. After reaching equilibrium overnight, the different phases were separated after centrifugation for further analysis. Sequential extraction is also summarized in **Figure 3.1**.

3.2.4 *pH Adjustment of Bio-oil*

The pH of the AqBO that was obtained from centrifuging crude bio-oil was adjusted by adding NaOH (50%) solution purchased from Sigma-Aldrich. Due to exothermic reactions, when NaOH solution was added to the AqBO (10 g), the temperature of the mixture increased up to 70°C. The mixture was centrifuged after it was

cooled down to make sure it reached equilibrium, and samples were taken for GC-MS analysis. The pH of the Boap was also measured after centrifugation.

3.2.5 GC-MS Analysis

GC-MS was performed at the BioAnalytical Mass Spectrometry Facility at the Georgia Institute of Technology (GIT). The column was an Agilent DB-5, 30 m long by 0.25 mm i.d. with a coating thickness of 0.25 μm . The program started with the oven at 35 $^{\circ}\text{C}$ for 1 minute. The oven temperature was ramped to 300 $^{\circ}\text{C}$ at a heating rate of 15 $^{\circ}\text{C}/\text{min}$. Then, the temperature was held at 300 $^{\circ}\text{C}$ for 6.3 minutes. The carrier gas was helium. A sample volume of 1 μL was injected with 50:1 ratio split mode. The inlet temperature was 280 $^{\circ}\text{C}$. The chemical species were identified from comparing with the mass spectral data library of the National Institute of Standards and Technology. Samples were prepared by diluting twenty times with methanol. The SolvB was analyzed without further treatment.

3.2.6 High-Performance Liquid Chromatography (HPLC) Analysis

The high-performance liquid chromatography (HPLC) system used was Agilent 1100. A BioRad Aminex HPX-87H column and a refractive index (RI) detector were used in HPLC analysis. The mobile phase was 5 mmol/L sulfuric acid (H_2SO_4), and the flow rate of the mobile phase was 0.6 mL/min. The samples were diluted twenty times with the mobile phase (H_2SO_4). A volume of 20 μL sample was injected, and each sample was run for an hour.

Table 3.1. Physical properties of switchgrass crude bio-oil.

Physical properties	Crude bio-oil
Water content (wt%)	42.3±0.66
Total solid (wt%)	1.7±0.25
pH value	2.8±0.07
Density (g/mL)	1.1±0.001
Ash (wt%)	0.3±0.04
Viscosity at 40 °C (centistokes, cSt)	6.5±0.82
TAN, mgKOH/g	137.4±2.96
Oxygen content of two switchgrass bio-oil batches (wt%)	47.11; 47.5
Heating value (BTU/lb) of centrifuged bio-oil	4,944

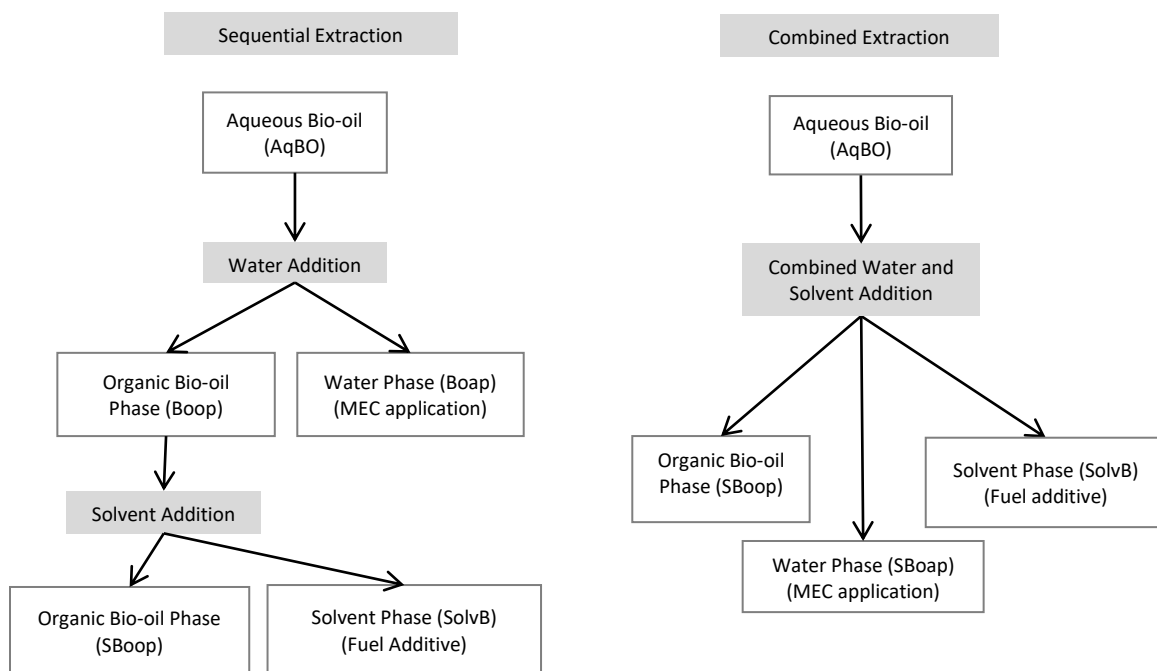


Figure 3.1. Flow charts for sequential and combined extractions.

3.3 Results and Discussion

3.3.1 Water Addition

Through centrifugation, the crude bio-oil was separated into water-like aqueous bio-oil (AqBO) and paste-like organic bio-oil (OrgBO). Previous work by other groups showed that phase separation occurred when water was added to bio-oil.¹⁸⁻²⁰ The centrifuged bio-oil of aqueous bio-oil (AqBO) had the oxygen content of 52.77 wt% and heating value of 4,944 BTU/lb. Deionized water was added to the AqBO at a weight ratio of 1:2 or 1:4 (AqBO to water ratio), as described in **Table A1** in **Appendix**. When water was added to single-phase AqBO, a second paste-like phase, Boop, formed at a relatively small quantity (see **Figure 3.1** and **Table A1**). The mass balance and water-content results before and after water addition (1:4 wt.) are presented in **Figure 3.2**. Boap, the aqueous phase obtained from water addition to AqBO was analyzed by GC-MS as shown in **Figure A2 (A)**. The chemicals corresponding to the peak numbers found in GC-MS figures (**Figures A2 – A4**, **Figure 3.3**, and **Figure 3.6**) are summarized in **Table A2**.

The major peaks found in Boap were hydrophilic chemical species, such as acetic acid (peak #3), 1-hydroxy-2-propanone (#8), and D-allose (#78); while phenolic species with a retention time from 6 to 13 minutes were found as major species in Boop. The acetic acid concentration was calculated from GC-MS spectra using a standard curve. The concentrations of acetic acid in Boap and Boop after water addition to AqBO are presented in **Table 3.2**. The concentration of acetic acid was approximately 28 times higher in Boap than in Boop (see **Figure A2** and **Table 3.2**). Chemical species found in the GC-MS analysis were categorized into groups. The relative percent areas of each

chemical group were calculated as shown in **Table 3.2**. Acid and alcohol groups were found largely in Boap, while phenolics were the major group in the Boop. Boop did not contain 1-hydroxy-2-propanone and D-allose unlike Boap. Most phenolic species were found within a retention time between 7 and 13 minutes. As compared to AqBO, some chemicals [e.g., 2-methyl phenol (#47) and 2,4,-dimethyl phenol (#50)] were not detected in the Boap. These phenolic species were partitioned in the Boop precipitated when water was added. Sugars such as glucopyranose (#53 and 82) and D-allose (#78) were only found in AqBO and Boap. The 1:2 ratio of AqBO to water represents the first step of sequential extraction.

The Boap with organic acids would produce hydrogen via MEC. Lewis et al.¹⁶ produced hydrogen using Boap obtained after adding water to crude bio-oil instead of AqBO. Moreover, it was observed that organic acids, including acetic acid, were transformed under batch and continuous conditions.¹⁶ Although Lewis et al.¹⁶ showed that phenolics were not problematic for MEC, the presence of less phenolic compounds but more organic acids (e.g., acetic acid) in Boap would be preferred for MEC applications. Furthermore, phenolics could be used for the production of higher value chemicals (e.g., phenolic resins).

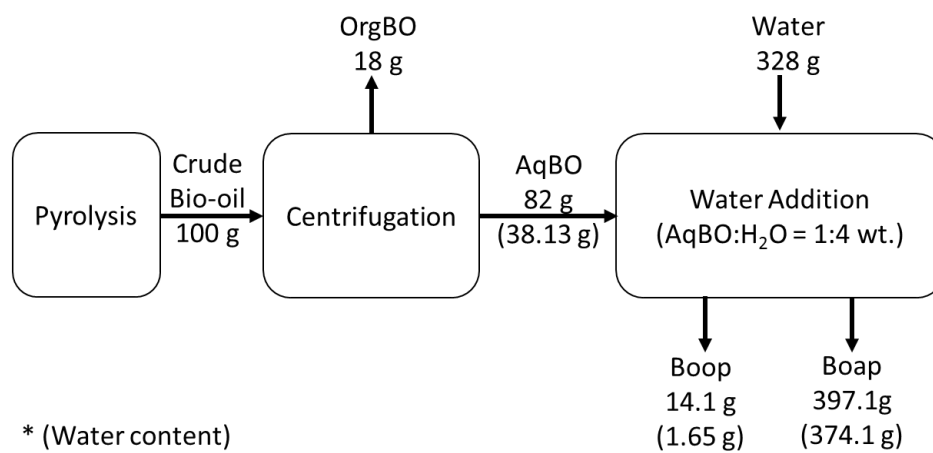
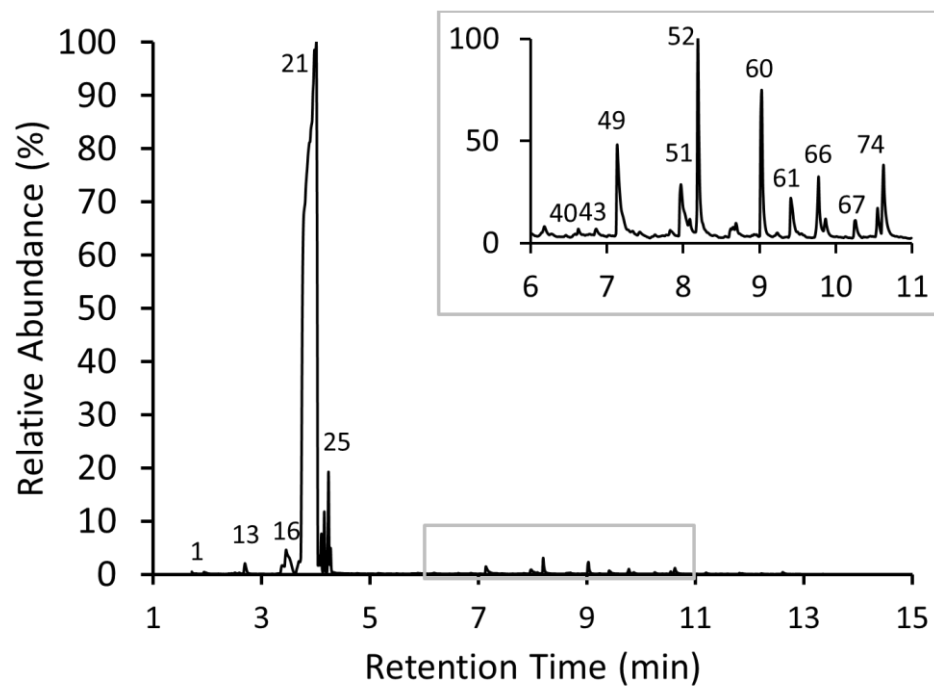
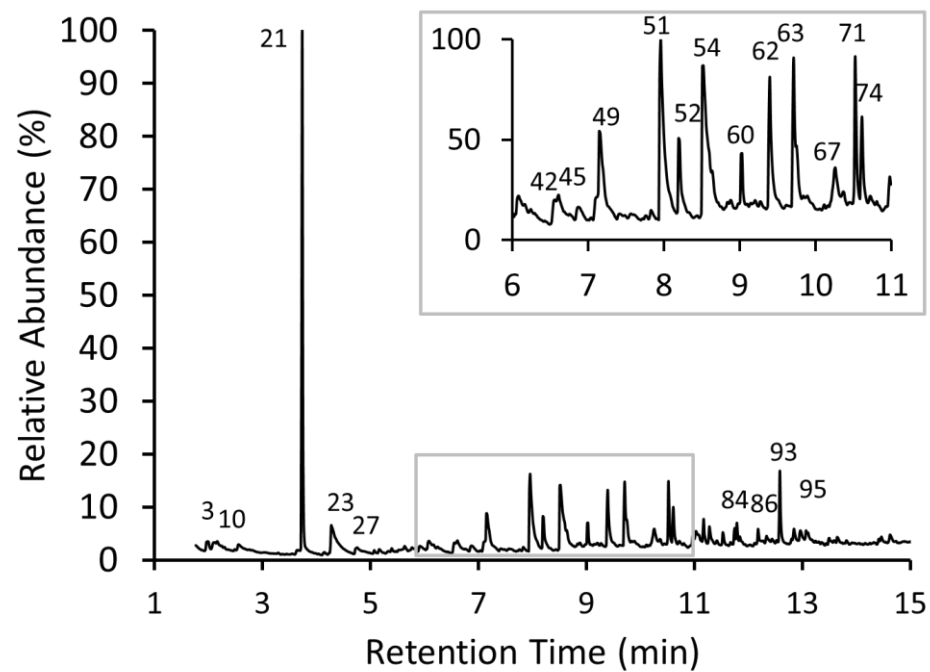


Figure 3.2. Mass-balance diagram for the water addition experiment (1:4 wt. ratio of AqBO to water; the mass of water is shown in parentheses)

(A)



(B)



(C)

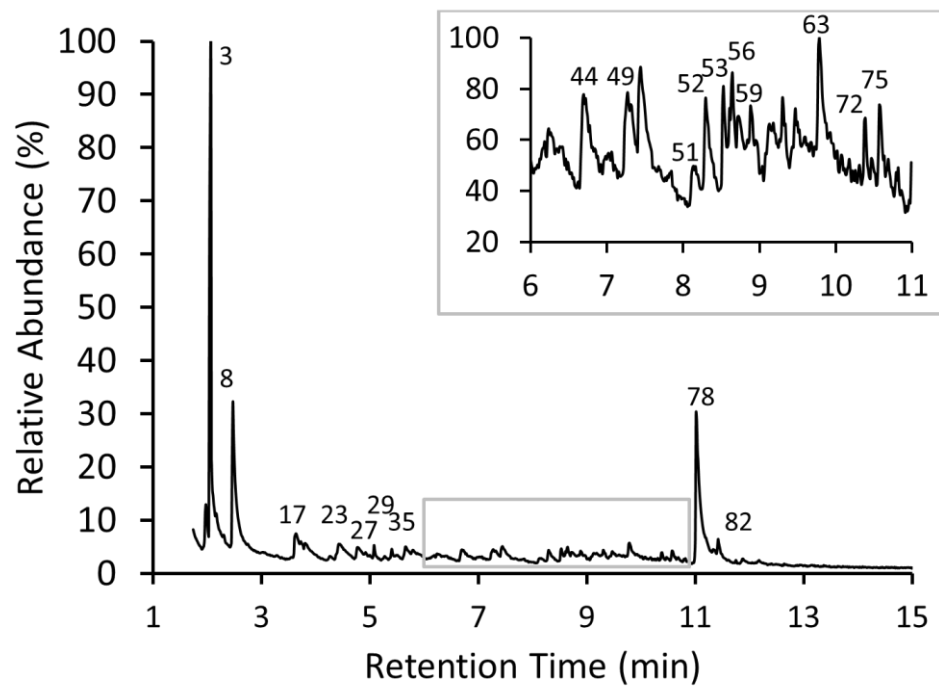


Figure 3.3. Chromatograms of (A) octane phase (SolvB-C8), (B) organic bio-oil phase (SBoop), and (C) water phase (SBoap) from combined extraction.

3.3.2 Organic Solvent Addition: Hexadecane vs. Octane

For organic solvent extraction, hexadecane (C16) and octane (C8) were chosen to represent diesel and gasoline components, respectively. The AqBO was extracted using organic solvents (C16 or C8) with a weight ratio of 1:4 (AqBO to organic solvents) to compare the results of combined and sequential extraction in further analysis.

The AqBO and organic solvents were not miscible; they formed two distinctive phases. The mixtures of AqBO and organic solvents were placed in a shaker overnight to reach equilibrium. The color of both organic solvents changed from colorless to yellow, indicating that some bio-oil components were extracted. The mixtures were separated into different containers after centrifugation by pouring out the solvent phase into a separate container. The changes in the weight of each phase were insignificant. However, the actual amount of AqBO components that partitioned to organic solvent phases (SolvB) might be larger than the overall difference because organic solvents were also partitioned to bio-oil phases (SBoap) as found in **Figures A3 (B) and (D)**.

The SBoap and the SolvB phases after extraction were analyzed by GC-MS as shown in **Figure A3**. For GC-MS analysis, the SBoap was diluted twenty times with methanol, while organic solvents were not further treated. It is noteworthy that C16 is a poor solvent for GC-MS analysis. The gas chromatography peaks from 11 to 13.4 minutes in **Figure A3 (A)** came mostly from C16 and its impurities. It was difficult to distinguish whether some of the chemicals that had similar retention time as C16 were extracted because C16 had a large and wide peak.

The amounts of acetic acid in SolvB and SBoap after organic solvent extraction of AqBO are shown in **Table 3.2**. In C16 and C8 phases, acetic acid was not found or was

under the detection limit (**Table 3.2**). Moreover, the relative percent areas of chemical species groups are shown in **Table 3.2**. More than 97 % of chemical species were alkanes. The alkane group was primarily from organic solvents. About 3 % relative percent area came from extracted chemicals. To compare the chemical species extracted, the relative percent areas were calculated by excluding the alkane group (bottom values in **Table 3.2**). Organic solvents could extract furan, ketone, and phenolics from AqBO. Phenolic compounds were extracted more by octane (70.6 %) as compared to C16 (34.3 %) according to **Table 3.2**. Alcohol was extracted to the hexadecane phase, while aldehyde was extracted to the octane phase. The SBoap was still similar to the initial AqBO. There were no SBoop formed by adding organic solvents, unlike the water addition experiment. The oxygen content and heating value of C8 phase from organic solvent extraction were 1.74 wt% and 20,140 BTU/lb, respectively, and those of C16 were 1.29 wt% and 20,200 BTU/lb, respectively.

3.3.3 *Combined Extraction vs. Sequential Extraction*

To determine whether single- or multi-stage extraction in series would be needed in a solvent extraction application, combined and sequential extractions were compared in a small scale. In combined extraction, water and the organic solvent were simultaneously added to bio-oil. Instead, AqBO was initially contacted with water, and the resulting Boop was subsequently contacted with the organic solvent in sequential extraction (see **Figure 3.1**). The reason that water addition was performed first was to prevent organic solvent partitioning into the water phase.

Combined extraction using AqBO formed three different phases: solvent (SolvB), water (SBoap), and organic bio-oil (SBoop) phases. Formation of three phases indicated

that even if combined extraction was performed, phase separation would be needed twice. Boap that was less viscous than SBoop became a brown-color liquid containing water-soluble chemicals such as acetic acid (#3), 1-hydroxy-2-propanone (#8), and D-allose (#78). The SolvB was organic solvent with extracted chemicals such as phenolics. The SBoop was dark-brown, the paste-like liquid that was similar to the Boop formed after water addition. The amounts of phases from combined and sequential extraction are presented in **Table 3.3**. Moreover, the mass balances with water content results are presented in **Figure 3.4** for combined extraction with C8 and in **Figure 3.5** for sequential extraction with C8. The changes in the weight of SolvB were insignificant indicating that no significant amounts of chemicals were extracted. However, the actual amount of chemicals extracted would be more than the weight changes indicated because organic solvents also partitioned to other phases. As found in **Figure A4**, **Figure 3.3**, and **Table 3.2**, the acetic acid in SolvB was under the detection limit. There was more acetic acid in the SBoap than in SBoop (**Table 3.2**). Phenolics were present the least in the water phases (**Table 3.2**). Methanol, the solvent used for the analysis of water and bio-oil samples, was not included in the relative percent area calculation. The SolvB-C16 from combined extraction included alcohols (20.2%), aldehydes (0.5 %), furans (12.8 %), ketones (7.5 %), and phenolics (59 %) while the SolvB-C8 from combined extraction included ketones (7.4 %) and phenolics (92.6 %) excluding alkanes (**Table 3.2**). As found in zoomed-in graphs in the upper right-hand corner of **Figures A4 (A)** and **Figure 3.3 (A)**, phenolic species extracted by C16 and C8 were similar. C16 extracted a variety of chemicals as compared to C8 (**Table 3.2**).

Table 3.2. Concentration of acetic acid, relative percentages of types of chemical species present in the samples of each phase, and relative percentages of chemical categories excluding alkanes from solvents.

Experimental Method			Conc. of acetic acid (g/L)	Chemical Categories (wt%)												
				Acid	Alcohol	Diol	Aldehyde	Ester	Furan	Ketone	Phenolic	Sugar	Ether	Alkane	Others	
Water Addition		Boap (1:2 wt.)	19.7	42.4	21.4	0	0	0	5.8	4.2	7.1	17.8	0.7	0	0.8	
		Boap (1:4 wt.)	19.6	36	24.5	0	0	0	6.4	7.7	9	14	1.2	0	1.2	
		Boop (1:4 wt.)	0.7	1.9	0.6	0.5	0	0	14.4	5.1	74.5	0	0.1	0	2.9	
Solvent Extraction	C16	SBoap	20.9	37 41	15.1 16.7	0 0	0 0	0 0	8.5 9.5	4 4.4	7.7 8.6	15.3 16.9	1.2 1.3	9.7 *	1.5 1.6	
			SolvB-C16	N/D	0 0	0.6 26.8	0 0	0 0	0 0	0.7 33	0.1 5.9	0.8 34.3	0 0	0 0	97.8 *	0 0
		C8	SBoap	20.8	34.7 37.1	17.3 18.6	0 0	0 0	0 0	4.3 4.6	4.8 5.1	6.4 6.8	23.5 25.2	1.2 1.2	6.7 *	1.2 1.3
	SolvB-C8			N/D	0 0	0 0	0 0	0.1 3.3	0 0	0.1 6.7	0.4 19.4	1.3 70.6	0 0	0 0	98.2 *	0 0
	Combined Extraction		C16	SBoap	6.8	35.4 36.1	20.9 21.3	0 0	0 0	0 0	4.9 5	5.4 5.5	8.6 8.8	20.3 20.7	1.4 1.5	1.9 *
		SBoop			6.2	11.8 28.9	0.9 2.1	0.5 1	0 0	0 0	5.1 12.5	1.6 4	16.9 41.3	3.3 8	0.1 0.3	59.1 *
SolvB-C16		N/D		0 0	0.4 20.2	0 0	0 0.5	0 0	0.2 12.8	0.1 7.5	1.1 59	0 0	0 0	98.1 *	0 0	
C8		SBoap	5.7	34.9 36	16.5 17	0 0	0 0	0 0	5.5 5.7	5.7 5.9	6.7 6.9	26.1 27	1.4 1.4	3.2 *	0 0	
			SBoop	1.3	5.8 7.1	1 1.2	0.6 1	2.9 3.5	0 0	14 17.1	3.1 3.8	51.4 62.7	2.3 2.8	0 0	18 *	0.9 1.1
		SolvB-C8	N/D	0 0	0 0	0 0	0 0	0 0	0 0	0.2 7.4	0.1 92.6	0 0	0 0	97.9 *	0 0	
Sequential Extraction	C16	SBoop	N/D	0.8 3.1	0.2 0.7	0.2 1	0.5 1.8	0 0	3.6 13.6	0.8 3	20.2 75.2	0 0	0 0	73.2 *	0.6 2.2	
			SolvB-C16	N/D	0 0	0.4 47.4	0 0	0 5.1	0 0	0 5.7	0 3.1	0.3 38.8	0 0	0 0	99.2 *	0 0
	C8	SBoop	N/D	0.2 0.2	0.5 0.7	0.4 1	1.6 2.2	0 0	9.8 13.3	2.3 3.1	56.5 76.5	0.9 1.2	0 0	26.2 *	1.7 2.3	
			SolvB-C8	N/D	0 0	0 0	0 0	0 0	0 0	0 2.4	0 3.1	0.6 94.5	0 0	0 0	99.4 *	0 0

* Notes: The top percentage value of chemical category in the solvent extraction experiment includes alkanes whereas the bottom value was calculated excluding alkanes from organic solvents. C16: hexadecane; C8: octane; N/D: not detected.

Table 3.3. Changes in the amount of each phase after combined and sequential extraction.

Combined Extraction	SBoap	SolvB- C16	SBoop	SBoap	SolvB-C8	SBoop
Initial amount (g)	14	14	7	14	14	7
Final amount (g)	20.23	13.92	0.85	20.25	13.89	0.86
Percent change (%)	45	-1	-88	45	-1	-88
Sequential Extraction	Boap	SolvB- C16	SBoop	Boap	SolvB-C8	SBoop
Initial amount (g)	14	14.04	7	14	14	7
Final amount (g)	20.29	14.06	0.79	20.16	14.01	0.84
Percent change (%)	45	0	-89	44	0	-88

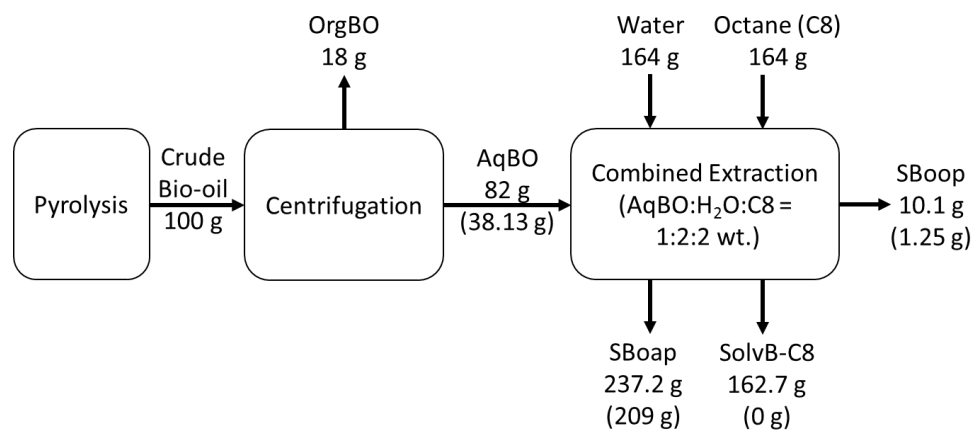


Figure 3.4. Mass-balance diagram for combined extraction with octane (the mass of water is shown in parentheses).

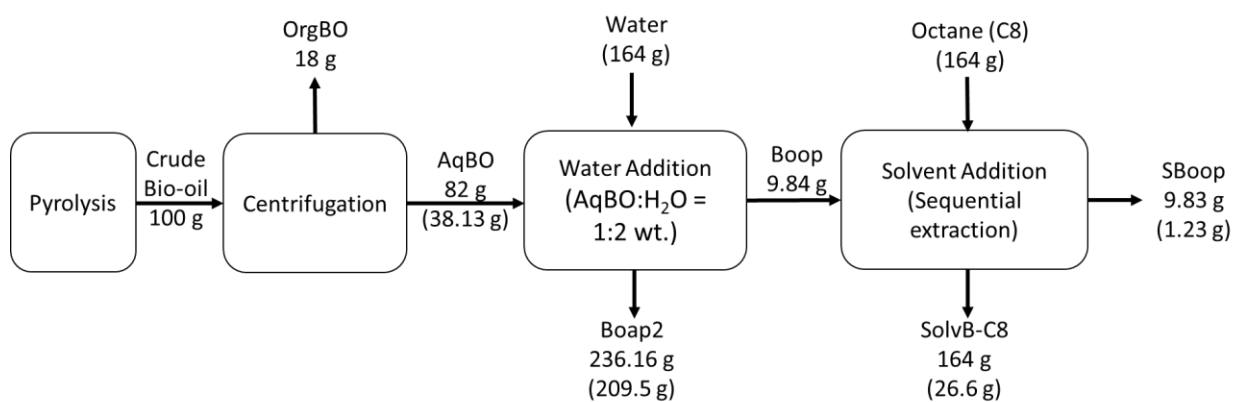


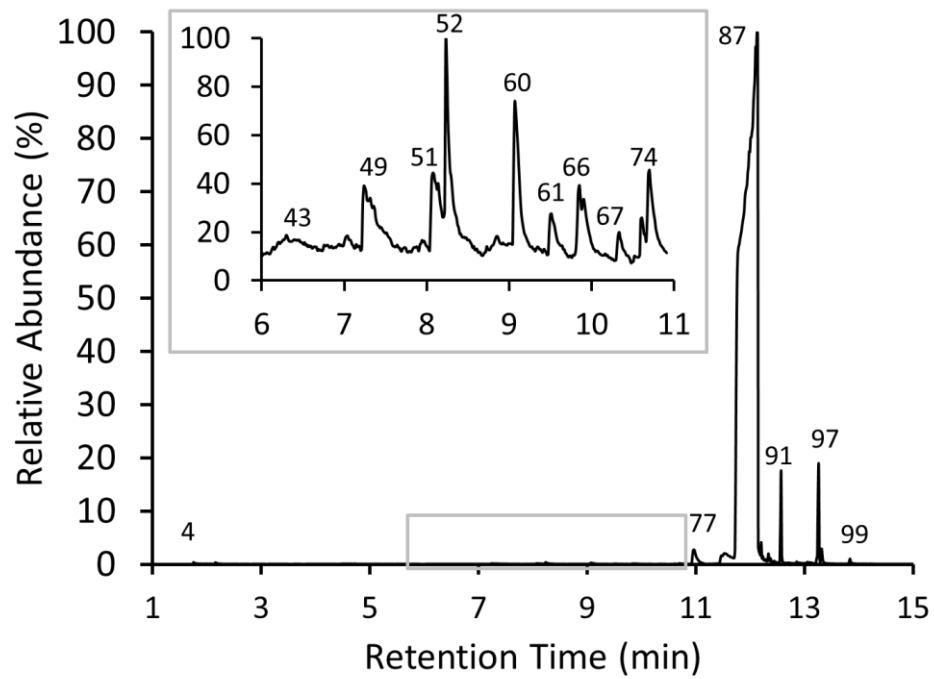
Figure 3.5. Mass-balance diagram for sequential extraction with octane (the mass of water is shown in parentheses).

The first step of sequential extraction was similar to the water addition experiment discussed previously, with a 1:2 AqBO to water ratio. Because the organic solvent was added to the system in the second step, the Boap from sequential extraction did not contain organic solvent unlike the SBoap from combined extraction. The Boop formed after water addition was contacted with organic solvents as the second step. Thus, the amount of chemicals exposed to organic solvents was smaller than those from combined extraction. The SolvB from sequential extraction was analyzed by GC-MS (**Figure 3.6**). Phenolics were found in SolvB at retention times from 6 to 13 minutes (mostly from 7 to 11 minutes). Some phenolic compounds were present in all SolvB including 4-ethyl-phenol (#51), 2-methoxy-4-methyl-phenol (#52), and 4-ethyl-2-methoxy-phenol (#60) (**Figure 3.3**, **Figure 3.6**, and **Figure A4**). From **Table 3.2**, the majority of chemicals in the SolvB detected by GC-MS are alkanes, which originated from organic solvents. This result indicated that about 1 % of relative percent area came from extracted chemicals. According to **Table 3.2** (bottom values), without alkanes, the majority of chemicals extracted by octane were phenolics. More diverse chemical species were found in the SolvB-C16 as compared to the SolvB-C8. As in the combined extraction, the phenolic species found in the SolvB-C16 and SolvB-C8 phases were similar, as shown in the close-up view of **Figure 3.6 (A)** and **(C)**.

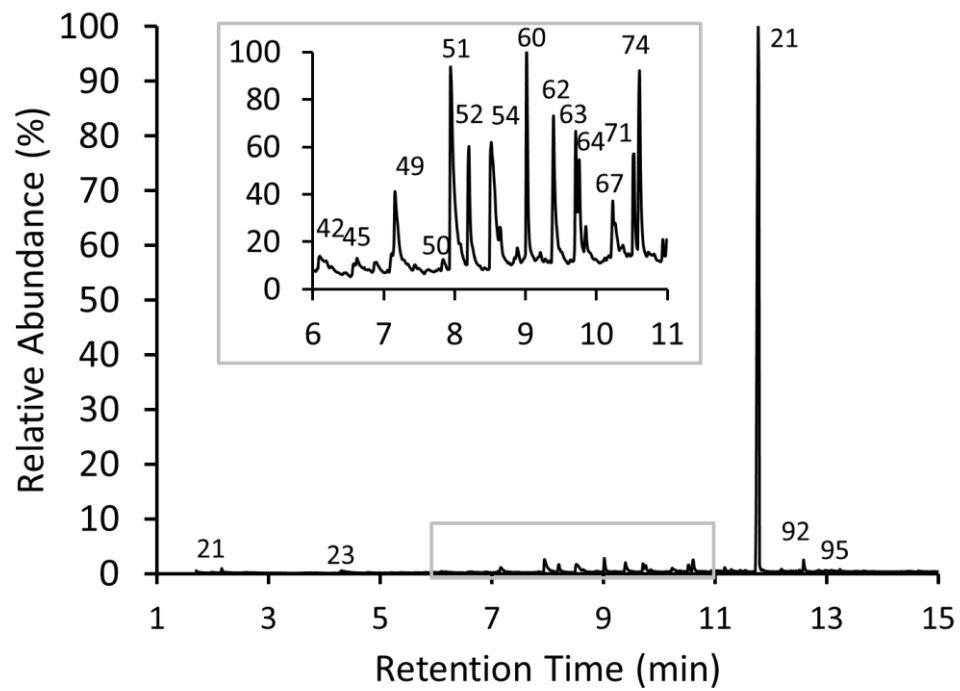
As shown in **Table 3.3**, the changes in the amounts of each phase from combined extraction and sequential extraction were comparable in general. However, according to GC-MS analysis, a larger variety of chemicals were found in SolvB from combined extraction than from sequential extraction (**Table 3.2**). The relative percent areas of phenolic compounds in SolvB from combined extraction were higher than those from

sequential extraction (**Table 3.2**). Therefore, combined extraction was considered better for extracting more phenolics by organic solvents. On the other hand, sequential extraction would be preferred for extracting more acetic acid by water without organic solvent partitioning to the water phase. Initially, combined and sequential extractions were compared to determine the number of extraction stages needed. One extraction stage for combined extraction and two for sequential extraction were assumed. However, even with combined extraction, two separation steps would be needed because three different phases formed. For extracting more chemicals both in quantity and variety, the combined extraction method would be preferred over the sequential extraction method. In contrast, the sequential extraction would be beneficial for further application of Boap in microbial electrolysis cells because having no organic solvents partitioned to the water phase would minimize the loss of the solvent.

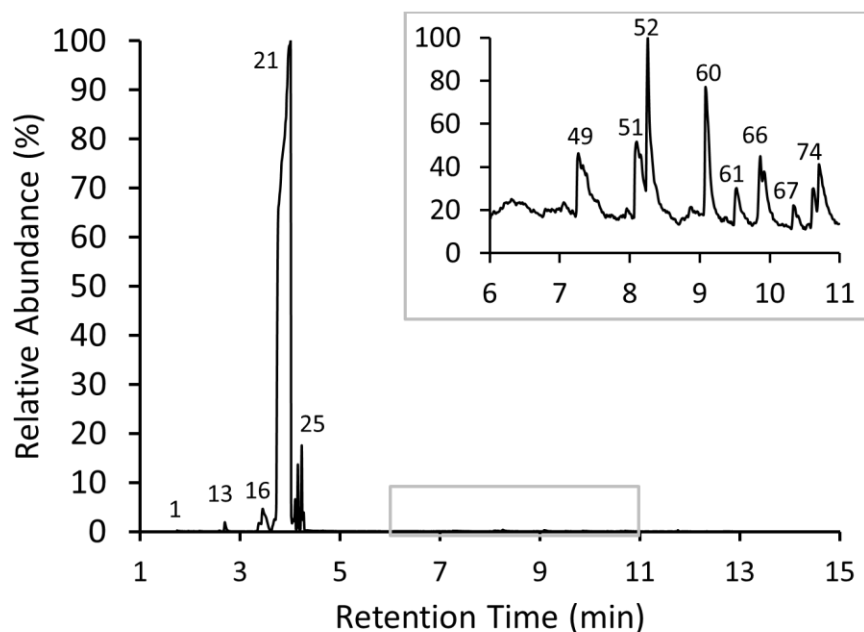
(A)



(B)



(C)



(D)

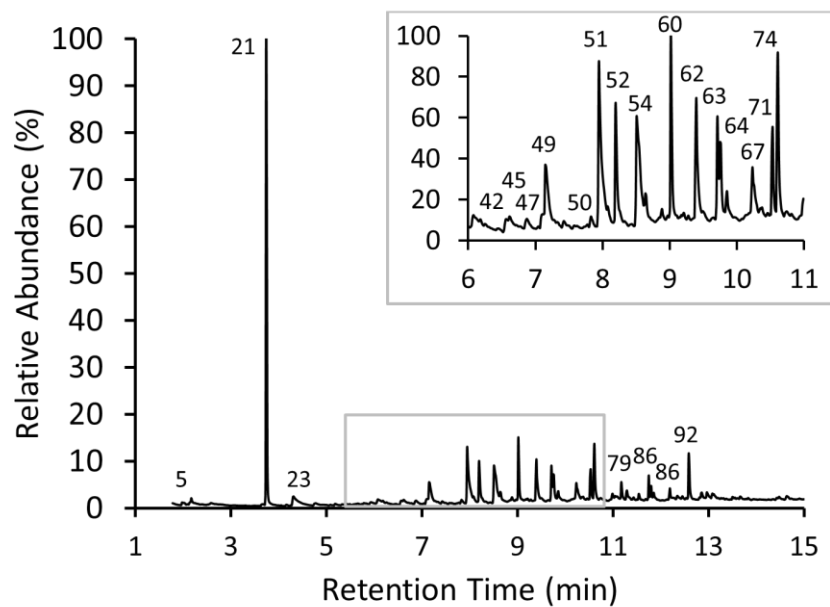


Figure 3.6. (A) Chromatogram of the hexadecane phase (SolvB-C16) from the sequential extraction of AqBO. (B) Chromatogram of the organic bio-oil phase (SBoop) after contact with hexadecane from sequential extraction. (C) Chromatogram of the octane phase (Solv-C8) from the sequential extraction of aqueous bio-oil. (D) Chromatogram of the organic bio-oil phase (SBoop) from sequential extraction with octane.

3.3.4 *pH Adjustment of Aqueous Bio-oil*

The pH of AqBO was adjusted by adding NaOH (50%) solution. The motivation behind these experiments was that pH neutralization generally reduces the solubility of organic species in the AqBO and forms an easily separable insoluble organic phase. This general trend, however, would not apply to some species, such as acetic acid. The pH value of crude bio-oil is between 2 and 3. The pK_a value for acetic acid is 4.76.

Therefore, most acetic acid would be present as the non-ionized form (CH_3COOH) in bio-oil at low pH, and as the ionized or deprotonated form (CH_3COO^-) at high pH. By adding 50% NaOH solution to AqBO, the pH value increased. The Boop, which contained chemicals including phenolics, precipitated as the pH increased. **Figure 3.7** shows the mass balance and water content results before and after pH adjustment (pH 6). **Figure 3.8** presents the conductivity of NBOAP as a function of pH. The conductivity of Boap increased as the pH value increased from 3 to 6.3. This increase in the conductivity indicated that the concentration of charged species, e.g., acetate, increased in the Boap. In basic Boap, the conductivity did not increase much as more NaOH solution was added. This plateau showed that most of deprotonation or speciation changes occur at low pH. Visual inspection revealed that the viscosity of the precipitated Boop also increased as the pH values increased. The optimum pH value with respect to percent weight of precipitated Boop seems to be around 6. The oxygen content and heating value of neutralized organic bio-oil (NBOOP) around pH 6 were 33.10 wt% and 9,878 BTU/lb, respectively. These data reveal that the oxygen content of neutralized bio-oil decreased by 37 % and the heating value increased by 100 % compared to the centrifuged bio-oil that was used for neutralization.

The amount of total acetic acid and acetate present in the Boap of pH-adjusted bio-oil was measured by HPLC analysis as shown in **Figure 3.9**. After dilution with the mobile phase (H_2SO_4), the pH of Boap samples became close to that of sulfuric acid (pH ~2). At around pH 2, acetate would become protonated and exist mostly as acetic acid, which was detected by HPLC. Thus, the measured acetic acid concentration would be roughly the same as the total concentration of acetate and acetic acid. The concentrations of acetate and acetic acid species were calculated using a $\text{p}K_a$ value of 4.76 and the measured acetic acid concentration at around pH 9 as total acetic acid concentration are found in **Figure 3.9**. Changes in the pH value of Boap as a function of 50 % NaOH solution added to 10 g of AqBO are plotted in **Figure 3.9**. The Boop formed by the addition of NaOH contained mostly phenolic compounds as shown in the chromatogram in **Figure 3.10 (A)**. Various phenolic compounds were found in the Boop, according to GC-MS analysis unlike the aqueous phase in **Figure 3.10 (B)** that contained mainly hydrophilic species such as acetic acid, 1-hydroxy-2-propanone, and D-allose. The remaining NBOAP after precipitation of the NBOOP will be investigated in future work for its suitability as feedstock for a microbial electrolysis process to produce hydrogen.

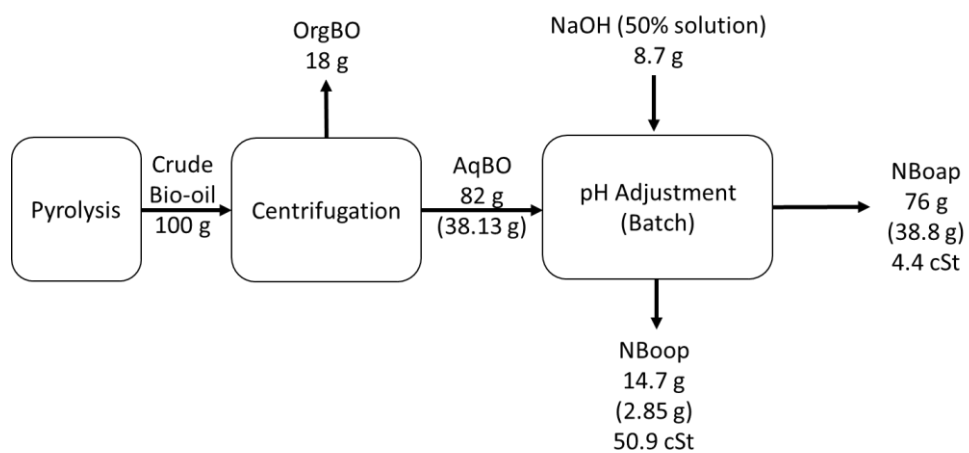


Figure 3.7. Mass-balance diagram for pH adjustment (the mass of water is shown in parentheses).

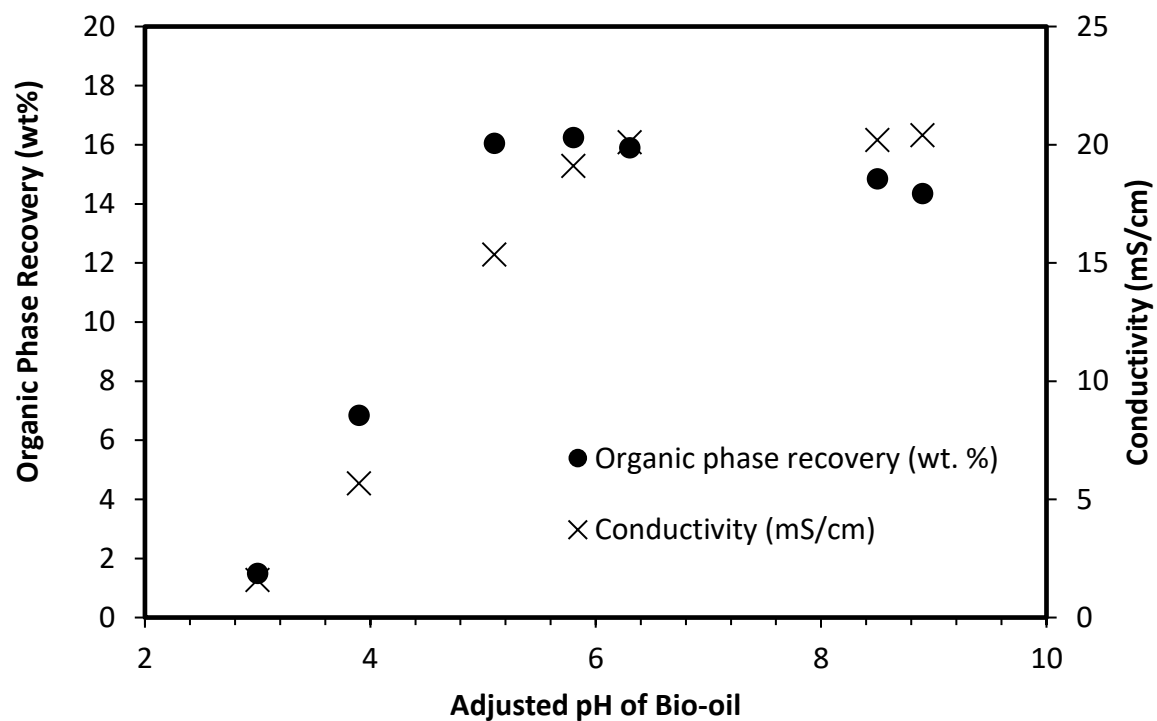


Figure 3.8. An organic phase (NBOOP) precipitated out of aqueous bio-oil as the pH was increased through the addition of NaOH (50%) solution. The conductivity of the aqueous phase (NBOAP) also increased with pH due to the addition of NaOH and precipitation of organic species.

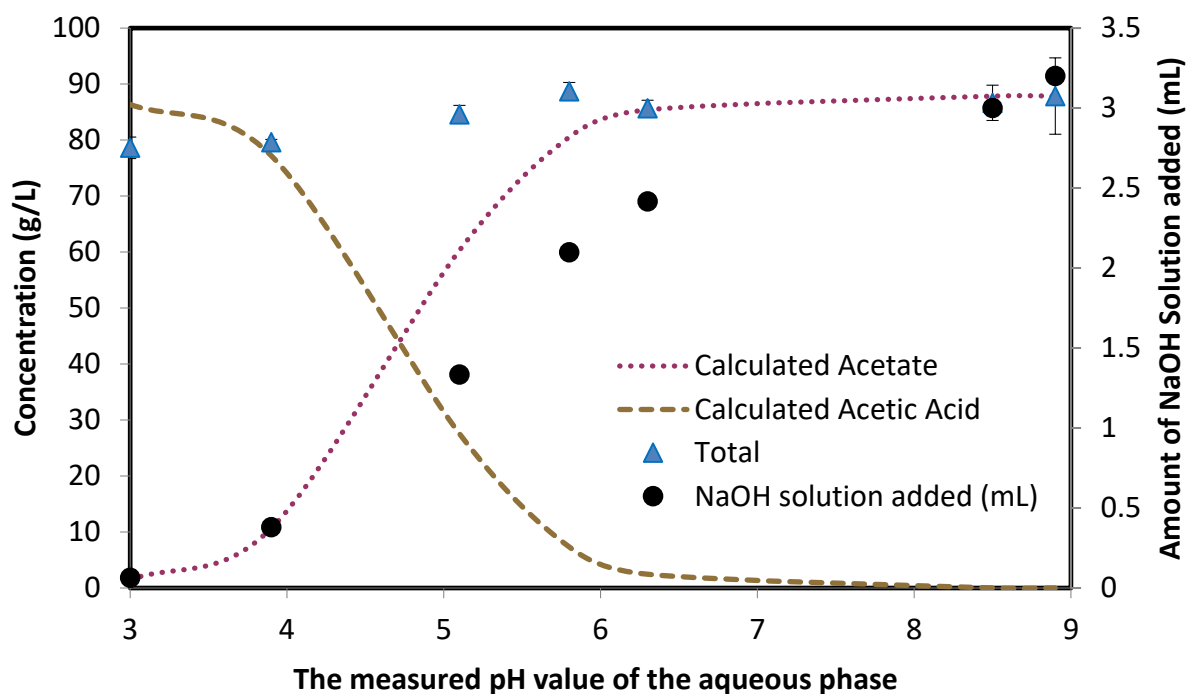


Figure 3.9. The amount of total acetate and acetic acid in the aqueous phase (NBOAP) of bio-oil as a function of pH measured by HPLC. The total concentration agrees with the addition of the calculated acetate and acetic acid concentrations. Changes in the pH value of the aqueous phase (NBOAP) as a function of NaOH (50 %) solution added to 10 g of AqBO.

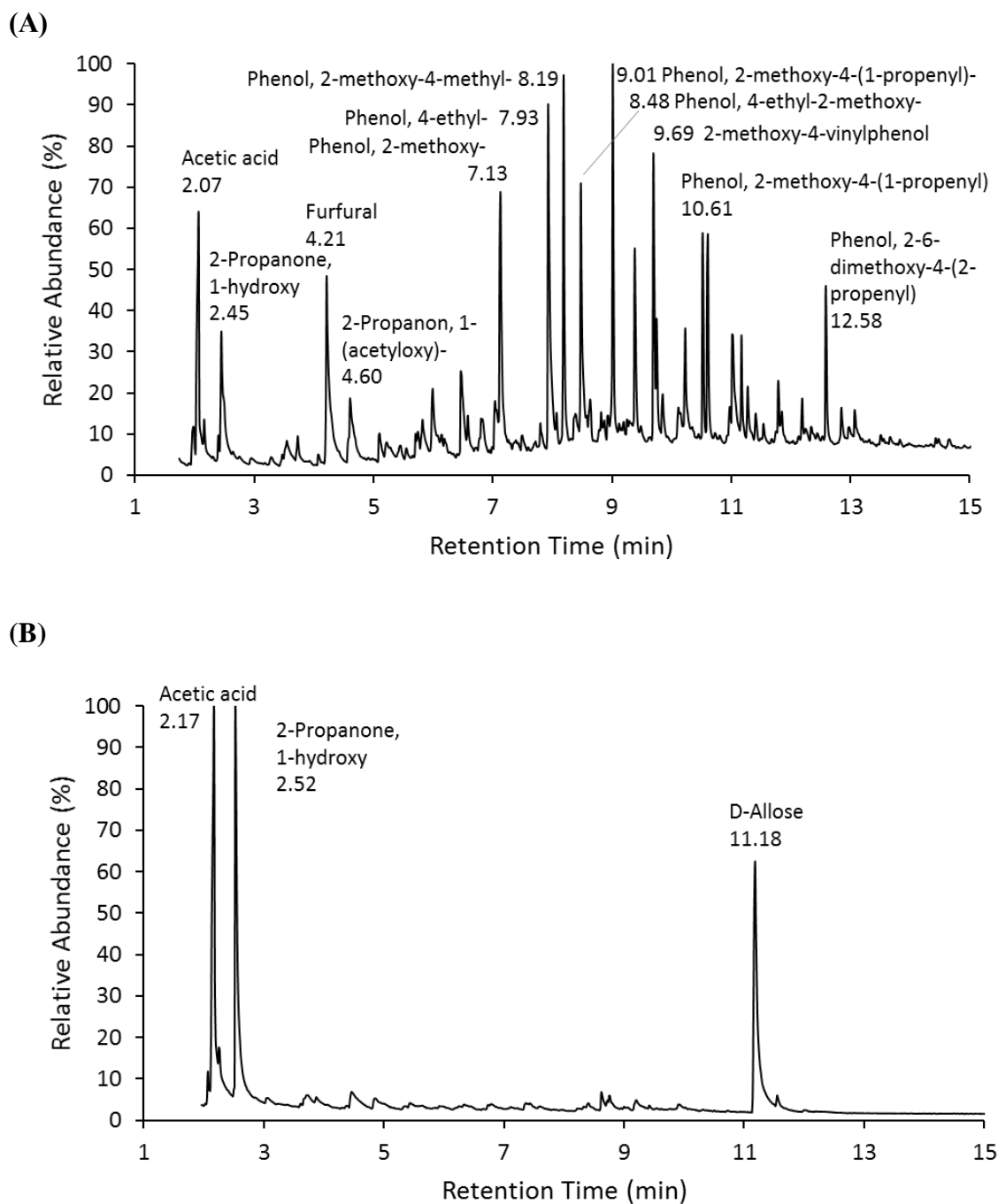


Figure 3.10. Representative GC-MS analysis of (A) organic phase (NBOOP) precipitated and (B) aqueous phase (NBOAP) after pH adjustment (pH 5.8).

3.4 Conclusions

Bio-oil phases are separated by adding water, organic solvents, and NaOH solution. The organic solvent phases contain phenolics and acetic acid. The mass of chemicals extracted by organic solvents is relatively small. Combined extraction is preferred for extracting more chemicals, especially phenolics. Sequential extraction is beneficial for a microbial electrolysis cell application for hydrogen production because organic solvents do not partition into the water phase. When the pH of the AqBO increases, an organic phase with phenolics is formed. The formation of organic phases is optimized at around pH 6.0. An application of the phenolics stream is needed for the improvement of process economics. The NBOAP with hydrophilic chemicals will be further investigated as a feedstock for MEC to produce hydrogen. Furthermore, NBOOP contained 37 % less oxygen and had double heating value compared to AqBO, which was used for neutralization. Less oxygen content and increased heating value of NBOOP demonstrate a significant quality improvement introduced by bio-oil neutralization.

3.5 Acknowledgments

This chapter contains contributions from coauthors and was published in: Park, L. K.-E., Ren, S., Yiacoumi, S. Ye, X. P., Borole, A. P., Tsouris, C. 2016. "Separation of Switchgrass Bio-Oil by Water/Organic Solvent Addition and pH Adjustment." *Energy & Fuels* **30**(3): 2164-2173.²⁴

CHAPTER 4. CONTRIBUTION OF ACIDIC COMPONENTS TO THE TOTAL ACID NUMBER (TAN) OF BIO-OIL

Bio-oil or pyrolysis oil — a product of thermochemical decomposition of biomass under oxygen-limited conditions — holds great potential to be a substitute for nonrenewable fossil fuels. However, its high acidity, which is primarily due to the degradation of hemicelluloses, limits its applications. For the evaluation of bio-oil production and treatment, it is essential to accurately measure the acidity of bio-oil. The total acid number (TAN), which is defined as the amount of potassium hydroxide needed to titrate one gram of a sample and has been established as an ASTM method to measure the acidity of petroleum products, has been employed to investigate the acidity of bio-oil. The TAN values of different concentrations of bio-oil components such as standard solutions of acetic acid, propionic acid, vanillic acid, hydroxybenzoic acid, syringic acid, hydroxymethylfurfural, and phenol were analyzed according to the ASTM D664 standard method. This method showed the same linear relationship between the TAN values and the molar concentrations of acetic, propionic, and hydroxybenzoic acids. A different linear relationship was found for vanillic acid, due to the presence of multiple functional groups that can contribute to the TAN value. The influence of the titration solvent on the TAN values has been determined by comparing the TAN values and titration curves obtained from the standard method with results from the TAN analysis in an aqueous environment and with equilibrium modeling results. Aqueous bio-oil samples with a known amount of acetic acid added were also analyzed. The additional acetic acid in bio-oil samples caused a proportional increase in the TAN values. The results of this research

indicate that the TAN value of a sample with acids acting as monoprotic acids in the titration solvent can be converted to the molar concentration of total acids. For a sample containing acids that act as diprotic and polyprotic acids, however, its TAN value cannot be simply converted to the molar concentration of total acids because these acids have a stronger contribution to the TAN values than the contribution of monoprotic acids.

4.1 Introduction

Increasing energy demand, climate change, and carbon dioxide emissions from fossil fuels raise serious concerns. The exploration, marketing, and transportation of fossil fuels cause additional pollution as well as social and political unrest.¹⁰⁴ In light of these circumstances, carbon-neutral biofuels produced from various lignocellulosic materials such as grass, wood, agricultural, or forest residues appear to be a promising substitute for fossil fuels. The currently available forms of biofuels include bioethanol, biodiesel, and bio-oil (pyrolysis oil).

Bioethanol and biodiesel are commercially used in blends of gasoline and diesel, respectively, for vehicle-use and heating. Bio-oil is produced, along with byproducts such as char and syngas, from pyrolysis in which biomass is heated under oxygen-limited conditions. Currently, bio-oil is the cheapest biofuel produced from lignocellulosic materials, with good potential of becoming a sustainable energy source.¹⁰⁵ However, it has some application-hindering properties including high moisture content, high viscosity, high density, low heating value, and high acidity.

High acidity is especially problematic for the storage and transportation of bio-oil, which has a typical pH of 2-3⁴⁵⁻⁴⁷). Acidic components can also cause instability by

generating protons (H^+) that can promote condensation and polymerization reactions.⁴³ Hence, there have been various attempts to reduce the acidity through neutralization and catalytic reactions.^{24, 43, 106} One approach to neutralizing acidic bio-oil is by adding alkaline solution.²⁴ To properly compare initial and final bio-oils after a neutralization treatment, however, the acidity of bio-oil must be accurately quantifiable.

Various techniques have been employed to measure the acidity of bio-oil including pH, ion chromatography (IC), high-performance liquid chromatography (HPLC), and gas chromatography-mass spectrometry (GC-MS), though each technique has some limitations. The pH, which measures the concentration of protons, does not provide the concentrations of acidic components, and also is found to be susceptible to errors.⁶⁰ Chemical analysis using IC, HPLC, and GC-MS can identify and quantify various chemicals including acids in bio-oil samples.^{47, 107} There are, however, some disadvantages associated with these techniques. Small changes in pH can greatly affect IC results by altering the binding profiles of IC resins.¹⁰⁸ On the other hand, HPLC and GC-MS may underestimate the acidic components in bio-oil samples. Specifically, GC-MS is known to detect only volatile compounds (e.g., acetic acid and propionic acid), which comprise 25 – 40 wt% of bio-oil, while other heavy carboxylic acids may not be detected.⁶¹ Moreover, due to a high diversity of chemicals in bio-oil, the use of HPLC and GC-MS has been linked to measurement inconsistencies among different laboratories, as demonstrated through the round-robin testing by Oasmaa et al.⁶⁰ Although recently Oasmaa et al.⁴⁶ suggested that capillary electrophoresis (CE) can accurately measure the acidic components in bio-oil, CE has disadvantages of lower injection precision and sensitivity as compared to HPLC.¹⁰⁹ Moreover, chemical analysis,

in general, cannot provide a single parameter that can be used for comparing samples with different chemical compositions.

Regardless of differing characteristics between various bio-oil samples, the total acid number (TAN) analysis can provide a single parameter that can be used for acidity comparisons. TAN is the amount of potassium hydroxide (KOH, in milligram) required to titrate one gram of a sample. The TAN analysis was originally developed for measuring the acidity of petroleum products but has been applied more recently to measure the acidity of biodiesel,⁴⁹⁻⁵⁸ biodiesel blends,^{50, 51, 55} vegetable oils,^{53, 110} lubricating oils,¹¹¹ heavy oil,¹¹² bitumens,¹¹² fats,¹¹⁰ and bio-oil.^{46, 59-61}

The current standard on biodiesel acidity is 0.50 mgKOH/g, according to the American Society for Testing and Materials (ASTM) D644 and European Standard (EN) 14104.⁵⁵ However, currently, there is no available standard for bio-oil. The typical TAN value of switchgrass intermediate pyrolysis bio-oil is 137.4 ± 3.0 mgKOH/g,⁴⁷ which is high compared to the standard for biodiesel.

Today, various standard methods (summarized in **Table 4.1** for comparison) are available to measure the TAN. Largely, there are potentiometric (ASTM D664⁶²) and colorimetric methods (ASTM D974,⁶³ ASTM D3339,⁶⁴ and American Oil Chemists' Society, AOCS Cd 3d 63⁶⁵). The colorimetric methods are known to be simple and better than potentiometric methods.^{50, 57} Moreover, the colorimetric methods (ASTM D974,⁶³ EN14104,¹¹³ and AOCS Cd 3d-63⁶⁵) were found to be more accurate for biodiesel analysis because these methods avoid errors introduced by the electrode.^{50, 57} The aqueous titration from EN14104, however, can cause some ester bonds to be hydrolyzed by the aqueous base, leading to consumption of base and elevating measurements.⁵⁵

Furthermore, the end point determination in colorimetric methods can be challenging.^{49, 54} Although ASTM D974 is known to be compatible for a colored sample, the dark brown (nearly black) color of bio-oil would most likely interfere with the endpoint determination during the analysis. Thus, for bio-oil analysis, the potentiometric method (ASTM D664⁶²) would be the appropriate option.

The potentiometric method, ASTM D664,⁶² has some challenges. While this method requires an electrode, the variability of the electrode dehydration may result in mediocre reproducibility and a lack of accuracy in the acidity analysis.^{50, 57} Additionally, a conventional pH electrode is originally designed to measure the pH in aqueous systems. Hence, the pH value would be different in non-aqueous systems (i.e., titration solvent) due to possible effects of the non-aqueous solvent on the pH and reference electrode, including effects on proton activity.¹¹⁴ All current standard methods require KOH/2-propanol as the titrant solution and the mixture of toluene and 2-propanol as a titration solvent. Thus, the measured pH refers to these conditions. Another challenge for using organic solvents is that toxic chemical waste is generated when analyzing the TAN value by standard methods due to the titration solvent. Therefore, many researchers have indicated that current standard methods are labor-intensive, expensive, error-prone, and harmful to the environment.^{49, 51, 52, 58}

Table 4.1. Standard methods of acidity analysis.

Standards	ASTM D664-11a	ASTM D974-14	ASTM D3339-12	AOCS Cd 3d 63
Methods	Potentiometric	Colorimetric	Colorimetric	Colorimetric
Alkaline of titrant	KOH	KOH	KOH	KOH
Solution for titrant	2-Propanol	2-Propanol	2-Propanol	2-Propanol
Concentration of titrant (M)	0.1	0.02	0.01	0.1
Titration solvent	Toluene: 2-propanol:water	Toluene: 2-propanol	Toluene: 2-propanol:water	Toluene: 2-propanol
Solvent volume Ratio	100:99:1	1:1	100:99:1	1:1
Titration solvent (mL)	125	10	40	125
Indicator	n/a	p-Naphtholbenzein	p-Naphtholbenzein	Phenolphthalein
Amount of indicator	n/a	8 drops	n/a	Until the appearance of a slightly pink color
Sample weight range (g)	0.1 - 20	0.2 - 20	0.1 - 5	Varies
TAN ranges (mgKOH/g)	0.05 - 260	0.0 - 250	0.0 – 3.0	n/a

To improve the currently available standard methods, many research groups have modified these methods to reduce the error in reproducibility. Furthermore, modified methods were quicker, simpler, cheaper, more environmentally friendly, and more accurate. Some modifications from other groups are summarized in **Table 4.2** and **Table 4.3** for reference. An organic titrant solution was replaced by aqueous solutions (KOH in water^{2, 46} or NaOH in water.^{49, 58, 110} The toxic titration solvent was substituted with less harmful solvents (e.g., only 2-propanol,⁵⁴ solely acetone,^{2, 46} a mixture of ethanol and water,^{49, 58, 110} and a mixture of acetone and tert-butanol⁶¹). Additionally, decreasing the amount of titration solvent^{2, 46, 49-51, 54, 58, 110} and the sample weight^{2, 50, 51} were attempted by many groups. Other modifications include changing the electrode filling solution⁵⁴ and introducing different electrode cleaning procedures^{58, 110} to address dehydration in the electrode.

Further steps have been made to develop new approaches to measuring acidity including a coulometric analysis,⁵² a 3D-printed flow injection analysis,¹¹⁵ and a sequential injection analysis with multivariate curve resolution-alternating least squares (SIA-MCR-ALS).⁵³ Although these new methods were developed for analyzing the acidity of plant oils,⁵³ biodiesel,^{52, 53} and thermal conductive oil,¹¹⁵ they may be applicable for analyzing the acidity of bio-oil as well.

Table 4.2. Modifications of total acid number analysis of biofuels.

Modifications	Baig et al. ^{50, 51}	Aricetti et al. ⁴⁹	Tubino et al. ^{58, 110}	Gonçalves et al. ⁵⁴
Standards	ASTM D974	AOCS Cd 3d-63	ABNT-NBR 14448 ⁵⁸ , AOCS Cd 3d-63 and ABNT-NBR 14448 ¹¹⁰	ASTM D664
Methods	Colorimetric	Colorimetric	Potentiometric	Potentiometric
Alkaline titrant	KOH	NaOH	NaOH	KOH
Solvent for titrant	2-Propanol	Water	Water	2-Propanol
Titration conc. (M)	0.02	0.02	0.02	0.01
Titration solvent	toluene:2-propanol:water	ethanol:water	ethanol:water	2-Propanol
Volume ratio	100:99:1	1:1	1:1	1
Solvent vol. (mL)	10	75	75	50
Indicator	p-naphtholbenzein	phenolphthalein	n/a	n/a
Amount of indicator	8 drops	n/a	n/a	n/a
Sample weight (g)	2	20	20	n/a
Sample type	Distilled biodiesel, biodiesel blends	Biodiesel	Biodiesel, ⁵⁸ oils and fats ¹¹⁰	Biodiesel
Other modifications	a 5 mL burette with division of 0.02 mL	n/a	Rinsing the electrode with ethanol and soaked it in water for 1 min	Electrode filling solution (3.0 M aqueous KCl solution)
Results	<ul style="list-style-type: none"> Reduced max error (from 42.88% to 5.92 %); good accuracy and repeatability ⁵⁰ Reduced max error (from 101% to 18%); repeatability decreased (from 290% to 100% ⁴⁹ 	<ul style="list-style-type: none"> Reliable, accurate, and precise TAN Same results as AOCS Cd 6d-63 with a little better precision 	<ul style="list-style-type: none"> Statistically equivalent results as ABNT NBR 14448 Less dehydration of the electrode ⁵⁸ Easier endpoints determination ¹¹⁰ 	<ul style="list-style-type: none"> Good repeatability that was lower than that of colorimetric method The difference in TAN for different solvents and filling solutions was < 5% Statistically similar results from standard methods and modifications
Advantages	Easy, reproducible, cost-effective, environmentally friendly, and time-efficient	Greener solvent, less solvent, aqueous titrant, cheaper (82%)	Minimizing dehydration of the electrode by using aqueous solution of ethanol as the solvent; quicker analysis, which decreases the possibility of dehydration of the electrode; less organic solvents, lower cost, greener method, lower toxicity	Less toxic and lower probability of causing possible aqueous hydrolysis of methyl esters
Challenges	Color changes at endpoint of titration of dark-colored samples could not be observed.	Difficult endpoint determination as a function of the yellow color of biodiesel	n/a	n/a

[ABNT: the Brazilian Association of Technical Standards (*Associação Brasileira de Normas Técnicas*)]

Table 4.3. Modifications of total acid number analysis of biofuels (continued).

Modifications	Fuhr et al. ¹¹²	Shao et al. ² and Oasmaa et al. ⁴⁶	Wu et al. ⁶¹
Standards	ASTM D664	ASTM D664	ASTM D664
Methods	Potentiometric	Potentiometric	Potentiometric
Alkaline titrant	KOH	KOH	tetramethylammonium hydroxide (TMAH)
Solvent for titrant	2-Propanol	water	methanol and 2-propanol (1:10 v.)
Titrant conc. (M)	0.05, 0.1, 0.15 (N)	0.1	0.12 mmol/L
Titration solvent	toluene:2-propanol	acetone	acetone: tert-butanol
Volume ratio	75:25	1	1:9
Solvent vol. (mL)	125	50	n/a
Sample weight (g)	1 - 2	0.1 - 0.5	n/a
Sample type	Heavy oils and bitumens	Bio-oil	Bio-oil
Others	time < 30 min; pretreatment of samples = heating to 60 °C	Used 0.1 M HCl in water as standard solution	Nonaqueous titration
Results	<ul style="list-style-type: none"> Concentrations of titrant have no effect Pretreatment is required for viscous samples More toluene in titration solvent can dissolve samples Good reproducibility 	<ul style="list-style-type: none"> Sample size (0.1 - 0.5 g) and solvent volume (50 - 125 mL) did not have effects on TAN analysis Possible recycling titration solvent (up to three times) 	<ul style="list-style-type: none"> Detected heavy carboxylic acids and phenolics as well as strong acids Differentiated the carboxylic acids and phenolic groups through a non-aqueous titration potentiometric titration
Advantages	Suitable analysis of viscous samples (perhaps this modification is applicable for organic phase of bio-oil) Titration without delay to avoid asphaltene precipitation	Less toxic, cost saving, and shorter analysis time	Nonaqueous titration: avoid leveling effect and obtain distinguishable endpoints Titration solution (acetone and tert-butanol) can dissolve bio-oil
Challenges	n/a	n/a	n/a

n/a: not available

Even though various modifications and new methods were recently developed for biofuels, it is important to understand the meaning of TAN values using the standard methods. Moreover, as compared to biodiesel, there are no in-depth studies on the TAN analysis of bio-oil, even though the TAN value has been primarily used for measuring the acidity of bio-oil. Understanding the relationship between TAN and the concentrations of acidic components found in bio-oil samples can help us develop methods to reduce the acidity of bio-oil. It is also important to determine if other non-acidic chemical species present in bio-oil (e.g., sugars, furans, ketones, aldehydes, phenolics) contribute to the TAN values.

Therefore, the objectives of this study were to: (1) analyze the acidity of switchgrass bio-oil in terms of TAN value; (2) compare measured TAN values with theoretically calculated ones for standard solutions; (3) investigate the relationship between TAN values and the concentrations of different chemicals species found in bio-oil using standard solutions; (4) examine the effect of the titration solvent on the TAN measurement by comparing the TAN values and titration curves obtained from the standard method with results from the TAN analysis in aqueous environment and with equilibrium modeling results; and (5) explore whether a variety of chemicals present in bio-oil have any influence on the TAN analysis by examining the recovery of added acetic acid in aqueous bio-oil samples (recovery test) through the TAN values. Because D664 ⁶² was previously employed for bio-oil acidity analysis, while D974 (colorimetric) was limited by the dark color of bio-oil as discussed above, we attempted to investigate the relationship between TAN values and concentrations of different standard solutions

using the D664 method.⁶² In this study, a minor modification to the electrode cleaning procedure — the 1-minute water-spray method described in Baig et al.⁵¹ — was adopted.

4.2 Materials and Methods

4.2.1 Materials

Acetic acid (analytical standard), propionic acid (analytical standard), vanillic acid ($\geq 97.0\%$), syringic acid ($\geq 95\%$), 4-hydroxybenzoic acid (HBA, $\geq 99\%$), 5-(hydroxymethyl)furfural (HMF, $\geq 99\%$), phenol ($\geq 99.5\%$), anhydrous 2-propanol (99.5 %), and toluene ($\geq 99.5\%$) were purchased from Sigma-Aldrich (Milwaukee, WI). A titrant solution, 0.1 mol/L KOH in 2-propanol was purchased from Fisher Scientific. Switchgrass bio-oil was produced via intermediate pyrolysis with a semi pilot-scaled auger pyrolysis system (Proton Power, Inc., Lenoir City, TN, USA) at the University of Tennessee (UT) Center for Renewable Carbon. More details on the production of bio-oil are available elsewhere.^{24, 47, 98} Switchgrass bio-oil had pH of 2.5.

4.2.2 Methods

4.2.2.1 Bio-oil Analysis

The chemical composition of crude, aqueous and organic bio-oil (**Table 4.4**) was analyzed by gas chromatography with a flame ionization detector (GC-FID) and high-performance liquid chromatography (HPLC). The methods involved in analyzing the chemical composition of bio-oil are found in Ren et al.^{25, 47} Briefly, 2(5H)-furanone, 1-hydroxy-2-butanone, 1,3-propanediol, 3-methyl-1,2-cyclopentanedione, guaiacol,

creosol, 2,6-dimethoxyphenol, and 3-ethylphenol were quantified using GC-FID using a HP-5 column (30 m \times 0.32 mm, 0.25 μ m film thickness).^{25, 47} The detailed setting for GC-FID is available in the literature.^{25, 47} The identification of compounds was performed by comparing their mass spectra with those from the National Institute of Standards and Technology (NIST) mass spectral data library. Acetic acid, propionic acid, levoglucosan, hydroxymethylfurfural (HMF), furfural, phenol, and 1,2-benzenediol were analyzed using an HPLC, Jasco 2000Plus (Jasco Analytical Instruments, Easton, MD) with an MD-2018 plus photodiode array detector, an RI-2031 Plus intelligent refractive index detector, and an AS-2055 plus autosampler. The chemical analysis using HPLC was performed at 50 °C with a Bio-Rad column HPX-87H (300 \times 8 mm). The injected sample volume was 20 μ L. Sulfuric acid (5 mmol/L) in deionized water was used as the mobile phase with the flow rate of 0.6 mL/min. The compounds were quantified using external standards in both the HPLC and GC-FID analyses. For water content measurements, a Schott TitroLine Karl Fischer volumetric titrator was used according to the ASTM D4377 (2011) method.¹¹⁶

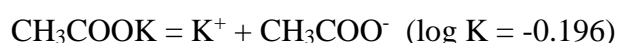
4.2.2.2 Total Acid Number Analysis

For the TAN analysis, the ASTM D664 method⁶² was followed except for the cleaning procedure. In brief, the titration solvent was prepared using toluene, anhydrous 2-propanol, and deionized water (100:99:1 v.). It should be mentioned here that one of the ASTM D664 modifications that have been suggested for biodiesel does not include toluene as one of the titration solvents. For the case of bio-oil, however, we did not follow that modification because, in contrast to biodiesel, bio-oil includes organic components that are not soluble in the 2-propanol/water mixture. For the titrant solution,

a concentration of 0.1 mol/L KOH in 2-propanol was used as received from Fisher Scientific. The volume of titration solvent used was 125 mL. Sample amounts varied depending on the range of TAN values (**Table 2.1**) according to ASTM D664-11a.⁶² The modified electrode cleaning procedure (spraying water for 1 min) was adapted from Baig et al.⁵¹ Samples were titrated to pH 11,⁴⁷ and the TAN values were calculated by following ASTM D664. Acetic acid, propionic acid, HMF, and phenol solutions were prepared in deionized water with concentrations of 2, 4, and 6 wt%. Sample analysis was performed in triplicate. Solutions of HBA and vanillic acid were prepared in 2-propanol due to its limited solubility in water and higher solubility in 2-propanol.¹¹⁷ Due to limited solubility of syringic acid in water or 2-propanol, syringic acid solution (0.6 wt%) was prepared in the titration solvent.

4.2.2.3 Equilibrium MINEQL+ Modeling and Aqueous Titration

The TAN analysis of acetic acid (2 wt%) was modeled using a solution equilibrium software called MINEQL+ for a closed system (with respect to air). The following chemical reactions were considered in modeling the TAN analysis of acetic acid (2 wt%). The equilibrium constants, K values, of these reactions were provided by the MINEQL+ library. The conditions of the MINEQL+ modeling are: aqueous system, closed to the atmosphere (i.e., no carbonate species considered), and room temperature (25 °C).



To imitate the MINEQL+ modeling experimentally, an aqueous TAN analysis was performed using water as titration solvent and 0.1 mol/L KOH solution in water as titrant solution.

4.2.2.4 Bio-oil Recovery Test

Crude bio-oil obtained from UT was centrifuged at 3000 rpm (1673 g) for 30 minutes using Beckman Coulter Avanti J-E centrifuge with a JLA 10.500 rotor to separate the aqueous and organic components of bio-oil. The chemical compositions of aqueous bio-oil (AqBO) and organic bio-oil (OrgBO) were analyzed. Due to the heterogeneity of crude bio-oil and organic bio-oil, AqBO was used in the recovery test for consistency. AqBO (9 g) was mixed with 1 g of acetic acid solutions (20, 40, and 60 wt% in deionized water) to yield an overall 2, 4, and 6 wt% of acetic acid, respectively. The TAN values of acetic-acid-added AqBO samples were analyzed in triplicate. Prepared samples were also analyzed using HPLC as described in **Section 4.2.2.5**.

4.2.2.5 High-Performance Liquid Chromatography (HPLC) Analysis for Bio-oil Recovery Test

Agilent 1100 was used as the HPLC system. A BioRad Aminex HPX-87H column and a refractive index detector were incorporated into this system. The mobile phase of the HPLC was 5 mmol/L sulfuric acid with a flow rate of 0.6 mL/min. Standard solutions were prepared with the mobile phase, and bio-oil samples were diluted 1000 times with the mobile phase. A volume of 20 μ L was injected, and each sample was analyzed for one hour.

4.3 Results and Discussion

4.3.1 Chemical Composition and TAN Analysis of Switchgrass Bio-oil

The chemical compositions of switchgrass crude bio-oil, aqueous bio-oil, and organic bio-oil from GC-FID and HPLC analyses are presented in **Table 4.4**. When the heterogeneous crude bio-oil is centrifuged, there were two different phases: aqueous bio-oil (supernatant) and organic bio-oil (precipitate). Aqueous bio-oil contains mostly water, levoglucosan, acetic acid, and propionic acid. Organic bio-oil contains less water but more furfural and phenolics than aqueous bio-oil. More than 70 wt% of organic bio-oil was not quantified by GC-FID and HPLC analyses. The TAN values of crude bio-oil and aqueous bio-oil were found as 109.7 ± 4.3 and 138.6 ± 14.7 mgKOH/g, respectively.

4.3.2 Comparison between Measured and Theoretical TAN Values

The relationship between measured TAN values of acetic acid and propionic acid solutions (2, 4, 6 wt%) and theoretical TAN values obtained from **Equation 4.1** are presented in **Figure 4.1**. The mean of the measured TAN values, theoretical TAN values, and their repeatability are found in **Table 4.5**. According to ASTM ⁶², the definition of repeatability calculated from **Equation 4.2-a** ^{2, 50, 62, 118} is given as follows: “the difference between successive test results obtained by the same operator with the same apparatus under constant operating conditions on identical test material would in the long run, in the normal and correct operation of the test method, exceed the following values only in one case in twenty.” Since the titration curves of the manual TAN analyses did not have defined inflection points, the acceptable repeatability for the manual titration mode is 5% of the mean based on the standard method ⁶². Thus, most of the data were

within the acceptable repeatability ($<5\%$) as shown in **Table 4.5**, while only one measurement exceeded the 5% limit.

Table 4.4. The chemical compositions of crude bio-oil, aqueous (centrifuged) bio-oil, and organic bio-oil.

(Weight %)	Crude Bio-oil	Aqueous Bio-oil	Organic Bio-oil
Water	43.3	43.65	15.18
Levogluconan	9.09	9.19	0.72
Acetic acid	7.71	8.06	6.16
Propionic acid	3.42	3.57	0.00
1-Hydroxy-2-butanone	1.37	1.08	0.86
1,3-Propanediol	0.29	0.07	0.06
HMF	0.59	0.58	0.19
Furfural	1.38	0.40	1.35
2(5H)-Furanone	0.38	0.41	0.26
3-Methyl-1,2-cyclopentanedione	0.25	0.17	0.25
1,2-Benzenediol	0.59	0.42	0.61
Phenol	0.26	0.12	0.31
Guaiacol	0.11	0.13	0.29
3-Ethylphenol	0.38	0.15	0.74
2-Methoxy-4-methylphenol (creosol)	0.42	0.24	0.47
2,6-Dimethoxyphenol	0.13	0.11	0.33
Quantified	69.67	68.34	27.78
Non-quantified	30.33	31.66	72.22

Table 4.5. Theoretical and measured TAN values of acetic and propionic acids standard solutions.

Chemicals	Concentration		Theoretical TAN (mgKOH/g)	Mean measured TAN (mgKOH/g)	Standard deviation	Repeatability (%)
	(wt%)	(mol/L)				
Acetic acid	2	0.33	18.69	18.96	0.24	3.5
	4	0.67	37.37	37.46	0.63	4.6
	6	1.00	56.06	58.75	0.90	4.2
Propionic acid	2	0.27	15.15	15.47	0.08	1.5
	4	0.54	30.30	30.55	2.00	18.2
	6	0.81	45.44	47.00	0.62	3.6

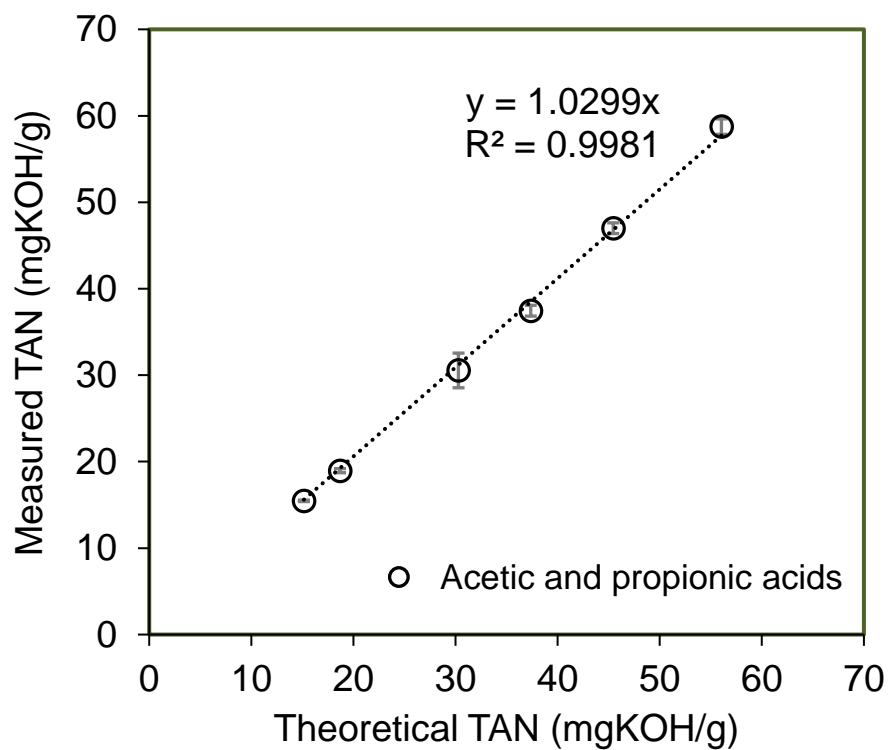


Figure 4.1. Relationship between measured TAN values of acetic acid and propionic acid solutions (2, 4, 6 wt%) and their theoretical TAN values obtained from **Equation (4.1)**.

$$\text{Theoretical TAN} = (\text{wt\% of acid}) \times (\text{MW of KOH}) / (\text{MW of acid}) \times 1000 \text{ (mg/g)} \quad (4.1)$$

where TAN is the total acid number (mgKOH/g) and MW is the molecular weight in g/mol (MW of KOH: 56.1056 g/mol)

$$\text{Repeatability (\%)} = [(2.77 \times \text{SD}) / (n \times \text{mean TAN})] \times 100 \% \quad (4.2-a)$$

$$\text{Error (\%)} = (\text{mean of measured TAN} - \text{theoretical TAN}) / (\text{theoretical TAN}) \times 100 \%$$

(4.2-b)

where n is the number of operators involved in the analysis (1 in this case), and SD is the standard deviation.

4.3.3 TAN Analysis of Standard Solutions

Oasmaa et al.⁴⁶ found that there were different linear relationships between TAN values and the concentrations of acetic acid and formic acid standard solutions (wt%). The reason for the different linear relationships, however, was not discussed. When the same data are replotted against molar concentrations, as shown in **Figure 4.2**, it is clear that both formic and acetic acids actually have the same linear relationship of TAN vs. molar concentrations. The combined data resulted in a slope of 58.494, which is very close to the combined slope (58.059) discussed later in this paper.

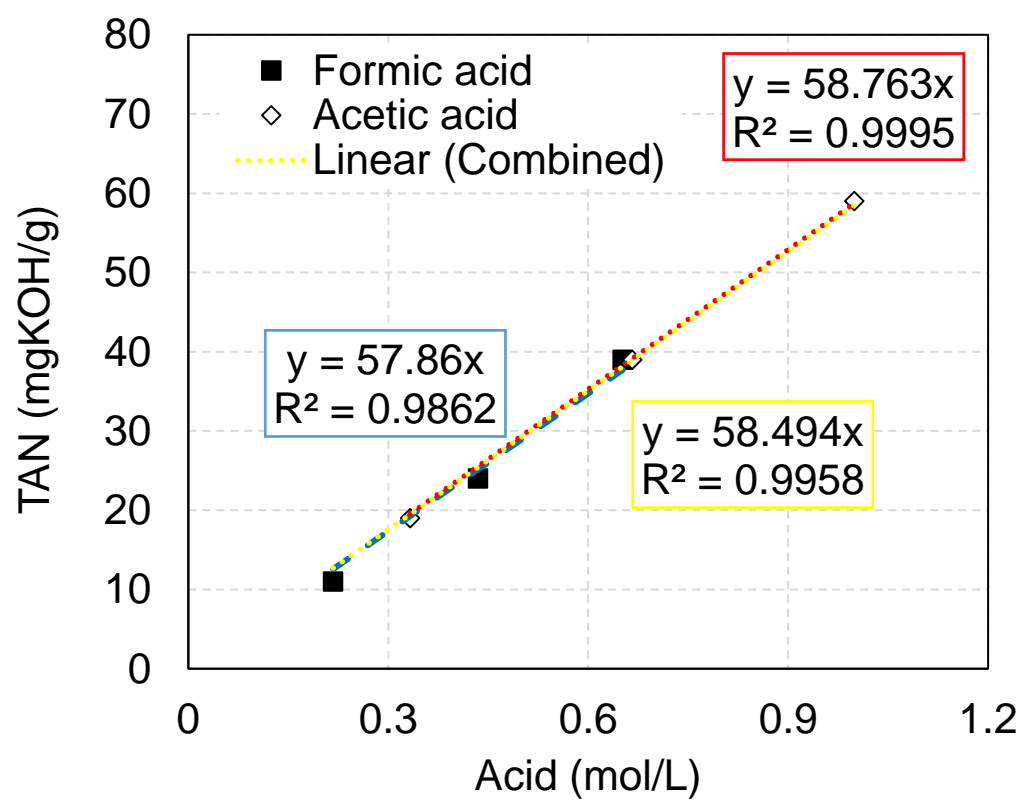


Figure 4.2. The same relationship is found when the TAN value is plotted vs. molar concentrations of formic and acetic acid (data obtained from Figure 5 in Oasmaa et al. ⁴⁶).

To further investigate the relationship between the TAN value and concentrations of various chemicals, the TAN analysis of standard solutions was performed for different concentrations (2, 4, and 6 wt%). All standard solutions except hydroxybenzoic, vanillic, and syringic acids were prepared in deionized water. Solutions of HBA and vanillic acid were prepared in 2-propanol due to its limited solubility in water.¹¹⁷ Preparing HBA and vanillic acid solutions in 2-propanol should not affect the TAN analysis because the titration solvent (125 mL) used contains 2-propanol (toluene: 2-propanol: water = 100:99:1 v.) at a relatively high concentration.

The measured TAN values are plotted vs. weight percent in **Figure 4.3**. As the concentration of the acidic solutions increased, the TAN values also increased. Unlike the acidic solutions, the phenol and HMF solutions did not influence the TAN measurements despite that phenols are more acidic than alcohols and may form phenoxide ions by reacting with hydroxide ions.⁴⁶ This is due to the high pK_a value (10.02) of the phenol, as well as the effect of the nonaqueous solvent. The low sensitivity of the standard method (ASTM D664) towards weak acids like phenol may be due to a suboptimal acidity of 2-propanol as Wu et al.⁶¹ pointed out.

The linear trendline of acetic acid, which has the lowest molecular weight, had the highest slope, while HBA and vanillic acid with high molecular weight had low slopes. The relationship between the TAN value and weight percent of standard solutions shown in **Figure 4.3** can be described by **Equations (4.3-a, b, c)**. As shown in **Equation (4.1-c)**, the slope of each line in **Figure 4.3** depends on the molecular weight of the sample.

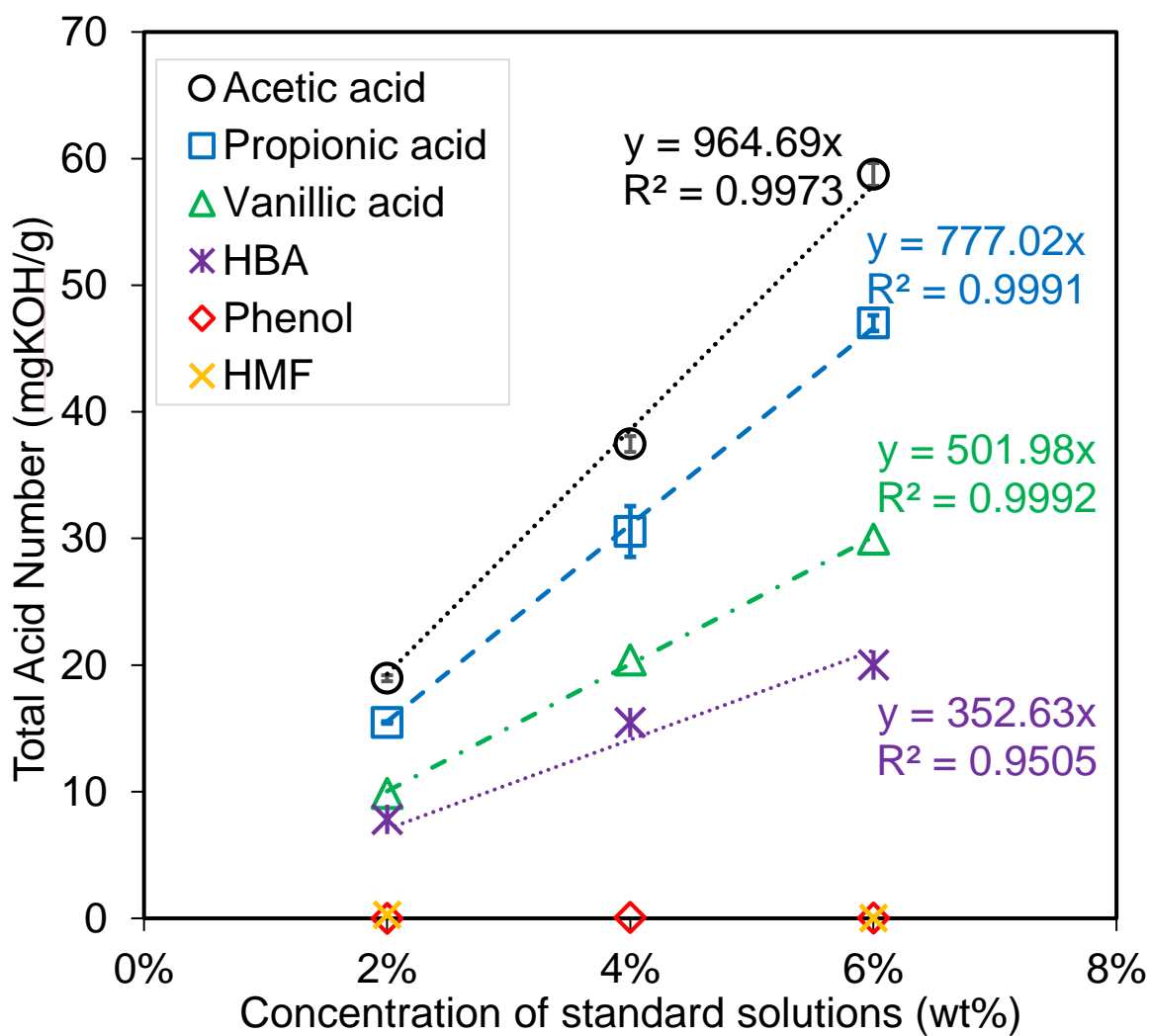


Figure 4.3. Different linear relationships between TAN values and weight percent concentrations of standard solutions of acetic acid, propionic acid, vanillic acid, and phenol.

Weight percent

$$TAN = [slope] \times [wt\%] \quad (4.3-a)$$

$$TAN(mgKOH/g) = \frac{MW \text{ of } KOH (g/mol)}{MW \text{ of Sample } (g/mol)} \times 1000 \left(\frac{mg}{g} \right) \times \frac{Sample (g)}{Total (g)} \% \times \alpha \quad (4.3-b)$$

$$[slope] = \frac{MW \text{ of } KOH (g/mol)}{MW \text{ of Sample } (g/mol)} \times 1000 \left(\frac{mg}{g} \right) \times \alpha \quad (4.3-c)$$

where $[wt\%] = \frac{Sample (g)}{Total (g)} \%$, where $Total (g) = Sample (g) + Solvent(g)$

Molar concentration

$$TAN = [slope] \times [M] \quad (4.4-a)$$

$$TAN = \frac{Sample (g)}{Total (L)} \times \frac{1}{MW \text{ of Sample } (g/mol)} \times \frac{Total (L)}{Total (g)} \times MW \text{ of } KOH (g/mol) \times 1000 \left(\frac{mg}{g} \right) \times \alpha \quad (4.4-b)$$

$$TAN \left(\frac{mgKOH}{g} \right) = \frac{Total (L)}{Total (g)} \times MW \text{ of } KOH (g/mol) \times 1000 \left(\frac{mg}{g} \right) \times \alpha \times [M] \quad (4.4-c)$$

$$TAN \left(\frac{mgKOH}{g} \right) = \frac{1}{\rho_{Total}} \times MW \text{ of } KOH (g/mol) \times 1000 \left(\frac{mg}{g} \right) \times \alpha \times [M] \quad (4.4-d)$$

$$[slope] = \frac{1}{\rho_{Total}} \times MW \text{ of } KOH (g/mol) \times 1000 \left(\frac{mg}{g} \right) \times \alpha \quad (4.4-e)$$

where $[M]: \text{molar concentration} = mol/L = \frac{Sample (g)}{Total (L)} \times \frac{1}{MW \text{ of Sample } (g/mol)}$

$$\rho_{Total}: \frac{Total (g)}{Total (L)}$$

Since the slopes of different linear relationships are inversely related to the molecular weight, the same data points were plotted with the x-axis as molar concentration as shown in **Figure 4.4**. Acetic, propionic, and hydroxybenzoic acids showed the same linear relationship; however, vanillic acid showed a different linear relationship. The

slope of vanillic acid in **Figure 4.4** is approximately two times the slope of acetic, propionic, and hydroxybenzoic acids. The relationship between TAN value and molar concentrations of standard solutions from **Figure 4.4** is described by **Equations (4.4-a through 4-e)**. The slope of each line in **Figure 4.4** is inversely related to the density of the standard solution. The different concentration standard solutions that were analyzed in this research were assumed to have similar density. However, at higher concentrations, the density of solutions may also cause a change in the slope of the line.

The slope of linear relationships is also related to the alpha factor. The alpha factor (α) in **Equations (4.3) and (4.4)** is the number of functional groups that contribute to the TAN value or the number of protons that can be removed during the TAN analysis. For instance, if a compound had more than one functional group that could react with KOH, consuming KOH with multiple functional groups would lead to a stronger effect on the TAN value as compared to compounds with only one acidic functional group. Even though vanillic acid has one carboxylic acid group, its slope, which is double the slope of other monoprotic acids, indicates that two protons were removed during the TAN analysis. This is because vanillic acid loses two protons and acts as diprotic acid during the TAN analysis (titration to pH 11) in the titration solvent system. Therefore, the alpha factor for formic, acetic, propionic, and hydroxybenzoic acids is 1, while the alpha factor for vanillic acid is found to be 2.

The results in **Figure 4.4** are summarized in **Table 4.6** with chemical structures and pK_a values. As expected, HMF that has pK_a value of 12.82 with the slope of 0 did not contribute to the TAN values. Because the samples were titrated to pH 11 during TAN analysis, hydrogen atoms with pK_a values less than 11 were expected to be titrated. The

pK_a of the hydrogen in phenol was less than 11; however, phenol did not contribute to the TAN value. As discussed in the following section (4.3.4), the reason for this behavior could be that the actual acid-base constants in the TAN standard titration solvent are different from pK_a values reported for the aqueous system. Acetic, propionic, and hydroxybenzoic acids had a slope of 58.059, which is close to the molecular weight of KOH. HBA has two hydrogens that have pK_a values of 4.38 and 9.67. Based on the slope of the linear relationship, only the hydrogen in the carboxylic group contributed to the TAN value and was removed during the TAN analysis. Vanillic acid has a very similar chemical structure as HBA except for the presence of a methoxy group. The slope of the linear relationship (**Figure 4.4**) for vanillic acid was 114, approximately double that for other acids. The slope of vanillic acid indicates that the two protons were removed during the TAN analysis (one from its carboxylic group and the other from its hydroxyl group). Perhaps the presence of the methoxy group helped the hydrogen in the hydroxyl group to be removed in the titration solvent – the mixture of toluene, 2-propanol, and water. It is noteworthy that the pK_a values presented in **Table 4.6** are based on aqueous systems. For consistency, the pK_a values of chemicals were obtained from chemical calculations from Chemicalize provided by ChemAxon¹¹⁹ except the pK_a value of HMF, which was obtained from another source.¹²⁰ In the titration solvent system (toluene, 2-propanol, and water – 100:99:1 v.), the pK_a values are certainly changing due to interactions between the titration solvent molecules and the various chemical species. Further investigations, which are not within the scope of this research, are needed to fully understand those interactions.

The data points for the TAN values of the acetic, propionic, and hydroxybenzoic acids were combined in **Figure 4.4**, and these data are well represented by a solid line, as shown on the graph. The combined slope for acetic, propionic, hydroxybenzoic acids is 58.059, which is close to the molecular weight of KOH (56.1056 g/mol). Thus, if a sample contains formic, acetic, propionic, and hydroxybenzoic acids, then the TAN value of the sample can be converted to the molar concentration of total acids using the following relationship, where M is the concentration in mol/L.

$$[\text{M of total acids}] = [\text{TAN (mgKOH/g)}] / [58.059 (\text{mgKOH M}^{-1} \text{ g}^{-1})] \quad (4.5)$$

If a sample such as bio-oil, however, contains acidic components such as vanillic acid, which have a stronger contribution to the TAN value than monoprotic acids, **Equation (4.5)** cannot be used to convert the TAN measurement to the molar concentration of total acidic components.

The TAN analysis of syringic acid solutions was also attempted. Due to limited solubility of syringic acid in water and 2-propanol, the TAN titration solvent (toluene: 2-propanol: water = 100: 99: 1 v.) was used to prepare the syringic acid solution. The maximum concentration that we were able to prepare was 0.6 wt% of syringic acid in the titration solvent. Unfortunately, the TAN value of 0.6 wt% of syringic acid could not be obtained because, during the TAN analysis of syringic acid, the pH value of the titration system could not reach 11, which is the end-titration pH according to the standard method. Instead, the maximum pH reached was 9.5. After reaching pH 9.5, precipitation of solids occurred, and the pH value dropped significantly. This means that, when a sample contains syringic acid, even at low concentrations, a strong contribution to the TAN value can be expected because syringic acid in the sample will consume the KOH

solution during titration; therefore, it would take more KOH solution for the system to reach pH 11, leading to a higher TAN value than that obtained in the absence of syringic acid.

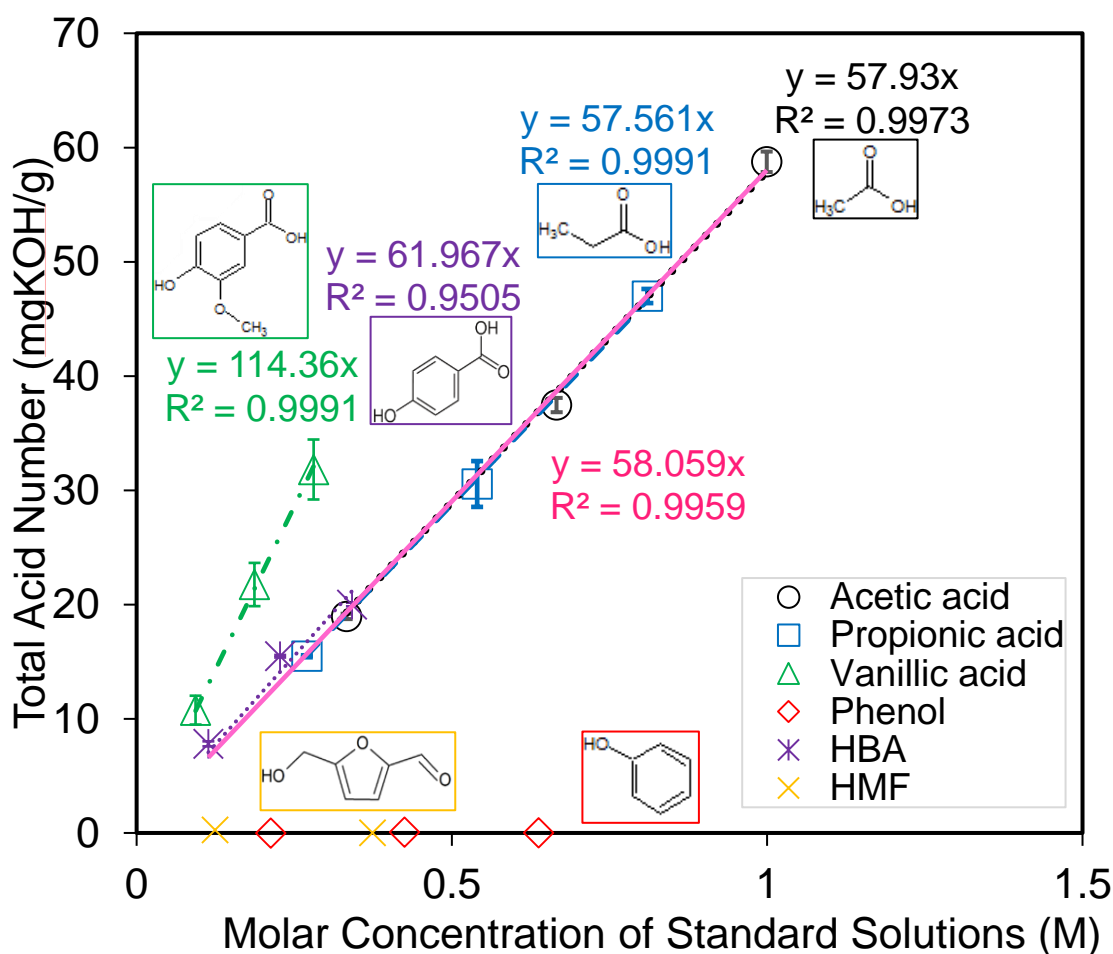
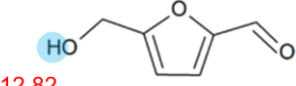
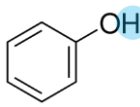
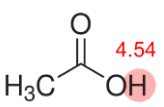
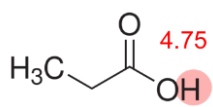
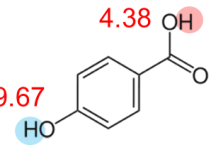
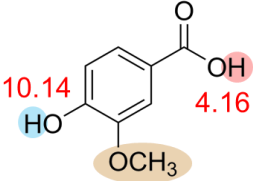


Figure 4.4. Relationship between TAN and molar concentrations of various bio-oil components. The TAN value of acetic, propionic, and hydroxybenzoic acids shows the same linear relationship vs. molar concentrations, represented by a solid trendline. The TAN vs. molar concentration line for vanillic acid shows a higher slope because of the release of 2 protons during titration to pH 11. Phenol and HMF show zero contribution to the TAN value.

Table 4.6. Slopes of the linear relationships between TAN value and the molar concentration of various chemicals found in bio-oil with their chemical structure and pK_a values obtained from the literature for HMF¹²⁰ and online chemical calculations from Chemicalize provided by ChemAxon¹¹⁹ for other chemicals.

Slopes	Chemical structures and pK_a values		
0 (TAN = 0)	 12.82 Hydroxymethylfurfural (HMF)	 10.02 Phenol	
58 (TAN = $58 \times [M]$)	 4.54 Acetic acid	 4.75 Propionic acid	 9.67 4.38 Hydroxybenzoic acid (HBA)
114 (TAN = $114 \times [M]$)	 10.14 4.16 Vanillic acid		

[M] is the molar concentration in mol/L.

4.3.4 Influence of Titration Solvent on TAN Analysis - MINEQL+ Modeling of Aqueous TAN Analysis

To investigate the effect of the titration solvent (i.e., the mixture of toluene, 2-propanol, and water), we employed MINEQL+, a solution equilibrium software, to model the TAN analysis. The MINEQL+ software is designed to model aqueous systems. Results from the MINEQL+ modeling are presented in **Figure 4.5**, where the molar concentration of potassium ions needed for the system to reach pH 11 is estimated at 3.67×10^{-3} mol/L. This amount can be converted to TAN value using the following equation based on the assumption that 1 g of sample is titrated in 125 mL of water [i.e., a total volume of 0.126 L (0.125 L of water and ~ 0.001 L of sample) was used in the calculation] as described in **Equations (4.6-a, b)**. Thus, the TAN value obtained from MINEQL+ modeling is 25.45 mgKOH/g [**Equation (4.6-b)**], which is different from the actual TAN value obtained from the TAN analysis using the ASTM D664 method (18.96 mgKOH/g).

Since the TAN values from the ASTM method and the MINEQL+ modeling were different, the TAN analysis in an aqueous system was performed using 2 wt% of acetic acid, water as the titration solvent, and 0.1 mol/L KOH solution in water. The experimental TAN analysis in the aqueous system is also presented in **Figure 4.5**. The amount of KOH solution added was measured during this analysis, and for comparison with the results from MINEQL+, the volume of KOH solution added was converted to molar concentration of KOH. From **Figure 4.5**, the amount of KOH required to titrate the system to pH 11 is estimated at 3.63×10^{-3} mol/L.

Similarly to **Equation (4.6-b)**, this concentration (3.63×10^{-3} mol/L) can be converted to TAN value as shown in **Equation (4.6-c)**.

Conversion from [KOH] to TAN (mgKOH/g sample)

$$= [\text{Concentration of KOH, (mol/L)}] \times [\text{molecular weight of KOH, (g/mol)}] \times [\text{unit conversion, (mg/g)}] \times [\text{total volume of the system, (L)}] / [\text{weight of a sample, (g)}]$$

(4.6-a)

$$= 3.67 \times 10^{-3} \text{ mol/L (KOH)} \times 56.1 \text{ g/mol} \times 1000 \text{ mg/g} \times 0.126 \text{ L} / 1 \text{ g} = \mathbf{25.45}$$

mgKOH/g (4.6-b)

$$= 3.63 \times 10^{-3} \text{ mol/L (KOH)} \times 56.1 \text{ g/mol} \times 1000 \text{ mg/g} \times 0.126 \text{ L} / 1 \text{ g} = \mathbf{25.66}$$

mgKOH/g (4.6-c)

Hence, the TAN value obtained from the TAN analysis in the aqueous system is 25.66 mgKOH/g, which is very close to the TAN value from MINEQL+ (25.45 mgKOH/g) but different from the TAN analysis using the ASTM method. The TAN analysis of acetic acid (2 wt%) using the ASTM D664 standard method is shown in **Figure 4.5**. To compare with the results from MINEQL+ and the experimental aqueous TAN analysis, the data were plotted as pH vs. molar concentrations of KOH added. Unlike the titration curves from MINEQL+ modeling and aqueous TAN analysis, the starting pH value is around 6.4, which is higher than the MINEQL+ model and the aqueous TAN analysis (~ pH 3.8). The TAN value from this analysis is 18.96 mgKOH/g, which is lower than the results from the model and aqueous system.

The results from MINEQL+, aqueous TAN analysis, and standard TAN analysis are summarized in **Table 4.7**. The MINEQL+ modeling results agree well with the experimental TAN analysis data for the aqueous system; however, these TAN values were significantly higher than the TAN value obtained from the ASTM D664 standard method. The initial pH value in the standard titration solvent was higher than those in aqueous systems. Different titration curves between aqueous and titration solvent systems also represent the different pK_a values in these systems. Rossini et al. compared different pK_a values of organic compounds in water, acetonitrile, dimethyl sulfoxide, and methanol.¹²¹ The pK_a values of organic compounds changed depending on the solvent used. These differences, as well as different TAN values, indicate that there may be different reactions and activities among the solvent molecules, sample molecules (e.g., acetic acid), and the titrant (i.e., KOH). As mentioned earlier, pK_a values in **Table 4.6** (i.e., the logarithm of acid dissociation constants) that represent dissociation in acid-base reactions, are reported for the aqueous system. Therefore, the TAN values obtain from the MINEQL+ modeling, which is based on the pK_a values, are comparable with results from aqueous TAN analysis. Since the ASTM method uses a mixture of toluene, 2-propanol, and water as a titration solvent, the dissociations of compounds in terms of acid-base reactions are expected to be different from those occurring in the aqueous system. In short, the pK_a values of compounds during the ASTM standard TAN analysis should be different from the known pK_a values for the aqueous system. In order to fully understand these differences, the reactions or activities among the sample and titration solvent molecules need to be further investigated.

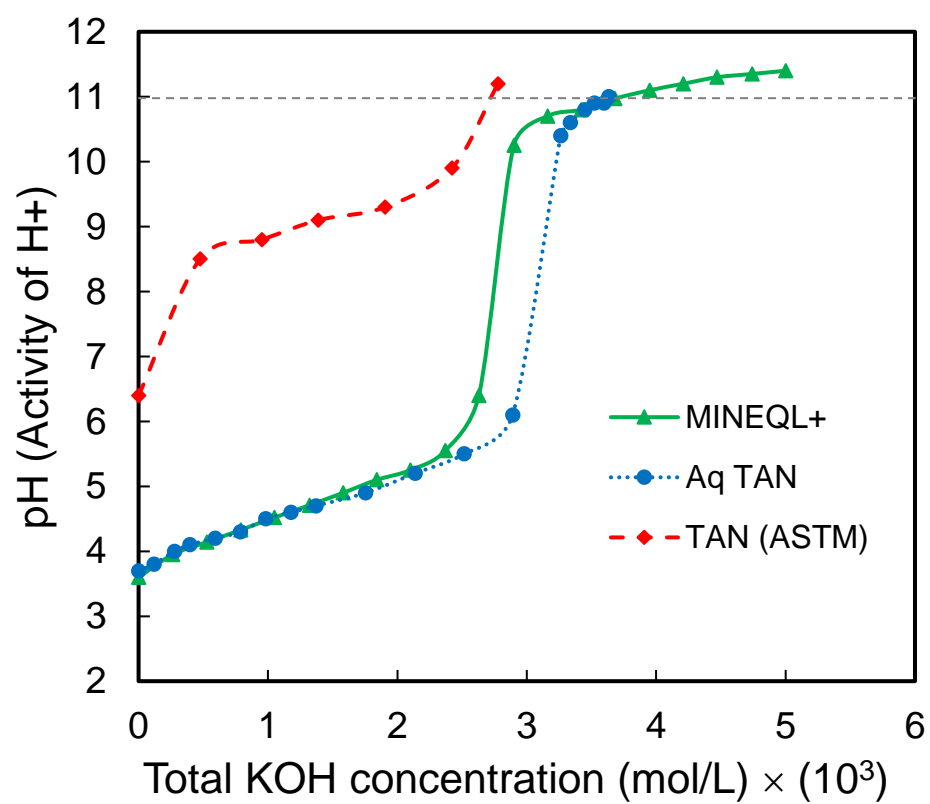


Figure 4.5. Titration curves of acetic acid (2 wt%) solution from MINEQL+ modeling, aqueous titration, and standard titration (ASTM D664).

Table 4.7. Summary of TAN values from MINEQL+ modeling and experimental TAN analysis in aqueous system and the titration solvent from ATSM D664.

	MINEQL+	Aqueous System	ASTM TAN Analysis
Sample (Conc.)	Acetic acid (2 wt%)	Acetic acid (2 wt%)	Acetic acid (2 wt%)
Titration Solvent	Water	Water	Toluene: 2-propanol: water (100:99:1 v.)
TAN (mgKOH/g)	25.45	25.66	18.96
[K+] (mol/L)	3.67×10^{-3}	3.63×10^{-3}	2.68×10^{-3}

4.3.5 Recovery Test on Acetic Acid in Bio-oil Samples

Here, to verify whether the addition of acetic acid can be detected by TAN analysis and whether the various chemical species in switchgrass intermediate-pyrolysis bio-oil affect the TAN analysis, a recovery test was performed. Previously, a recovery test with biodiesel samples was performed by a coulometric titration method⁵². In this study, a similar recovery test, which involved adding known amounts of acetic acid to aqueous bio-oil, was performed to verify whether the TAN analysis can accurately recover the mass of acetic acid added to aqueous bio-oil. Since known amounts of acetic acid were added to the aqueous bio-oil sample, the TAN values of aqueous bio-oil samples should be directly related to the increasing acetic acid concentration.

Results from the TAN and HPLC analyses of aqueous bio-oil samples with added acetic acid are presented in **Figure 4.6**. To incorporate the dilution effect after adding acetic acid solution, 90% of the measured TAN of the aqueous bio-oil (the first data point) was plotted with the measured TAN of aqueous bio-oil samples with acetic acid added, displayed by black circular markers in **Figure 4.6**. The samples (overall 2, 4, and 6 wt% of acetic acid in aqueous bio-oil) were prepared with 90% of aqueous bio-oil and 10% of the acetic acid solution as described in **Section 4.2.2.4**. The first data point (black circle marker) represents the aqueous bio-oil without any acetic acid added, diluted by 10% with water to make it comparable with the other analyzed samples that had acetic acid because those samples contained only 90% aqueous bio-oil. Based on the measured TAN of the aqueous bio-oil and the measured TAN of the acetic acid standard solution from **Section 4.3.3**, the calculated TAN values were estimated using **Equation (4.7)**, similarly to Baig et al.⁵⁰, and represented by a gray dashed line in **Figure 4.6**. The

measured TAN values of aqueous bio-oil samples were slightly higher than the calculated TAN values. The calculated TAN values, however, were still within the range of measured TAN values, which are marked with error bars that indicate the standard deviation. Moreover, the relationship of data points for aqueous bio-oil samples was linear with an R^2 value of 0.9963.

The TAN analysis of aqueous bio-oil samples with added acetic acid led to less than $\pm 5\%$ error, calculated using **Equation (4.2-b)** and based on the calculated TAN from **Equation (4.7)**.

$$\text{Calculated TAN} = [(\text{TAN of AqBO}) \times (\text{wt\% of AqBO}) + (\text{TAN of AA}) \times (\text{wt\% of AA})] / 100 \quad (4.7)$$

AqBO: centrifuged or aqueous bio-oil, AA: acetic acid

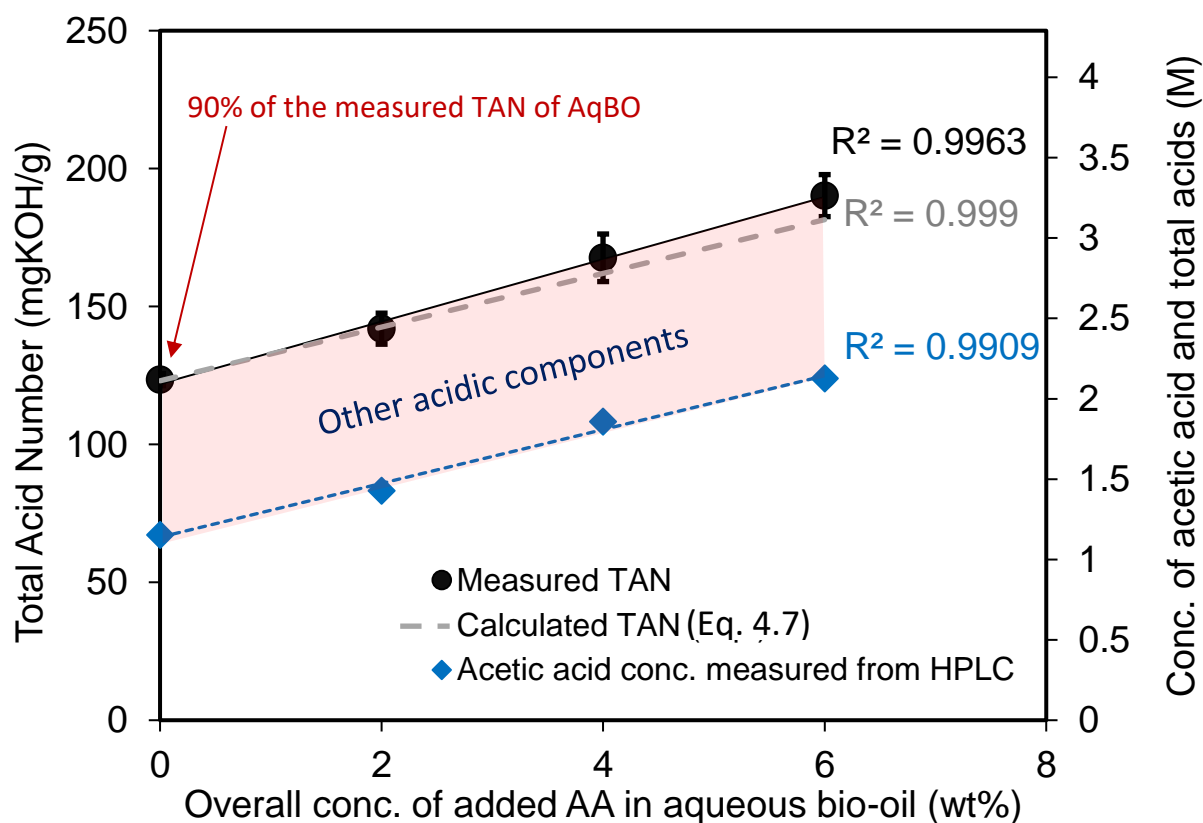
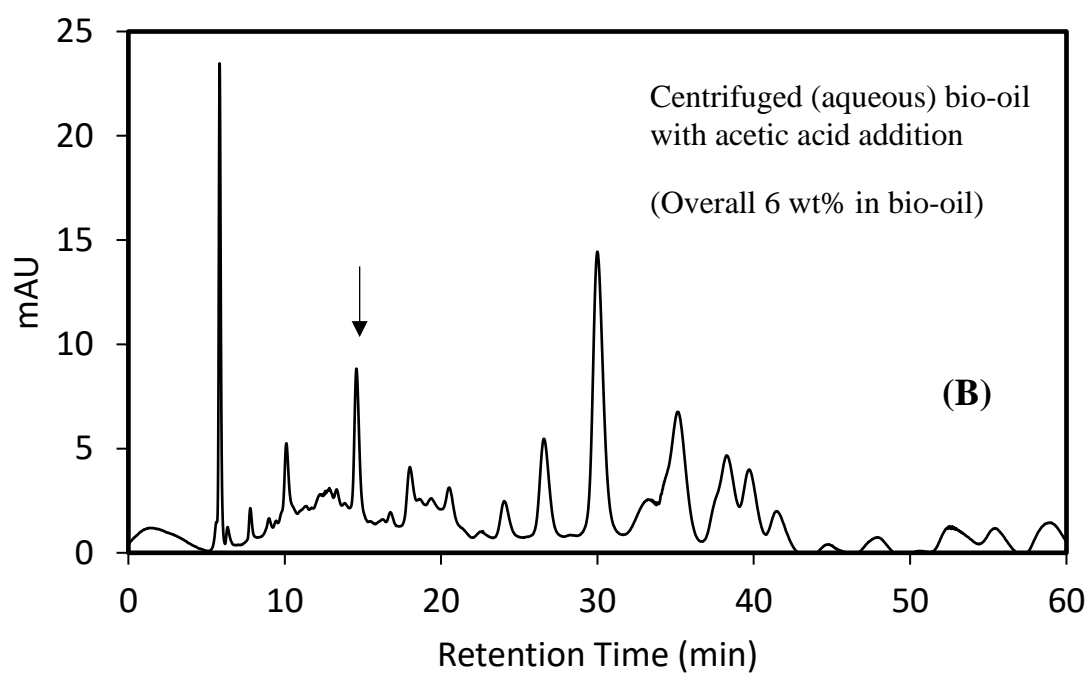
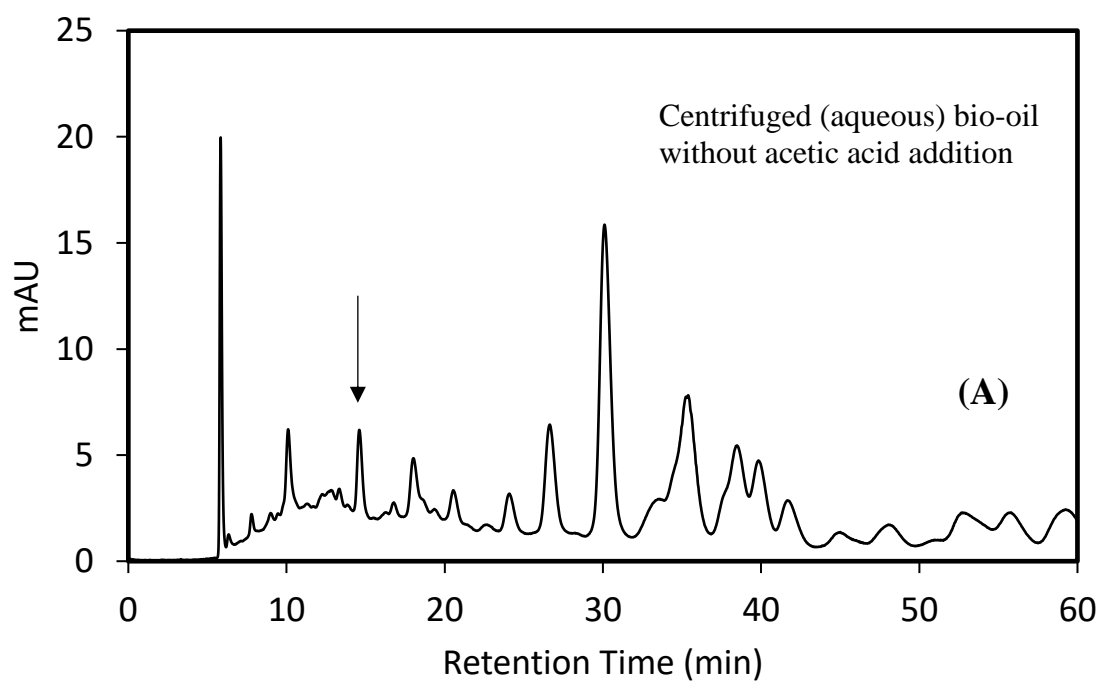


Figure 4.6. Measured TAN values of aqueous bio-oil (90% of the value) and aqueous bio-oil samples with known amounts of acetic acid added, calculated TAN of aqueous bio-oil samples using the measured TAN values of aqueous bio-oil (90%) and acetic acid standard solutions (2, 4, and 6 wt%) through Equation (4.7) (broken line), and measured molar concentrations of acetic acid from HPLC analysis vs. overall concentration of added acetic acid.

Aqueous bio-oil samples were also analyzed by HPLC to quantify the acetic acid concentration. The molar concentrations of acetic acid in aqueous bio-oil samples were also included in **Figure 4.6**. Chromatographs from the HPLC analysis are found in **Figure 4.7**. As expected, the concentration of acetic acid detected by HPLC increased as more acetic acid was added to aqueous bio-oil samples. Using the known relationship between TAN and molar concentrations of acetic acid solutions [**Equation (4.5)**], we converted the molar concentrations of acetic acid in aqueous bio-oil samples to the TAN values, represented as diamond markers in **Figure 4.6**. As shown in **Figure 4.6**, there is good agreement between measured and calculated TAN values for different amounts of acetic acid added. Also, the differences between TAN from total acids and TAN from acetic acid were consistent, as presented with the shaded area. It may be noteworthy to mention that the concentrations of the shaded area may be overestimated because some of these acidic components (e.g., vanillic acid) have a stronger effect on TAN values than monoprotic acids. The consistent difference between total acids and acetic acid indicates that acidic components, other than acetic acid, in aqueous bio-oil contributed similarly to the TAN value because no other acidic components were added besides acetic acid. From the recovery test results, it can be concluded that the presence of various chemicals, other than acetic acid, in bio-oil did not interfere the detection of additional acetic acid. Moreover, the TAN values of bio-oil samples are proportional to the amount of acetic acid present in bio-oil. In other words, the TAN values can reflect the amount of acetic acid—the major acidic component present in switchgrass bio-oil.



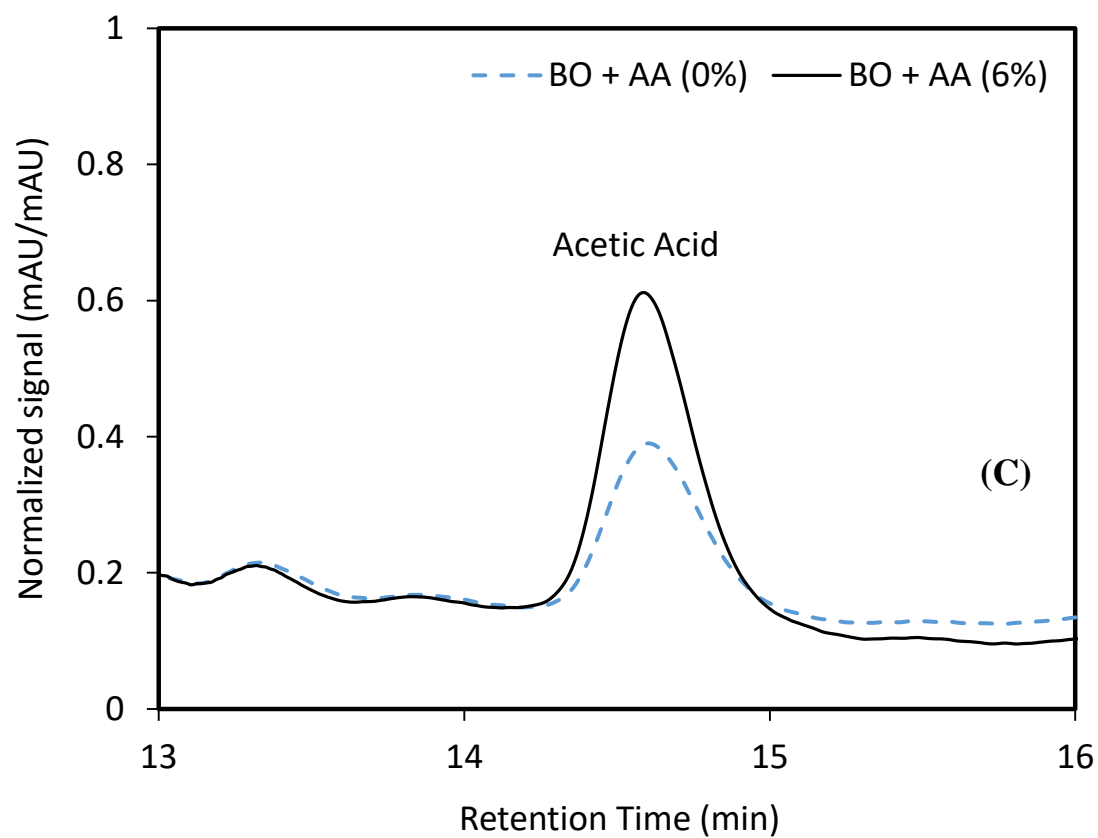


Figure 4.7. (A) HPLC chromatographs of aqueous bio-oil, (B) aqueous bio-oil with added acetic acid (overall 6 wt% in aqueous bio-oil), and (C) zoomed-in view for acetic acid peaks from aqueous bio-oil (dotted line) and aqueous bio-oil with added acetic acid (solid line).

Two major carboxylic acids—acetic and propionic acids—and other chemicals that contribute to the TAN value of aqueous bio-oil are shown in **Figure 4.8**. It was found that 54% of the TAN value of the aqueous bio-oil comes from the acetic acid. According to the chemical analysis of crude switchgrass bio-oil (prior to centrifugation), the propionic acid content in the switchgrass bio-oil is roughly half of the acetic acid content. Thus, assuming that the propionic acid content in the switchgrass bio-oil is half of the acetic acid content, 27% of the TAN value should be attributed to propionic acid. The remaining 20% of the TAN value is due to other chemicals, such as vanillic and syringic acids. The total molar concentration of other chemicals may be smaller than the concentration of propionic and acetic acids, however, as shown in **Section 4.3.3** from the TAN analysis of standard acids, the effects of these chemicals on the TAN value may be important, showing a fraction of 20% in **Figure 4.8**.

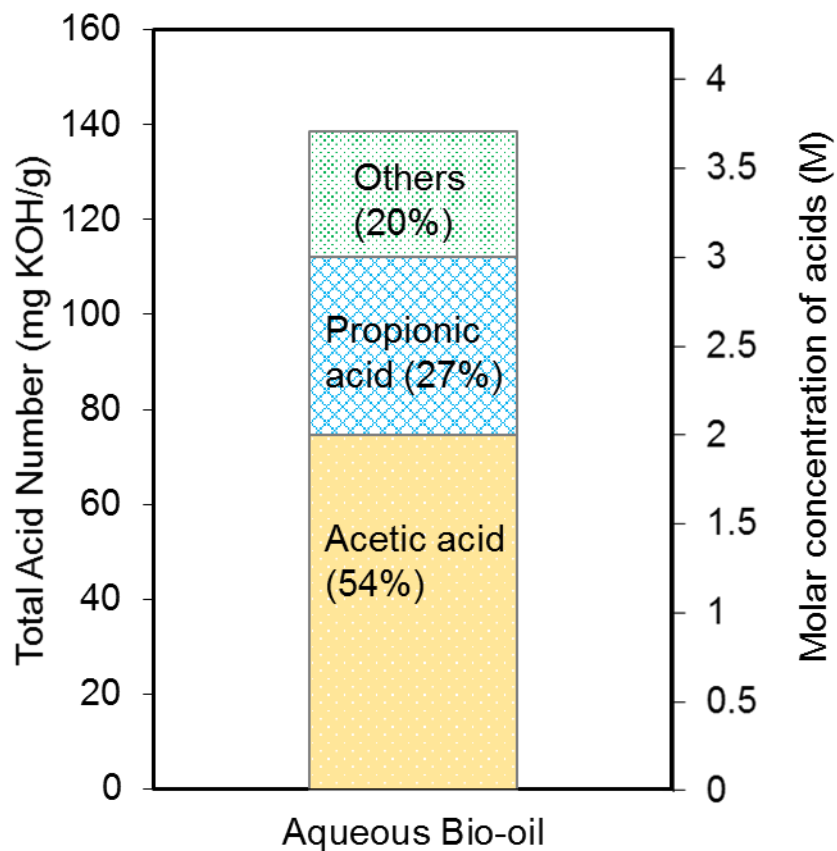


Figure 4.8. Carboxylic acids and other chemical components that contribute to the TAN value of the aqueous bio-oil. The molar concentration equivalent to others (20%) is overestimated in the graph because chemical species other than acetic and propionic acids (e.g., vanillic acid) have a stronger effect on the TAN value than monoprotic carboxylic acids.

4.3.6 *Limitations of the Bio-oil TAN Analysis*

Using a glass pH electrode in organic solvents is not ideal because the electrode is calibrated with aqueous buffer solutions. Moreover, the current standard titration solvent (mixture of toluene, 2-propanol, and water) is suitable for analyzing petroleum products but inappropriate for analyzing bio-oil. For the TAN analysis of bio-oil, other solvents may be appropriate because the standard titration solvent cannot dissolve all the components of bio-oil. Some research groups modified the titration solvent for the TAN analysis to overcome the solubility issue of bio-oil. Different titration solvents used in modified TAN analysis include methanol,¹²² ethylene glycol,¹²³ and acetone.² Currently, there is no standard method available specifically for the bio-oil analysis. As shown in this study, the TAN values would be different depending on the titration solvents. Thus, an alternative solvent for the bio-oil analysis needs to be standardized, and the relationship between the concentrations of acids and the TAN values in such titration solvent needs to be investigated. In addition, measuring or estimating pK_a values of bio-oil components in the alternative titration solvent would be beneficial in understanding the TAN measurement of bio-oil.

4.4 Conclusions

This study investigated how monoprotic and diprotic acid bio-oil components contribute to the overall acidity of bio-oils. An accepted ASTM potentiometric method for KOH titration of a variety of standard samples and switchgrass aqueous bio-oil has been employed to yield the TAN value of the samples. The analyses were performed in triplicate using both aqueous and organic solvents. The bio-oil was separated into aqueous and organic fractions by centrifugation and analyzed accordingly to provide consistent measurements. An appropriate recovery analysis has also been performed.

A similar linear relationship was found between the TAN values vs. molar concentrations of acetic, propionic, and hydroxybenzoic acids, which act as monoprotic acids in the titration solvent. This result indicates that the TAN values can be converted to molar concentrations of total acids if a sample contains only these acids. For more complex organic acid molecules that act as polyprotic acids during the TAN analysis (e.g., vanillic and syringic acids), a higher slope of TAN values vs. molar concentrations was obtained. The higher slope indicates a stronger contribution to the TAN value than that of chemicals acting as monoprotic acids. The stronger effect on the TAN values from vanillic acid is interesting because vanillic acid is considered a weaker acid than acetic and propionic acids. Thus, the TAN analysis does not discriminate between weak and strong acids, since the respective protons are titrable and the pH end point in the TAN analysis is 11. The TAN analysis is, in general, an acceptable method to determine the acidity of bio-oil; however, a comparison of TAN values of different types of bio-oil (produced from different sources of biomass or with different pyrolysis settings) should take into consideration the type and concentration of acidic components in each bio-oil.

In other words, the standard TAN analysis method should be used with caution when we want to compare different bio-oils.

Different titration curves and TAN values found for aqueous systems, both in modeling and experiments, as expected, indicate that the pK_a values in the standard titration solvent are different from those in aqueous systems. These differences indicate different interactions and activities among chemical species analyzed and titration solvent molecules. In a recovery test, the TAN values of aqueous bio-oil samples increased proportionally to the amount of acetic acid added. Thus, the recovery test demonstrated that the TAN value is proportional to the acetic acid content in bio-oil samples, and the various chemicals present in AqBO do not interfere with the TAN analysis. This study demonstrates the usefulness of TAN analysis in determining the acidity of bio-oil before and after treatment and helps us understand how strongly different bio-oil components contribute to the TAN value and, therefore, to the acidity of a complex chemical system like bio-oil.

4.5 Acknowledgments

This chapter involves contributions from coauthors and was submitted for publication: Park, L. K.-E., Liu, J., Yiacoumi, S., Borole, A. P., Tsouris, C. 2017 “Contribution of Acidic Components to the Total Acid Number (TAN) of Bio-Oil.” *Fuel* 200: 171-181.¹²⁴

CHAPTER 5. PH NEUTRALIZATION OF BIO-OIL FROM SWITCHGRASS INTERMEDIATE PYROLYSIS USING PROCESS INTENSIFICATION DEVICES

Despite the potential carbon-neutrality of switchgrass bio-oil, its high acidity and diverse chemical composition limit its utilization. The objectives of this research are to investigate pH neutralization of bio-oil by adding various alkali solutions in a batch system and then perform neutralization using process intensification devices, including a static mixer and a centrifugal contactor. The results indicate that sodium hydroxide and potassium hydroxide are more appropriate bases for pH neutralization of bio-oil than calcium hydroxide due to the limited solubility of calcium hydroxide in aqueous bio-oil. Mass and total acid number (TAN) balances were performed for both batch and continuous-flow systems. Upon pH neutralization of bio-oil, the TAN values of the system increased after accounting for the addition of alkali solution. A bio-oil heating experiment showed that the heat generated during pH neutralization did not cause a significant increase in the acidity of bio-oil. The formation of phenolic compounds during neutralization was initially suspected of increasing the system overall TAN value because some of these compounds (e.g., vanillic acid) act as polyprotic acids and have a stronger influence on the TAN value than monoprotic acids (e.g., acetic acid). However, the amount of phenolics in bio-oil phases did not change significantly after pH neutralization. Process intensification devices provided sufficient mixing and separated the organic and aqueous phases, demonstrating a scale-up route for the bio-oil pH neutralization process.

5.1 Introduction

Switchgrass bio-oil or pyrolysis oil is a biorenewable energy carrier that can have a net zero-carbon footprint. Despite its potential carbon-neutrality, its low pH (high acidity) limits its applications. High acidity is problematic for transport and storage. Bio-oil also has another challenging characteristic; it contains a broad range of chemicals such as acids, sugars, furans, diols, and phenolics that have various chemical and physical properties. To overcome these challenges, various attempts have been made for phase separation of bio-oil using water, aqueous salt solutions,^{125, 126} organic solvents,^{22, 24, 25, 127} switchable hydrophilicity solvents,¹²⁸ and supercritical fluids.^{90, 129, 130}

In addition, phenolic compounds were targeted during phase separation by adding alkali.^{24, 97, 131} Amen-Chen et al.¹³¹ separated phenolic compounds such as phenol, cresols, guaiacol, 4-methylguaiacol, catechol, and syringol from wood tar through a five-stage extraction process by adding alkali and an organic solvent. The solvent extraction successfully isolated phenolics especially under alkaline conditions.¹³¹ More recently, Wang et al.⁹⁷ adjusted the pH of bio-oil to 14, 6.4, and 1.5 by adding alkaline and acid solutions after water extraction. As a result, different phases containing phenolics were separated from bio-oil.⁹⁷ The second and third phases obtained at pH 6.4 and 1.5 contained 94.4% and 54.3% of phenolics, respectively.⁹⁷

According to a previous study, alkali addition can reduce the acidity of bio-oil and also induce organic-phase formation and separation of bio-oil into an organic phase and an aqueous phase.²⁴ The separated aqueous phase contains mostly water, acids, sugars, and other hydrophilic compounds, while the organic phase contains phenolics, furans,

and other hydrophobic compounds.²⁴ It was found that a pH value of 6.0 is optimal for phase separation in a batch system using sodium hydroxide solution, NaOH(aq).²⁴

In this study, different alkaline solutions and solids (sodium hydroxide, calcium hydroxide, and potassium hydroxide) were added to aqueous bio-oil (AqBO) in batch systems. Solid calcium hydroxide [Ca(OH)₂] was tested because of its low cost. Liquid potassium hydroxide, KOH(aq), was examined as it simplifies the total acid number (TAN) balance. Solid potassium hydroxide, KOH(s), was also tested to eliminate water addition.

The use of a static mixer and a centrifugal contactor allows process intensification of the pH neutralization process. The static mixer provides in-line mixing, while the centrifugal contactor provides high-shear mixing followed by phase separation at the exit.⁸² The use of such devices eliminates one or more unit operations such as mixers, reactors, and separators. Process intensification is encouraged in various fields of chemical process engineering.⁷⁵ According to Kiss, process intensification is “a set of innovative principles applied in process and equipment design, which can bring significant benefits regarding process efficiency, lower capital and operation expenses, higher quality of products, fewer wastes, and improved process safety.”¹³² The static mixer and centrifugal contactor used in this study are innovative process devices that can advance process intensification. The centrifugal contactor has recently been demonstrated for continuous biodiesel production.⁶⁶

This work introduces process intensification tools, including the static mixer and centrifugal contactor, to the switchgrass bio-oil neutralization process. TAN and mass balances are performed to analyze changes in the acidity after pH neutralization and

evaluate the process. TAN values, i.e., the amount (in mg) of KOH required to titrate 1 g of a sample to pH 11, is used as the acidity indicator for bio-oil samples. The (American Society for Testing and Materials) ASTM D664 method was performed for TAN analysis with a minor modification in the electrode cleaning method (1-minute water spray method⁵¹). The main objectives of the study were to (1) investigate bio-oil neutralization in a batch system by adding various alkali compounds and (2) compare pH-neutralization in a batch process and in continuous-flow systems in which process intensification devices have been employed.

5.2 Materials and Methods

5.2.1 Production of Bio-oil

As described in previous studies,^{24, 47, 98, 127} bio-oil or pyrolysis oil was produced by intermediate switchgrass pyrolysis with a semi pilot-scale auger pyrolysis system (Proton Power, Inc., Lenoir City, TN, USA) at the Center for Renewable Carbon of the University of Tennessee (UT). Air-dried switchgrass (*Panicum virgatum* L.) from a local producer in eastern Tennessee was used as a biomass feedstock. The details of switchgrass composition and the auger pyrolysis system were described in previous studies.^{24, 47, 98, 127} Intermediate pyrolysis was conducted using 20 kg of switchgrass (less than 2-mm particle size; 7-8 wt% water content) at 550 °C with a residence time of 90 s and feeding rate of 10 kg h⁻¹ in the presence of N₂.

5.2.2 Analysis of Bio-oil Samples

The pH value was measured using a glass electrode (Orion 9172BNWP) with an Accumet pH meter. The ASTM D4377 standard method¹⁰⁰ was followed for the water content analysis using a Schott Titro Line Karl Fischer volumetric titrator. The ASTM D664 standard method⁶² was employed for the TAN measurement with a minor modification on the electrode cleaning procedure (1-min water spray method⁵¹ was used).

Chemical compounds in the bio-oil and neutralized bio-oil phases were identified by gas chromatography with a flame ionization detector (GC-FID), and high-pressure liquid chromatography (HPLC) similarly to previous studies.^{25, 47, 127} GC-FID with an HP-5 column (30 m × 0.32 mm, 0.25-μm film thickness) was used to quantify compounds including 2(5H)-furanone, 1-hydroxy-2-butanone, 1,3-propanediol, 3-methyl-1,2-cyclopentanedione, guaiacol, creosol, 2,6-dimethoxyphenol, and 3-ethylphenol. The detailed settings for GC-FID are available elsewhere.^{25, 47, 127} Identification of compounds was performed by comparing their mass spectra with those from the National Institute of Standards and Technology (NIST) mass spectral data library.

An HPLC (Jasco 2000Plus, Jasco Analytical Instruments, Easton, MD) equipped with an MD-2018 plus photodiode array detector, an RI-2031 Plus intelligent refractive index detector, and an AS-2055 plus autosampler^{10, 11} was used to analyze acids, levoglucosan, hydroxymethylfurfural, furfural, phenol, and 1,2-benzenediol. The HPLC analysis was performed at 50 °C using a Bio-Rad column HPX-87H (300 × 8 mm). The volume of sample injected was 20 μL. The mobile phase was 5 mmol/L sulfuric acid (H₂SO₄) in deionized water. The volumetric flow rate of the mobile phase was 0.6 mL/min. The compounds were quantified using external standards in both the HPLC and GC-FID analyses.

Gas chromatography-mass spectrometry (GC-MS) analysis was performed at the BioAnalytical Mass Spectrometry Facility of the Georgia Institute of Technology. Details of this GC-MS analysis are also available in the literature.²⁴ The GC-MS was equipped with an Agilent DB-5 column (30-m long by 0.25-mm i.d. with a coating thickness of 0.25 μm). The program of the analysis began with the oven at 35 °C, and this temperature was held for 1 minute. Then, it was raised to 300 °C at a heating rate of 15 °C/min, and held at 300 °C for 6.3 minutes. Helium was used as the carrier gas, and samples were prepared with methanol. A sample of 1 μL was injected with a 50:1 ratio split mode, and the inlet temperature was 280 °C. The chemicals were identified by comparing with the mass spectral data library of NIST.

5.2.3 *pH Neutralization of Bio-oil*

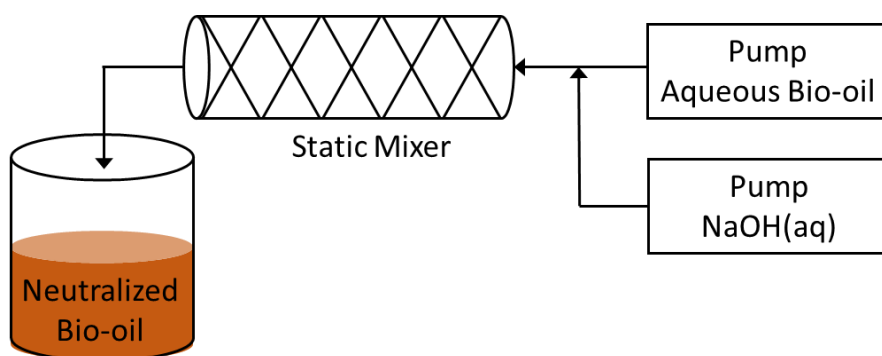
Sodium hydroxide (NaOH) solution (50%), calcium hydroxide $[\text{Ca}(\text{OH})_2]$ powder, and potassium hydroxide (KOH) pellets were purchased from Sigma-Aldrich. KOH solution (50 wt%) was prepared using KOH pellets and deionized water. Crude switchgrass bio-oil from UT was centrifuged using a Beckman Coulter Avanti J-E centrifuge with a JLA 10.500 rotor at 3000 rpm (1673 g) for 30 minutes to remove the highly viscous, solid-like organic phase and obtain the AqBO before neutralization experiments. It should be noted that the fraction of AqBO is approximately 75% of the crude switchgrass bio-oil. For the batch neutralization system, alkali was added to AqBO in a beaker with magnetic stirring. All batch experiments were performed at room temperature. The mixture was centrifuged after reaching equilibrium to separate aqueous and organic phase that were formed during neutralization.

A static mixer (Solid Kynar PVDF 3/8-80-10-12H-2, 8”) purchased from Koflo Corporation, IL, and a centrifugal contactor purchased from CINC Industries, NV, were employed for continuous pH neutralization. Two peristaltic pumps from Dynamax and Cole-Parmer were used to introduce AqBO and NaOH(aq) to the static mixer and the centrifugal contactor (**Figure 5.1 A and B**). For a combined static-mixer and centrifugal-contactor (SM-CC) experiment, AqBO and NaOH(aq) were introduced to the static mixer by the pumps, and the outlet of the static mixer was connected to one of the input ports of the centrifugal contactor (**Figure 5.1C**). The flow rates of AqBO and NaOH(aq) through the reactors were 100 mL/min and 13 mL/min, respectively.

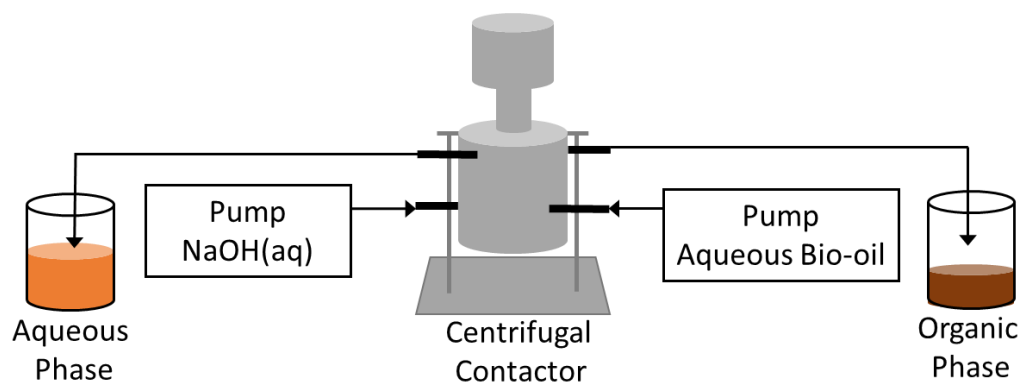
5.2.4 Bio-oil Heating Experiments

For this set of experiments, AqBO obtained after centrifugation was placed in glass bottles. A water bath was set at 70 °C, and the bottles with AqBO were placed in the water bath for 1, 4, and 8 hours. The heated AqBO was then cooled down to room temperature, and TAN analysis of the heated AqBO was performed in triplicates.

(A)



(B)



(C)

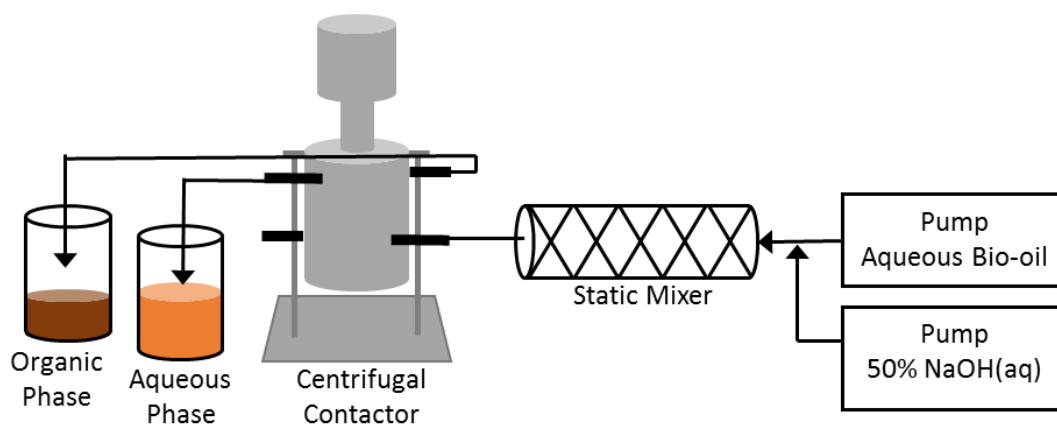


Figure 5.1. Schematics of the pH neutralization experiment using (A) a static mixer, (B) a centrifugal contactor, and (C) both a static mixer and a centrifugal contactor in series.

5.3 Results and Discussion

5.3.1 Batch Systems

5.3.1.1 NaOH(aq) addition in a batch system

NaOH(aq) addition in a batch system has been discussed by Park et al.²⁴ In brief, it was reported that pH neutralization causes the formation of two phases, neutralized bio-oil aqueous phase (NBOAP) and neutralized bio-oil organic phase (NBOOP). The optimal pH for maximum NBOOP volume-fraction was found to be 6.0.²⁴ Maximizing the amount of NBOOP precipitates is significant because NBOOP has potential to be utilized for energy and other applications, such as microbial electrolysis. In addition, removing heavy organic compounds from AqBO as NBOOP is important because those compounds have a negative effect on microbial electrolysis performance. Compared to AqBO, the heating value and oxygen contents improved in the produced organic phase after pH neutralization.²⁴ Based on the previous results, all pH neutralization experiments in this study were designed to reach pH 6.0.

The general schematic of the pH neutralization treatment of AqBO is presented in **Figure 5.2**. The weights and TAN values before and after pH neutralization of bio-oil are organized in **Table 5.1**. The chemical compositions of separated NBOAP and NBOOP from NaOH(aq) addition to AqBO are shown in **Table 5.2**. The ratio values shown in **Table 5.2** were calculated by dividing the weight percent of chemical species in NBOAP by that in NBOOP. Ratio values larger than one indicate that more chemical species were extracted to NBOAP than to NBOOP. Ratio values less than one show that more chemicals were extracted to NBOOP than to NBOAP. The mean ratio values presented in **Table 5.2** represent the average of ratio values obtained from batch and continuous-flow

neutralization experiments. The chromatograms of NBOAP and NBOOP from the GC-MS analysis are found in **Figure 5.3**. NBOAP contained mostly polar compounds (e.g., acetic and propionic acids) and water, whereas NBOOP contained mostly nonpolar compounds (e.g., furans, diols, and phenolics). The concentration of acetic acid—the major acid in switchgrass bio-oil—was much higher in NBOAP than in NBOOP.

The mass and TAN balances over bio-oil neutralization in the batch system using NaOH(aq) are shown in **Figure 5.4**. The mass and TAN balances are demonstrated in **Equations 5.1** and **5.2 (a-d)**. Because the TAN values are in units of mgKOH/g, the amount of NaOH solution added was converted to units of KOH using molecular weights for TAN value of alkali in **Table 5.1** [i.e., $\text{g NaOH(aq, 50\%)/g} \times (56.1056 \text{ g KOH/mol} / 39.997 \text{ g NaOH/mol}) \times 1000 \text{ mg/g} \times 50\% = 701.4 \text{ mgKOH/g}$]. TAN values of alkali in **Table 5.1** are negative because alkali has been added to the system resulting in a negative effect on the overall TAN value of the system. Unexpectedly, the TAN balance did not close. Further discussion on non-balanced TAN is found in later sections.

Mass balance

$$[\text{wt. of AqBO (g)}] + [\text{wt. of alkali (g)}] = [\text{wt. of NBOAP (g)}] + [\text{wt. of NBOOP (g)}] + [\text{Loss (g)}] \quad (5.1)$$

TAN Balance

Initial TAN (mgKOH):

$$[\text{wt. of AqBO (g)}] \times [\text{TAN of AqBO}] - [\text{wt. of alkali (g)}] \times [\text{conversion (if necessary)}] \quad (5.2-a)$$

Final TAN (mgKOH):

$$[\text{wt. of NBOAP (g)}] \times [\text{TAN of NBOAP}] + [\text{wt. of NBOOP (g)}] \times [\text{TAN of NBOOP}]$$

(5.2-b)

Difference (mgKOH): (Final TAN) – (Initial TAN) **(5.2-c)**

Change of TAN (%): (Difference) / (Initial TAN) \times 100% **(5.2-d)**

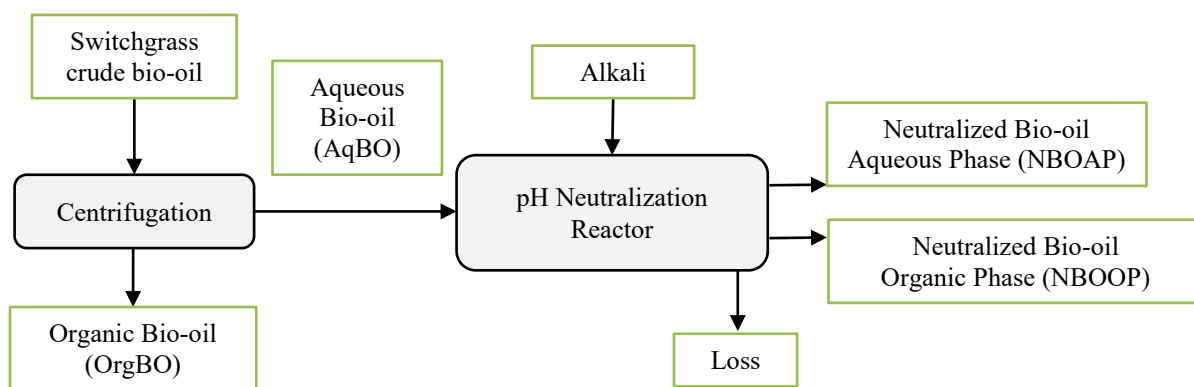
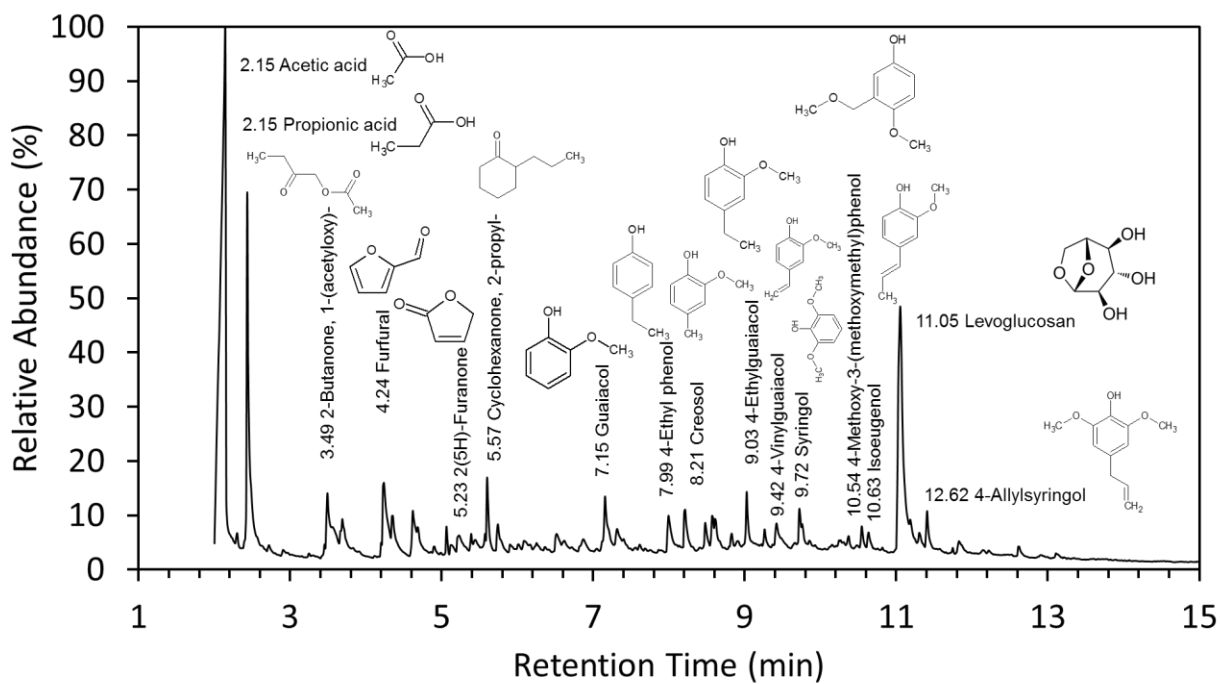
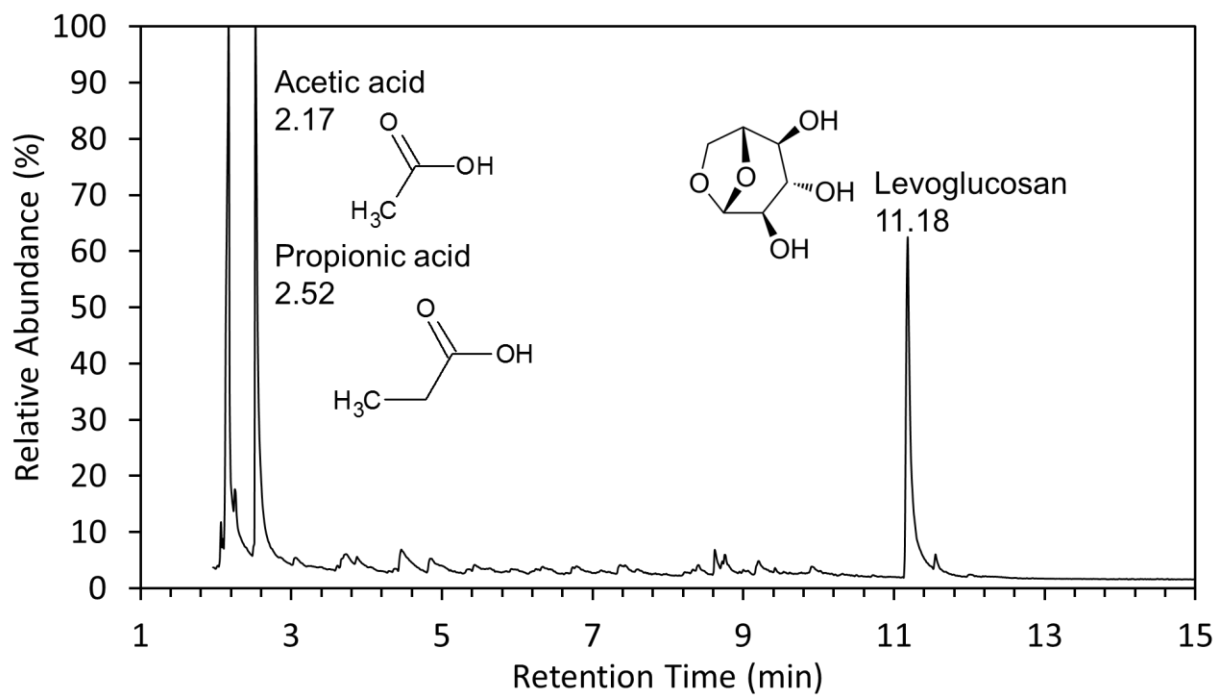


Figure 5.2. Schematic of pH neutralization of AqBO from switchgrass crude bio-oil.

(A)



(B)



(C)

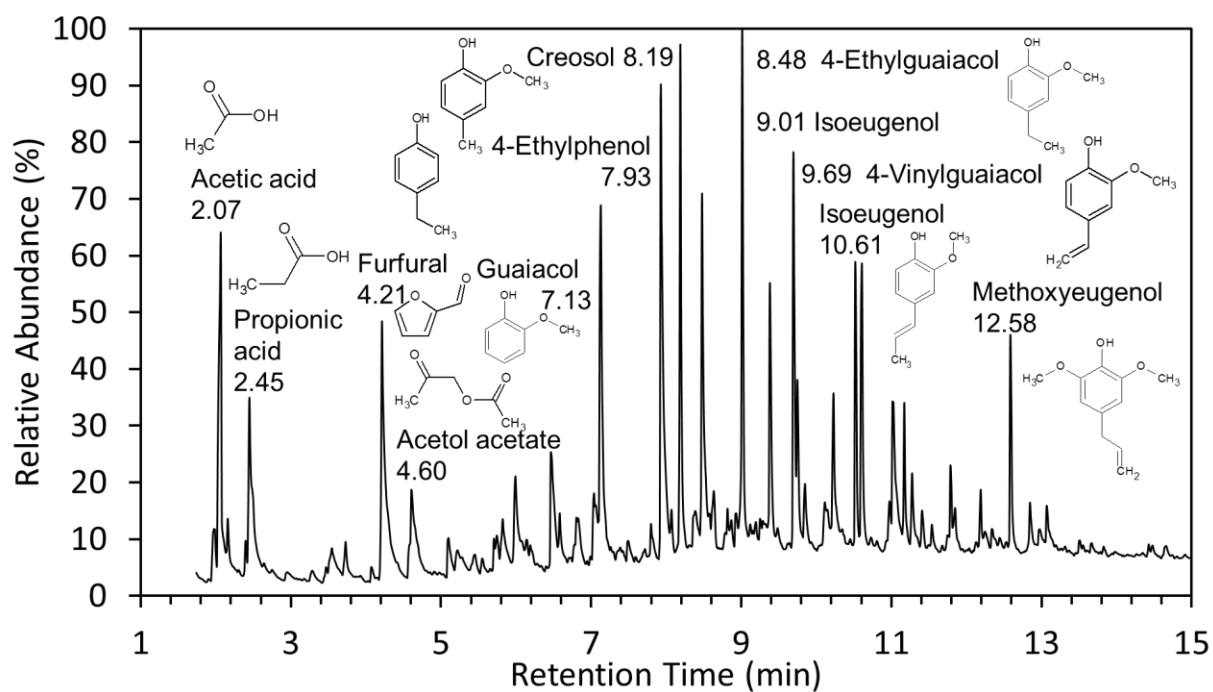


Figure 5.3. Chromatograms of (A) AqBO, (B) NBOAP, and (C) NBOOP from the GC-MS analysis.

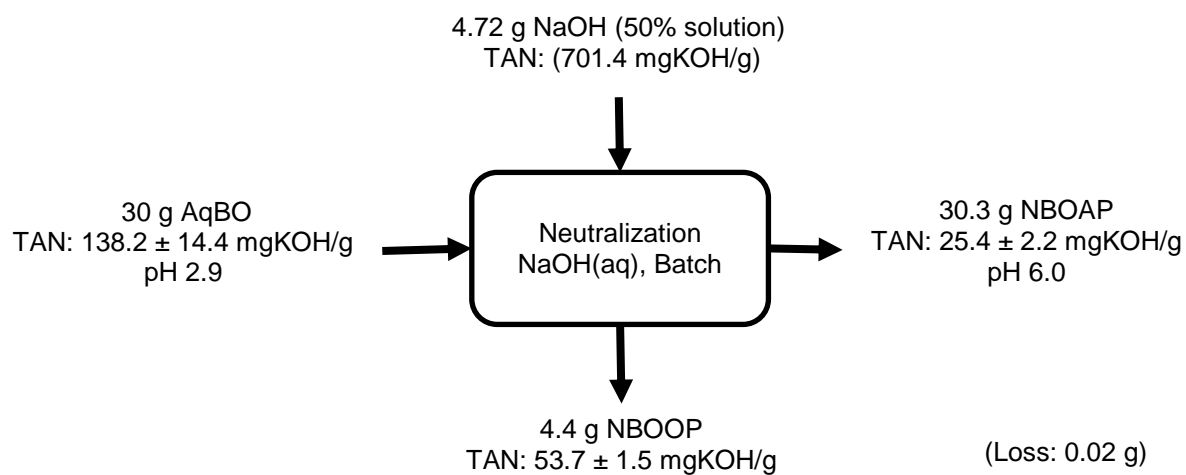


Figure 5.4. Mass and TAN balances over pH neutralization with NaOH(aq) in a batch system.

Table 5.1. Mass and TAN balances of pH neutralization of AqBO.

Alkali	Experimental Setting	AqBO		Alkali		Initial TAN (Eq. 2-a) mgKOH	NBOAP		NBOOP		Loss Weight (g)	Final TAN (Eq. 2-b) mgKOH	Difference (Eq. 2-c) mgKOH	Change of TAN (Eq. 2-d) (%)
		Weight (g)	TAN (mgKOH/g)	Weight (g)	TAN (mgKOH/g)		Weight (g)	TAN (mgKOH/g)	Weight (g)	TAN (mgKOH/g)				
NaOH (aq)	Batch	30	138.2±14.4	4.72	-701.4	847.4	30.3	25.4±2.2	4.4	53.7±1	0.02	1005.9	158.5	20.4
Ca(OH) ₂ (s)	Batch	30	138.2±14.4	2.285	N/A	N/A	25.39	N/A	3.21	N/A	3.685	N/A	N/A	N/A
KOH (aq)	Batch	33.96	138.2±14.4	7.55	-3775.0 ^a	931.9	36.12	36.3±0.4	2.61	51.7±1	2.78	1446.1	514.2	57.5
KOH (s)	Batch	34.03	138.2±14.4	3.45	-3447.6 ^b	1269.0	32.43	39.5±0.7	3.14	52.3±0	1.91	1445.2	176.2	15.1
NaOH (aq)	SM	960.55	138.2±14.4	151.5	-701.4	26485	979.15	27.8±0.7	123.68	43.9±3	9.22	32649.9	6164.0	23.3
NaOH (aq)	CC	955.05	138.2±14.4	147.7	-701.4	28391.1	945.29	23.9±0.1	121.92	45.3±1.6	35.54	28117.8	-273.3	-1.0
NaOH (aq)	SM-CC	1111	128.0±3.6 ^c	171	-701.4	22268.6	1095	21±2	81	32±1	106	25587.0	3318.4	14.9

AqBO: aqueous bio-oil obtained after centrifuging crude bio-oil (AqBO was used in neutralization experiments)

OrgBO: organic bio-oil obtained after centrifuging crude bio-oil

NBOAP: neutralized aqueous bio-oil phase, NBOOP: neutralized organic bio-oil phase

SM: static mixer, CC: centrifugal contactor

^a Calculated based on the amount of solution added and the density of the KOH solution (50%)

(5 mL KOH × 1.51 mg/mL × 50% × 1000 mg/g = 3775 mgKOH)

^b Calculated based on the amount of KOH solid added (3.4476 g × 1000 mg/g = 3.4476 mgKOH)

^c Different batch of bio-oil produced at slightly different condition.

Table 5.2. Total acid numbers, water contents, and chemical composition of bio-oil samples before and after pH neutralization.

	Initial			Batch System									Continuous Flow System							Mean Ratio
Weight%	AqBO	OrgBO	Ratio	NaOH(aq)		Ratio	KOH(aq)		Ratio	KOH(s)		Ratio	SM		Ratio	CC		Ratio		
				NBOAP	NBOOP		NBOAP	NBOOP		NBOAP	NBOOP		NBOAP	NBOOP		NBOAP	NBOOP			
TAN (mgKOH/g)	138.2 ±14.7	121.81	-	25.44 ± 2.19	54.29 ± 1.70	-	36.26 ± 0.40	51.65 ± 1.13	-	39.46 ± 0.74	52.25 ± 0.63	-	27.80 ± 0.78	43.93 ± 3.07	-	23.90 ± 0.11	45.34 ± 1.63	-	-	
Water	43.65	15.18	2.88	52.09	21.18	2.46	53.1	18.55	2.86	49.96	21.46	2.33	52.17	16.93	3.08	53.69	17.73	3.03	2.75	
Levogluconan	9.19	0.72	12.76	6.39	0.56	11.41	6.11	1.01	6.05	6.62	1.52	4.36	7.76	0.52	14.92	6.44	0.59	10.92	9.53	
Acetic acid	8.06	6.16	1.31	8.93	2.12	4.21	7.63	3	2.54	8.51	3.54	2.40	10.01	2.17	4.61	7.73	2.35	3.29	3.41	
Propionic acid	3.57	N/M	H/N	3.07	N/M	H/N	2.54	N/M	H/N	2.76	N/M	H/N	4.03	N/M	H/N	3.29	N/M	H/N	H/N	
1-Hydroxy-2-butanone	1.08	0.86	1.26	0.43	0.63	0.68	0.52	0.22	2.36	0.65	0.22	2.95	0.49	0.72	0.68	0.52	0.85	0.61	1.46	
1,3-Propanediol	0.07	0.06	1.17	0.01	0.02	0.50	0.13	0.5	0.26	0.19	0.49	0.39	0.01	0.03	0.33	0.01	0.03	0.33	0.36	
HMF	0.58	0.19	3.05	0.06	0.21	0.29	0.02	0.32	0.06	0.01	0.3	0.03	0.16	0.31	0.52	0.06	0.34	0.18	0.21	
Furfural	0.4	1.35	0.30	0.03	1.12	0.03	0.07	0.46	0.15	0.09	0.42	0.21	0.04	1.34	0.03	0.04	1.55	0.03	0.09	
2(5H)-Furanone	0.41	0.26	1.58	0.08	0.14	0.57	0.04	0.1	0.40	0.06	0.1	0.60	0.1	0.21	0.48	0.08	0.32	0.25	0.46	
3-Methyl-1,2-cyclopentanedione	0.17	0.25	0.68	0.05	0.25	0.20	0.08	0.36	0.22	0.11	0.34	0.32	0.06	0.3	0.20	0.06	0.32	0.19	0.23	
1,2-Benzenediol	0.42	0.61	0.69	0.28	0.66	0.42	0.26	0.68	0.38	0.3	0.61	0.49	0.27	0.78	0.35	0.27	0.83	0.33	0.39	
Phenol	0.12	0.31	0.39	0.05	0.35	0.14	0.05	0.42	0.12	0.08	0.4	0.20	0.05	0.47	0.11	0.05	0.53	0.09	0.13	
Guaiacol	0.13	0.29	0.45	0.04	0.38	0.11	0.05	0.44	0.11	0.06	0.41	0.15	0.05	0.46	0.11	0.05	0.5	0.10	0.11	
3-Ethylphenol	0.15	0.74	0.20	0.05	0.75	0.07	0.04	0.94	0.04	0.06	0.87	0.07	0.05	0.89	0.06	0.05	0.96	0.05	0.06	
2-Methoxy-4-methylphenol (creosol)	0.24	0.47	0.51	0.12	0.42	0.29	0.05	0.09	0.56	0.07	0.1	0.70	0.1	0.52	0.19	0.1	0.65	0.15	0.38	
2,6-Dimethoxyphenol	0.11	0.33	0.33	0.05	0.47	0.11	0.05	0.6	0.08	0.05	0.55	0.09	0.05	0.54	0.09	0.05	0.57	0.09	0.09	
Identified (wt%)	68.34	27.78	-	71.72	29.27	-	70.73	27.69	-	69.59	31.32	-	75.39	26.18	-	72.48	28.13	-	-	
Unidentified (wt%)	31.66	72.22	-	28.28	70.73	-	29.27	72.31	-	30.41	68.68	-	24.61	73.82	-	27.52	71.87	-	-	

Ratio = aqueous phase: organic phase

N/M: not measureable

H/N: high number (>>1)

5.3.1.2 Ca(OH)₂ powder addition in a batch system

AqBO (30 g) was mixed with Ca(OH)₂(s) to examine the feasibility of using Ca(OH)₂, which is cheaper than NaOH, for large-scale neutralization of bio-oil. As the amount of Ca(OH)₂ increased, the pH value increased as shown in **Figure 5.5**. Similar with NaOH, Ca(OH)₂ also separated bio-oil to NBOAP and NBOOP at pH 6. The final pH value of neutralized bio-oil (NBO) from Ca(OH)₂ powder addition was 6.0 at room temperature. Compared to the NaOH batch experiment, the amount of NBOOP (9.9 wt%) formed was smaller in the Ca(OH)₂ addition experiment. Detailed data on the weight of each phase are found in **Table 5.1**. It is also noteworthy that the added Ca(OH)₂ powder was not completely dissolved in AqBO. The Ca(OH)₂ powder seemed to form clusters in AqBO. Therefore, the amount of Ca(OH)₂ to reach the pH shown in **Figure 5.5** has probably been overestimated because not all Ca(OH)₂ powder added contributed to pH neutralization of bio-oil. Furthermore, the amount of NBOOP formed could also be overestimated because the undissolved Ca(OH)₂ powder precipitated in the NBOOP phase. The same batch experiment was also performed with sonication and at a different temperature to promote dissolution of Ca(OH)₂. Added Ca(OH)₂ powder could not be dissolved completely in AqBO even with sonication, and an attempt to increase its solubility by raising the temperature also failed because it was later found that the solubility of Ca(OH)₂ decreases as the temperature increases. Although Ca(OH)₂ can still be used on a larger scale for economical pH neutralization, due to its incomplete dissolution that would cause inaccuracies in the measurements, it was excluded from further experiments in this study. The TAN and chemical composition analyses of

NBOAP and NBOOP from $\text{Ca}(\text{OH})_2$ addition were not pursued because $\text{Ca}(\text{OH})_2$ could not be fully dissolved in AqBO resulting in a nonhomogeneous NBOOP.

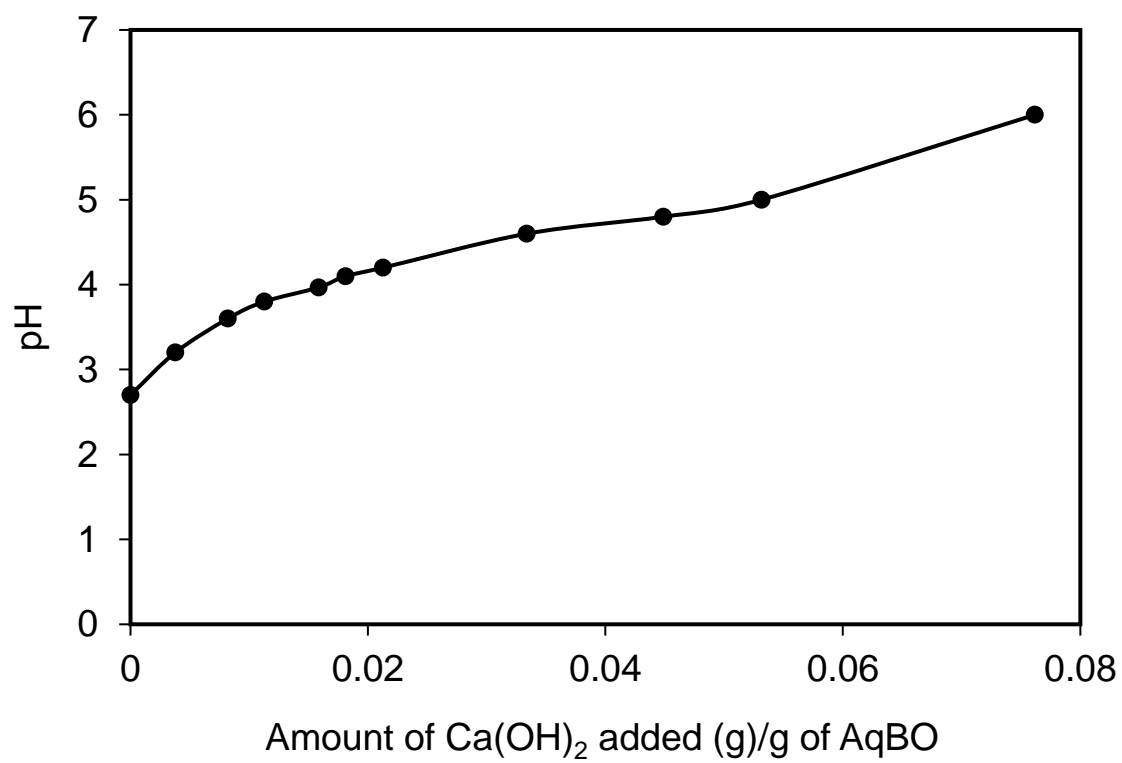


Figure 5.5. Measured pH values of bio-oil after adding Ca(OH)_2 powder.

5.3.1.3 KOH(aq) addition in a batch system

To simplify the TAN balance calculation by avoiding the conversion of different alkali solutions to KOH during calculation, KOH(aq) was added to neutralize AqBO to pH 6. Chemical compositions of the separated NBOAP and NBOOP from the KOH(aq) addition experiment are found in **Table 5.2**. Similar to the NaOH(aq) addition experiments, NBOAP contained water (53.1 wt%) and hydrophilic compounds such as levoglucosan (6.11 wt%), acetic acid (7.63 wt%), and propionic acid (2.54 wt%), while NBOOP contained furans (0.88 wt%), diols (1.18 wt%), phenolics (1.95 wt%), and many unidentified compounds (72.31 wt%). The water content of NBOAP (53.1 wt%) was much higher than that of NBOOP (18.55 wt%). Even though NBOAP contained more acids (e.g., acetic and propionic acids) than NBOOP, the TAN value of NBOAP (36.26 ± 0.4 mgKOH/g) was lower than that of NBOOP (51.56 ± 1.13 mgKOH/g).

The mass and TAN balances over pH neutralization using KOH(aq) are shown in **Table 5.1**. The TAN value for added KOH(aq) in **Table 5.1** was calculated based on the amount of solution added and the density of the KOH solution [the concentration of the solution and the unit conversion ($5 \text{ mL} \times 1.51 \text{ mg/mL} \times 50\% \times 1000 \text{ mg/g} = 3775 \text{ mgKOH}$)]. The unit of TAN for alkali found in **Table 5.1** for KOH(aq) is mgKOH. The loss of 2.78 g (**Table 5.1**) is due to the residue (mostly organic phase) remaining in the beaker after transferring the NBO to the centrifuge tubes for phase separation. Also, there may be some volatile species that escaped from the system due to the heat generated during pH neutralization.

The TAN balance was performed as shown in **Equation 5.2** and **Table 5.1** with the assumption that acidic components are conserved during neutralization. Similar to the

NaOH(aq) addition case, however, the overall final TAN values from NBOAP and NBOOP were higher than the overall initial TAN values from AqBO and added KOH(aq). There was 57.5% increase in the overall TAN values after pH neutralization of AqBO using KOH(aq). One potential reason for the increased TAN could be changes in the system due to exothermic reactions during neutralization. It was thought that the heat generated from KOH addition might be causing aging. Accelerated aging techniques, including heating, are commonly used to study the stability of bio-oil.¹³³⁻¹³⁸ One common accelerated aging condition is heating bio-oil at 80 °C for 24 hours.¹³⁶⁻¹³⁸ During neutralization, the temperature of the system reaches a temperature of 70–75 °C. The heat generated from pH neutralization is dissipated to the room atmosphere within a few hours. Even though the generated heat lasts for a relatively short time, it was initially thought that the elevated temperature of the NBO has a similar accelerated aging effect on bio-oil. Thus, a bio-oil heating experiment has been performed, and the results with discussion can be found in **Section 5.3.3**.

5.3.1.4 KOH(s) pellet addition in a batch system

It is known that addition of water causes phase separation of bio-oil.^{20-22, 139} Previous pH neutralization experiments using NaOH(aq)²⁴ and KOH(aq) did not differentiate the effect of adding water from that of adding base. Therefore, a batch experiment using KOH pellets was performed to differentiate the effect of alkaline solution addition from that of water addition. KOH(s) was added to AqBO (30 mL) to increase the pH value to 6.0. Due to the finite size of KOH pellets, however, it was difficult to reach exactly pH 6.0. The pH value of the separated NBOAP was 6.1.

As shown in **Table 5.1**, the amounts of aqueous and organic phases were close to the amounts of the two phases formed in the previous batch KOH(aq)-addition experiment. The amounts and TAN values of phases before and after KOH(s) addition are summarized in **Table 5.1**. In **Table 5.1**, the TAN value of KOH(s) was obtained from the conversion from grams to milligrams of KOH. Thus, the unit of TAN for alkali found in **Table 5.1** for KOH(s) is mgKOH.

Chemical compositions of the separated NBOAP and NBOOP from the KOH(s)-addition experiment are found in **Table 5.2**. Similar to other alkali-addition experiments, NBOAP had water (49.96 wt%) and hydrophilic compounds such as levoglucosan (6.62 wt%), acetic acid (8.51 wt%), and propionic acid (2.76 wt%), while NBOOP had furans (0.82 wt%), diols (1.10 wt%), phenolics (2.33 wt%), and many unidentified compounds (68.68 wt%). The water content of NBOAP (49.96 wt%) was much higher than that of NBOOP (21.46 wt%). Even though NBOAP contained more acetic and propionic acids than NBOOP, the TAN value of NBOAP (39.46 ± 0.74 mgKOH/g) was lower than that of NBOOP (52.25 ± 0.63 mgKOH/g). Due to the addition of KOH, however, both the TAN values of NBOAP and NBOOP were much lower than the TAN value of the initial AqBO. Also, it can be observed in **Table 5.2** that the TAN value of NBOAP after neutralization with KOH(s) is slightly higher than the corresponding value after neutralization with KOH(aq) or NaOH(aq) in which water was added with the base diluting mostly the NBOAP.

Analogous to previous results, the TAN balance over KOH(s) addition did not close as shown in **Table 5.1**. The final TAN value was 15.1% higher than the initial value in the system, and the TAN value of NBOOP was greater than that of NBOAP. The

increase in TAN values indicates that some acidity was added to the system by the products of neutralization reactions. The non-balanced TAN is further discussed in **Section 5.3.4**.

5.3.2 *Continuous-Flow Systems with NaOH Solution*

5.3.2.1 Static mixer

A static mixer experiment for pH neutralization of bio-oil was performed first because the static mixer is the simplest reactor for a continuous process. Compared to two-phase reactors, the static mixer reactor does not require energy to mix the bio-oil and alkaline solution and eliminates the need for a reactor vessel. The experimental arrangement for the static mixer experiment is shown in **Figure 5.1 (A)** and **Figure A5** from **Appendix**. The flow-rate ratio of AqBO and NaOH(aq) was selected based on the experimental conditions and results of the corresponding batch experiments to yield a pH value of 6.0 for NBOAP. Details of the experimental conditions and results are summarized in **Table 5.3**.

AqBO and NaOH(aq) were introduced and mixed in the static mixer. The temperature of the NBO at the output was 65 °C at the time of collection. The NBO had been cooled down to room temperature after two hours. After one day of gravitational settling, NBOOP accumulated at the bottom of the bottle. Gravitational settling, however, for one day was not enough to separate completely NBOOP from NBOAP. When a sample obtained from the top (mostly NBOAP) was centrifuged, NBOOP accumulated at the bottom. Therefore, for effective separation of the two phases after pH neutralization with a static mixer, centrifugation or longer settling time is needed.

The weight and TAN values of phases after pH neutralization using the static mixer are found in **Table 5.1**. Chemical compositions of both NBOAP and NBOOP obtained after centrifugation of the output of the static mixer were analyzed, and results are shown in **Table 5.2**. Results were very similar with those from NaOH(aq) addition in the batch system. NBOAP from the static mixer experiment contained mostly water and polar compounds such as acetic acid, propionic acid, and levoglucosan. NBOOP contained phenolics, furans, diols, and many other unidentified chemicals. With the higher content of acetic and propionic acids, NBOAP should have a higher TAN value than that of NBOOP. The TAN value of NBOAP, however, was lower than that of NBOOP. This behavior was initially speculated to be due to the formation of phenolic acids that act as polyprotic acids (e.g., vanillic acid) in NBOOP because it was previously¹²⁴ revealed that weak phenolic acids have a higher influence on the TAN value than acids such as acetic and propionic acids.

The mass and TAN balances for the static mixer experiment were summarized in **Table 5.1**. There were some losses due to residual liquid remaining inside the static mixer and bottles. Overall, the mass balance closed while the TAN balance did not close. The difference between the initial and final TAN values amounted to 23.3% of the initial TAN values. It is noteworthy that the TAN balance did not include the loss (9.22 g). If the loss was included in the TAN balance, the difference would have been greater than the currently calculated value. The non-balanced TAN over pH neutralization is further discussed in **Section 5.3.4**.

Table 5.3. Experimental conditions and results of the static mixer and centrifugal contactor experiments.

	Static Mixer	Centrifugal Contactor
Pump 1 (AqBO) (mL/min with water)	100	100
Pump 2 (NaOH) (mL/min with water)	13	13
Duration (min:sec)	08:16.9	08:32.4
Initial pH of AqBO	2.9	2.8
AqBO added (g)	960.55	955.05
NaOH added (mL)	100	97.5
NaOH added (g)	151.5	147.7
Final pH of NBO (room temp.)	6.0	6.0
NBO (g)	1104.69	1067.21
NBOAP (g)	979.15	945.29
NBOOP (g)	123.68	121.92

5.3.2.2 Centrifugal Contactor

In this part of the study, pH neutralization of bio-oil was performed using a centrifugal contactor as shown in **Figure 5.1 (A)** and **Figure A6** from Appendix. Peristaltic pumps with the same setting as those for the static mixer experiments were used to introduce NaOH(aq) and AqBO into the centrifugal contactor. The centrifugal contactor has a shear-mixing zone and a rotor where the centrifugal force causes phase separation. Thus, this system provides mixing for bio-oil neutralization to form NBOAP and NBOOP and then separates the two phases at the exit of the contactor. Due to the relatively low volume of AqBO used in this experiment, however, only the NBOAP product exited the contactor/reactor. The organic phase (NBOOP), which was the heavy phase and had much lower volume than that of NBOAP, accumulated in the contactor and was drained after the completion of the neutralization experiment. NBOOP is very viscous but, due to the exothermic reactions in the mixing zone of the contactor, the temperature of the liquid increased, thus reducing the viscosity of the liquid.

The NBO from the centrifugal contactor was centrifuged to further separate NBOAP and NBOOP for chemical analysis. The chemical compositions of NBOAP and NBOOP are shown in **Table 5.2**. Similar to the batch and static mixer experiments, NBOAP was found to contain mostly water, acids, and sugars, while NBOOP contained phenolics, furans, and diols. Based on the chemical analysis, the results from the static mixer and the centrifugal contactor were similar with those from the batch experiments. This consistency in the chemical compositions of NBOAP and NBOOP after pH neutralization in both batch and continuous-flow systems indicates that both the

centrifugal contactor and the static mixer provide sufficient mixing. Thus, these devices can be employed to scale up the pH neutralization process of bio-oil.

The mass and TAN balances were carried out as described in **Equations 5.1** and **5.2 (a-d)** and summarized in **Table 5.1**. The difference between the initial and final TAN values obtained from **Equations 5.2 (a-d)** seems to be small; however, due to the loss (35.55 g) in the system, a significant portion of bio-oil was not included in the TAN balance. A large fraction of this loss was due to NBOOP remaining inside the centrifugal contactor after draining. If this loss was accounted for in the TAN balance, assuming the TAN value is between 23.9 and 45.3 mgKOH/g (TAN values of NBOAP and NBOOP, respectively), the difference between the initial and final TAN values would be +2% to +5%. Although the difference between initial and final TAN from the centrifugal contactor was smaller than the batch and static mixer experiments, it can still be concluded that the overall TAN values after pH neutralization increased.

This increase in the overall TAN values of the system was consistent in all pH neutralization experiments. As mentioned earlier, it was initially assumed that the heat generated during pH neutralization raised the overall TAN values of the system. Thus, a bio-oil heating experiment was performed as discussed in **Section 5.3.3**. Further investigation on the increase in the overall TAN values is discussed in **Section 5.3.4**.

5.3.2.3 Combined Static Mixer – Centrifugal Contactor (SM-CC) in Series

It has been established that, after pH neutralization, centrifugation will be needed for phase separation of NBOAP and NBOOP. The centrifugal contactor can be used for both neutralization and phase separation. In this part of the study, the static mixer was placed before the centrifugal contactor to increase the contact time between AqBO and

alkali solution and thus investigate the influence of contact time on the neutralization process.

The static mixer and the centrifugal contactor were connected in series, as shown in **Figure 5.1 (C)** and **Figure A7** from Appendix, to perform pH neutralization using the same experimental conditions as those used in the previous continuous-flow experiments. The behavior of the centrifugal contactor was the same as if the AqBO and alkali solution were fed directly into the centrifugal contactor from different ports, indicating that no additional contact time was necessary. Due to the small volume of bio-oil used, NBOAP was collected at the exit of the contactor while NBOOP accumulated inside the contactor and drained at the end of the experiment.

As shown in **Table 5.1**, the TAN values of NBOAP and NBOOP obtained from the combined SM-CC system were consistent with those from the previous batch and continuous-flow systems. The TAN values in the overall system increased by 14.9% after pH neutralization, which is consistent with observations from the previous batch and continuous-flow systems.

5.3.3 *Bio-oil Heating Experiments*

As bio-oil ages, its acidity and moisture content increase, and phase separation occurs.^{135, 136, 138} Due to the heat generated during pH neutralization, bio-oil may experience a similar behavior with that observed during aging. Heating is a commonly used method to induce accelerated aging of bio-oil.¹³³⁻¹³⁸ To simulate the heating effect during pH neutralization, AqBO without alkali added was heated at 70 °C for eight hours. Changes in TAN values of the heated AqBO over eight hours are shown in **Figure 5.6**. After one hour, the TAN of the heated bio-oil was 141.6 ± 3 mgKOH/g, which represents

a slight increase over the initial TAN value of 138.2 mgKOH/g. This increase, however, is not significant enough to explain the increase in the TAN value observed after the pH neutralization. Moreover, the TAN value of the heated AqBO was 138.3 ± 1.1 mgKOH/g and 139.8 ± 2.1 mgKOH/g after four and eight hours of heating, respectively. Based on the results of the heating experiment, it can be concluded that the heat generated during pH neutralization is not the major reason for the increase in acidity.

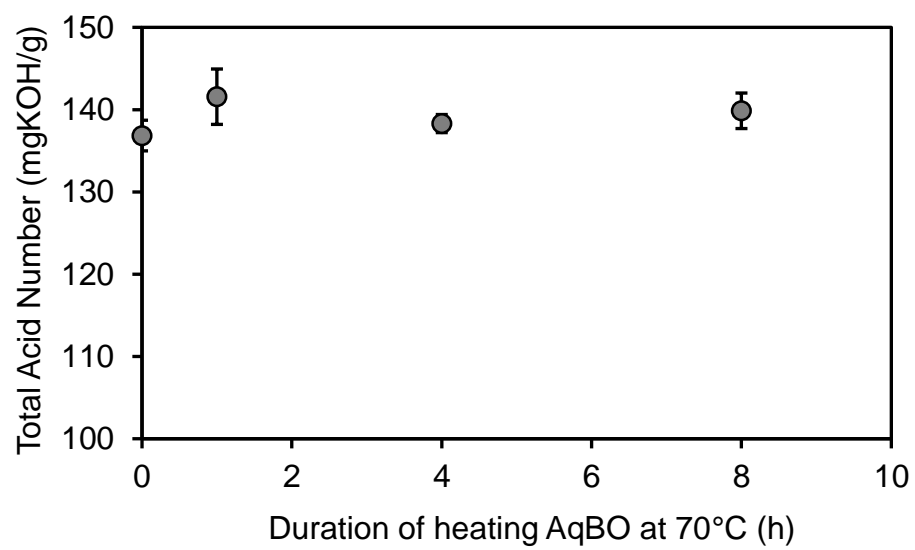


Figure 5.6. TAN (mgKOH/g) values of AqBO heated at 70 °C for 0, 1, 4, and 8 hours.

5.3.4 Discussion of increased TAN value of the system after pH neutralization

The overall TAN values of both batch and continuous-flow systems increased significantly after pH neutralization with different bases. TAN balances revealed a percent increase ranging from 13% to more than 55%. In the centrifugal-contactor system, the overall change in TAN values was -1%; however, if the mass lost in the system is included in the calculations, the change would be positive and ranging from +2% to +5%.

Previously, the same linear relationship was found between the TAN values and the molar concentrations of formic, acetic, propionic, and hydroxybenzoic acids, which act as monoprotic acids during the TAN analysis.¹²⁴ A different linear relationship, with double slope compared to that of monoprotic acids, was observed between the TAN values and the molar concentrations of vanillic acid, which acts as a diprotic acid in the TAN analysis.¹²⁴

Based on the chemical analyses of NBOAP and NBOOP obtained after pH neutralization (**Table 5.2**), NBOAP had higher concentrations of acetic and propionic acids, which are the major acids in bio-oil samples, than NBOOP. The TAN values of NBOAP, however, were lower than those of NBOOP. The reason that NBOOP had higher TAN values than NBOAP is probably due to the variety of phenolics that behave like vanillic acid during the TAN analysis. As shown in **Figure 5.3**, the concentration of phenolics in NBOOP is higher than that in NBOAP. During alkali addition, phenolic compounds were initially thought to be formed and partitioned in NBOOP, and the formation of phenolic acids caused an overall increase of the TAN value of the system. **Table 5.4** presents the changes in the weight of water and chemical species in bio-oil for

the batch NaOH(aq) addition experiment. It also shows the mean difference and deviation values of chemicals from various pH neutralization experiments. As shown in **Table 5.4**, however, the content of identified phenolics in the system after pH neutralization did not change significantly. Thus, phenolic compounds did not form during pH neutralization, and probably did not cause the increase in the overall TAN values that was observed after neutralization. As found in **Table 5.4**, the overall contents of water and acetic acid increased by $4.81 \pm 1.47\%$ and $0.91 \pm 0.78\%$, respectively while the levoglucosan content decreased by $1.95 \pm 0.55\%$ after pH neutralization. This small increase in acetic acid cannot fully explain why the overall TAN values increased after pH neutralization. The increase in water and acetic acid contents still indicates that pH neutralization is similar to the aging reactions of bio-oil because the water content and acidity are known to increase after bio-oil aging reactions.

Due to the diverse chemical species present in bio-oil, many chemical reactions can occur during bio-oil aging. Aging of bio-oil typically occurs at room temperature for long duration, but is often investigated at elevated temperatures for a much shorter period (i.e., accelerated aging). In aging of bio-oil, some general chemical reactions are expected to play a significant role, as follows:¹⁴⁰

1. Organic acids with alcohols to form esters and water
2. Organic acids with olefins to form esters
3. Aldehydes and water to form hydrates
4. Aldehydes and alcohols to form hemiacetals, or acetals and water
5. Aldehydes to form oligomers and resins
6. Aldehydes and phenolics to form resins and water

7. Aldehydes and proteins to form oligomers
8. Organic sulfur to form oligomers
9. Unsaturated compounds to form polyolefins
10. Air oxidation to form more acids and reactive peroxides that catalyze the polymerization of unsaturated compounds

Reactions 1 through 5 can occur when there is a change in temperature or relative amounts of water and other reactive compounds.¹⁴⁰ Reactions 4 through 10 can produce resins, oligomers, or polyolefins and result in irreversible changes in bio-oil composition.¹⁴⁰ Although bio-oil heating experiments demonstrated that heat did not increase the TAN values of aqueous bio-oil in the absence of alkali, chemical reactions similar to the aging reactions might have occurred at elevated temperatures in the presence of an alkali such as NaOH. Further investigations are needed to understand the chemical reactions occurring during pH neutralization and the relationship between the TAN values and different chemicals (e.g., ester, resin, and acetals) in complex bio-oil phases.

Table 5.4. Changes in amounts of chemicals in bio-oil phases after pH neutralization for the batch NaOH(aq) addition experiment and the mean difference and deviations over all pH neutralization experiments.

	AqBO	NaOH	Initial (NBO)	NBOAP	NBOOP	Final (NBOAP + NBOOP)	Difference ¹	Mean difference over all pH neutralization experiments
Weight (g)	86.4	13.6	100.0 ²	87.3	12.7	99.94	0.06	
Water	37.72	6.80	44.51	45.46	2.68	48.14	3.63	4.81 ± 1.47
Levoglucosan	7.94	-	7.94	5.58	0.07	5.65	-2.29	-1.95 ± 0.55
Acetic acid	6.96	-	6.96	7.79	0.27	8.06	1.10	0.91 ± 0.78
Propionic acid	3.08	-	3.08	2.68	N/M	-	-	-
1-Hydroxy-2-butanone	0.93	-	0.93	0.38	0.08	0.46	-0.48	-0.41 ± 0.04
1,3-Propanediol	0.06	-	0.06	0.01	0.00	0.01	-0.05	0.02 ± 0.10
HMF	0.50	-	0.50	0.05	0.03	0.08	-0.42	-0.41 ± 0.06
Furfural	0.35	-	0.35	0.03	0.14	0.17	-0.18	-0.18 ± 0.05
2(5H)-Furanone	0.35	-	0.35	0.07	0.02	0.09	-0.27	-0.27 ± 0.03
3-Methyl-1,2-cyclopentanedione	0.15	-	0.15	0.04	0.03	0.08	-0.07	-0.05 ± 0.02
1,2-Benzenediol	0.36	-	0.36	0.24	0.08	0.33	-0.03	-0.04 ± 0.01
Phenol	0.10	-	0.10	0.04	0.04	0.09	-0.02	0.00 ± 0.01
Guaiacol	0.11	-	0.11	0.03	0.05	0.08	-0.03	-0.02 ± 0.01
3-Ethylphenol	0.13	-	0.13	0.04	0.10	0.14	0.01	0.02 ± 0.01
2-Methoxy-4-methylphenol (creosol)	0.21	-	0.21	0.10	0.05	0.16	-0.05	-0.09 ± 0.05
2,6-Dimethoxyphenol	0.10	-	0.10	0.04	0.06	0.10	0.01	0.01 ± 0.01
Identified (wt%)	59.05	-	59.05	62.59	3.71	66.30	7.25	7.93 ± 3.02
Unidentified (wt%)	27.36	-	27.36	24.68	8.96	33.64	6.29	5.67 ± 1.68

N/M: not measurable

1: Difference = Final – Initial

2: The percent values are calculated based on AqBO (g) + Alkali (g) = 100%.

5.4 Conclusions

Comparisons of the results from the batch and continuous-flow systems indicate that pH neutralization can be the first step of the bio-oil upgrading process because it can be used to optimize the formation and separation of the aqueous and organic phases. The pH neutralization process can be performed in batch or continuous-flow systems. Process intensification devices, including a static mixer and a centrifugal contactor, can be used to reduce the processing cost by making the process continuous with less processing steps. The neutralization reactions occur in a delivery pipe equipped with special baffles to enhance mixing in the static mixer, while the centrifugal contactor separates the two phases at the exit. Both systems can be easily scaled up to handle commercial-scale flow rates.

The ASTM standard TAN analysis has been employed to investigate changes in the acidity during pH neutralization. A TAN balance over pH neutralization revealed that, after considering the TAN contribution of the alkali solution added, the overall TAN value of the system increase after neutralization. A bio-oil heating experiment confirmed that the heat generated during pH neutralization is not the major factor that contributed to the increase in the overall TAN of the system. Chemical analysis showed that NBOOP contains higher concentrations of phenolics and other unidentified chemicals than those in AqBO and NBOAP. These phenolics and unidentified chemicals were initially assumed to be formed after alkali addition. A comparison of the initial and final masses of chemicals after pH neutralization, however, revealed that changes in mass of phenolics were insignificant. Thus, formation of phenolics in NBOOP may not be the reason for the

increase in the overall TAN values. Further investigations are, therefore, needed to fully understand the reason for the increase in the overall TAN values after pH neutralization.

The organic and aqueous phase separated after pH neutralization can be used to manufacture useful products. Extension of this work, for example, could focus on generating hydrogen through microbial electrolysis cells^{16, 141} utilizing NBOAP. NBOOP, on the other hand, may further be upgraded to generate fuel or used to produce other products, such as resins.

5.5 Acknowledgments

This chapter contains contributions from coauthors and has been submitted for publication: Park, L. K.-E., Ren, S., Yiacoumi, S., Ye, X. P., Borole, A. P., Tsouris, C. “pH Neutralization of Bio-Oil from Switchgrass Intermediate Pyrolysis Using Process Intensification Devices.” (*Submitted*).

CHAPTER 6. ELECTROSORPTION OF ACIDS FROM BIO-OIL FOR HYDROGEN PRODUCTION VIA MICROBIAL ELECTROLYSIS

Capacitive deionization (CDI) is a desalination technology that separates ions from solutions by applying an electric field. After pH neutralization of bio-oil, acidic components are present as anions in the neutralized bio-oil aqueous phase (NBOAP). In addition, some acidic components remain in the neutralized bio-oil organic phase (NBOOP). The objectives of the work presented in this chapter are to (1) collect acidic components from the NBOOP through water extraction and (2) capture acids in the NBOAP, as well as the NBOOP-contacted water phase, via CDI. The results showed that the CDI treatment was effective with the diluted solutions. Capture of acids through CDI would allow the microbial electrolysis cell (MEC) application to effectively produce renewable hydrogen, which is essential in hydrodeoxygenation (HDO) of bio-oil and would lead the entire pyrolysis process to be a carbon-neutral process.

6.1 Introduction

Acetic and propionic acids, the major acids in switchgrass bio-oil, are present as ions (acetate and propionate ions, respectively) in the neutralized bio-oil. These acidic components are problematic in bio-oil due to their contributions to the acidity and corrosivity problems. However, these acidic components can be valuable for other applications. For example, microbes can utilize acids to produce hydrogen, which is a

valuable component for further treating bio-oil through HDO. Recently, Lewis et al.¹⁶ reported a novel application of microbial electrolysis to produce renewable hydrogen using an aqueous phase obtained from adding water to switchgrass bio-oil. Among various components found in the aqueous phase, acids (e.g., acetic acid) are known to be easily and effectively converted to hydrogen. Some other compounds, such as furanic and phenolic compounds, are known to inhibit hydrogen production in MEC¹⁴¹⁻¹⁴³. Thus, it is important to collect as much acid as possible with no or less phenolic compounds from bio-oil for acidity reduction as well as the MEC application.

One approach to separate acids from bio-oil is by employing CDI. CDI has been developed mainly for desalination of brackish water because of its ability to remove ions from solutions. When an electric field is applied to the CDI reactor, the two electrodes are charged positively and negatively. Then, the charged electrodes can attract oppositely charged ions (counterions) from the solution. Electrodes with high conductivity and surface area can form electrical double layers (EDLs) on their external and internal surfaces, where ions accumulate. This phenomenon is also known as electrosorption. After electrosorption is completed, the solution between the electrodes can be removed, and a rinsing stream or water can be introduced into the CDI cell to collect the electrosorbed ions after turning off the electric field. Compared with other technologies, e.g., ion exchange, evaporation, and reverse osmosis, CDI is considered to have several advantages of reversibility, non-requirement of chemicals, and less energy use.

CDI can be used to capture acidic ions from the NBOOP-contacted water phase. A CDI cell was set up in our laboratories, with carbon aerogel electrodes, and was operated in a batch mode for concept demonstration. It was demonstrated that carbon

aerogel works well as an electrode material because of its high electrical conductivity and large surface area.¹⁴⁴ In general, carbon aerogel has low electrical resistivity ($\leq 40 \text{ m}\Omega \text{ cm}$), high porosity, high specific surface area ($400\text{--}1000 \text{ m}^2/\text{g}$), and controllable pore size distribution ($\leq 50 \text{ nm}$).¹⁴⁴⁻¹⁴⁷ The same type of carbon aerogel that was used by Ying et al.¹⁴⁴ was also employed in this study.

The water phase that was contacted with the NBOOP, after pH adjustment of AqBO, has been utilized as the initial solution for CDI. Water was added to NBOOP to extract remaining acids that were partitioned in NBOOP during pH neutralization. Mixtures of the neutralized aqueous phase and the NBOOP-contacted water, as well as diluted NBOAP, were also utilized as initial solutions for CDI to recover acids from neutralized bio-oil. An overall schematic of the pH neutralization, water extraction, and CDI treatment processes is provided in **Figure 1.1**.

6.2 Materials and Methods

6.2.1 Extraction of Acids from Neutralized Bio-oil Organic Phase using Water

After adjusting the pH of AqBO by adding sodium hydroxide solution [NaOH(aq), 50%] in a batch system, as described elsewhere,²⁴ the NBOAP was removed after centrifugation of the neutralized bio-oil using a Beckman Coulter Avanti J-E with a JLA 10.500 rotor at 3000 rpm (1673 g) for 30 minutes. Then, deionized water was added to the NBOOP at various dilution factors ranging from 2 to 50. Water was contacted with NBOOP for 24 h to extract acids that have been partitioned in NBOOP after pH

neutralization. The water phase was then separated from NBOOP via centrifugation for further treatment and analysis.

6.2.2 CDI Experiments

Batch CDI experiments were performed using a laboratory-scale CDI cell with a pair of carbon aerogel electrodes (**Figure 6.1**). Carbon aerogels were obtained from Marketch (Port Townsend, WA). Details on the carbon aerogels can be found in Ying et al.¹⁴⁴ Two sheets of carbon aerogel electrodes used in experiments 1–7 were 1.08 g and 1.04 g, respectively. Another pair of carbon aerogel sheets for experiments 8 and 9 had the same mass, 1.04 g each. The two sheets of carbon aerogel electrodes were in contact with titanium sheets, which were used as current collectors. The edges of the carbon sheets were taped on the titanium sheets. A plastic mesh [**Figure 6.1 (4)**] was placed in between the two electrodes to prevent any shortage. The distance between the two electrodes, which were separated by a central hollow piece of viton gasket [**Figure 6.1 (2)**], was 0.6 cm. The titanium sheets [**Figure 6.1 (3)**] were connected to a direct-current (DC) power supply (Hewlett Packard E3630A Triple output DC power supply) with a voltage range of 0 to 15 V and a current range of 0 to 7 A.

Approximately 11–14 mL of the initial solution was placed in the CDI reactor using a syringe. After initializing the CDI cell by allowing the electrodes to reach equilibrium with the initial solution, a potential of 1.4 V was applied between the two electrodes. The electric field was applied for at least 20 minutes and until the current reached 0.02 A. While the electric field was on, the CDI-treated solution was removed from the CDI cell using a syringe. Then, the electrical potential was turned off to 0 V, and the current in the cell eventually became 0 A. Then, deionized water was introduced

into the CDI cell to recover desorbed ions and regenerate the electrodes. Finally, after at least 2 hours of regeneration, the rinsing water phase was collected for analysis.

6.2.3 *Characterization of Carbon Aerogel*

The carbon aerogel used in this study is of the same type as the carbon aerogel described in Ying et al.¹⁴⁴ The characteristics of the carbon aerogel were analyzed as described in Tsouris et al.⁸⁴ In brief, nitrogen adsorption isotherms were collected on a Micromeritics Tristar 3000 at 77 K (−196 °C) after degassing at 200 °C for 18 hours in flowing nitrogen. The surface area was calculated using the Brunauer–Emmet–Teller (BET) method or a comparative method.¹⁴⁸ The pore size distribution, which is the available surface area for electrosorption, was analyzed by following the Barrett–Joyner–Halenda (BJH) method.¹⁴⁹ The carbon aerogel characterization analysis was performed by Dr. Richard Mayes at Oak Ridge National Laboratory (ORNL).

6.2.4 *Physical and Chemical Analyses of Solutions*

The pH value was measured using an Accumet pH meter 50 from Fisher Scientific with Orion sureflow combination pH glass electrode (9172BNWP), the conductivity was measured using an Amber Scientific, Inc. (Eugene, Oregon) EC meter Model 2052.

The concentrations of acetate and propionate ions were measured using an HPLC unit equipped with a UV–vis detector (Agilent 1100, Santa Clara, CA).¹⁴³ An HPX-87H column (BioRad, Hercules, CA) was used with an eluent of 5 mmol/L H₂SO₄ at a flow rate of 0.6 mL/min. The wavelength of 210 nm was used.

Chemical oxygen demand (COD) analysis was performed using the Hach COD method. Samples (2 mL) were added to Hach COD digestion vials. Then, the samples were placed in a Hach DRB 200 reactor at 150 °C for 2 hours. Before spectroscopic analysis, samples were cooled to room temperature. Using 10 concentrations ranging from 25 to 1000 mg/L of COD standard solutions (potassium hydrogen phthalate), a calibration curve was generated prior to running the samples. Absorbance readings were taken at 620 nm on a Spectronic 20 Genesys. These readings were converted to concentration based on the calibration curve.

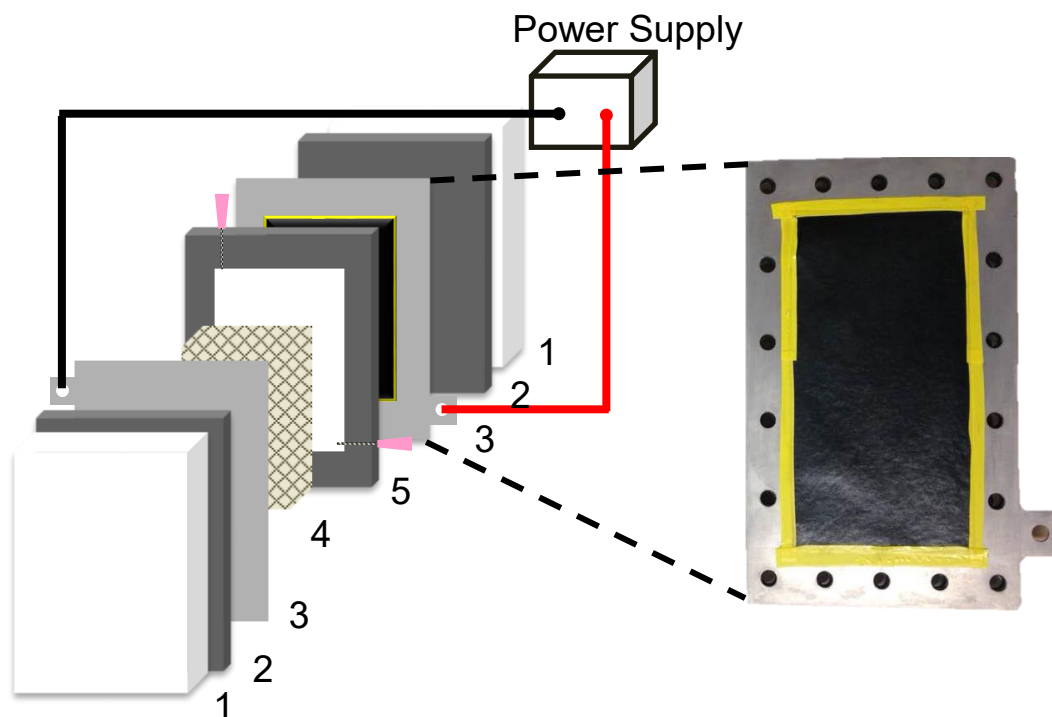


Figure 6.1. CDI cell with two half cells, each of which contains (1) a Plexiglas cover, (2) a viton gasket, (3) a titanium plate (current collector) with a carbon sheet, (4) a plastic mesh, and (5) a hollow middle viton gasket with syringe needles for input/output. Right: a picture of a carbon sheet taped to a current collector plate made of titanium.

6.3 Results and Discussion

6.3.1 Water Extraction

As found in **Table 6.1**, NBOOP still contains some acetic acid (2.12 wt%). To recover this acid, as well as other acidic components in NBOOP, with the objective to use them in MEC for hydrogen production, water was used to extract organic acids from the NBOOP. Initially, pH neutralization of AqBO was performed in a batch system with NaOH(aq). The NBOAP was removed from the container after centrifugation of neutralized bio-oil for 30 minutes at 3000 rpm. Then, deionized water was added to the remaining NBOOP at various dilution factors (ranging from 2 to 50) to extract hydrophilic compounds, especially acids, from the NBOOP. The water phase was contacted with the NBOOP for 24 hours to allow the system to reach equilibrium, and then the two phases were separated via centrifugation. The produced phases were the NBOOP-contacted water phase and the remaining NBOOP after contact with water. Mass and TAN balances over the pH neutralization and the water extraction experiments were performed. Results from these experiments are summarized in a flow chart shown in **Figure 6.2**. The differences in weights presented in **Figure 6.2** are due to wetting of containers and experimental errors.

The NBOOP-contacted water phase and the mixture of NBOAP and NBOOP-contacted water phase were used in CDI experiments as discussed in the following section. Various properties including pH, conductivity, concentrations of acetate and propionate ions were monitored for the initial water phase used in the CDI experiments, and these data are presented in the following section. In addition, a mixture of the

NBOAP and the NBOOP-contacted water phase was sent to collaborators at ORNL for the MEC application for hydrogen production.

Table 6.1. TAN values and chemical compositions of initial aqueous and organic bio-oil and neutralized aqueous and organic phases from NaOH(aq) addition to AqBO.

Weight%	Initial		Batch system with NaOH(aq)	
	AqBO	OrgBO	NBOAP	NBOOP
Water	43.65	15.18	52.09	21.18
Levogluconan	9.19	0.72	6.39	0.56
Acetic acid	8.06	6.16	8.93	2.12
Propionic acid	3.57	0.00	3.07	0.00
1-Hydroxy-2-butanone	1.08	0.86	0.43	0.63
1,3-Propanediol	0.07	0.06	0.01	0.02
HMF	0.58	0.19	0.06	0.21
Furfural	0.40	1.35	0.03	1.12
2(5H)-Furanone	0.41	0.26	0.08	0.14
3-Methyl-1,2-cyclopentanedione	0.17	0.25	0.05	0.25
1,2-Benzenediol	0.42	0.61	0.28	0.66
Phenol	0.12	0.31	0.05	0.35
Guaiacol	0.13	0.29	0.04	0.38
3-Ethylphenol	0.15	0.74	0.05	0.75
2-Methoxy-4-methylphenol (creosol)	0.24	0.47	0.12	0.42
2,6-Dimethoxyphenol	0.11	0.33	0.05	0.47
Identified (wt%)	68.34	27.78	71.72	29.27
Unidentified (wt%)	31.66	72.22	28.28	70.73
TAN (mgKOH/g)	138.2 ±14.7	121.81	25.44 ± 2.19	54.29 ± 1.70

AqBO: aqueous bio-oil obtained from centrifuging the crude bio-oil

OrgBO: organic bio-oil obtained from centrifuging the crude bio-oil

NBOAP: neutralized AqBO phase obtained after adding NaOH(aq) to AqBO

NBOOP: neutralized organic bio-oil phase obtained after adding NaOH(aq) to AqBO

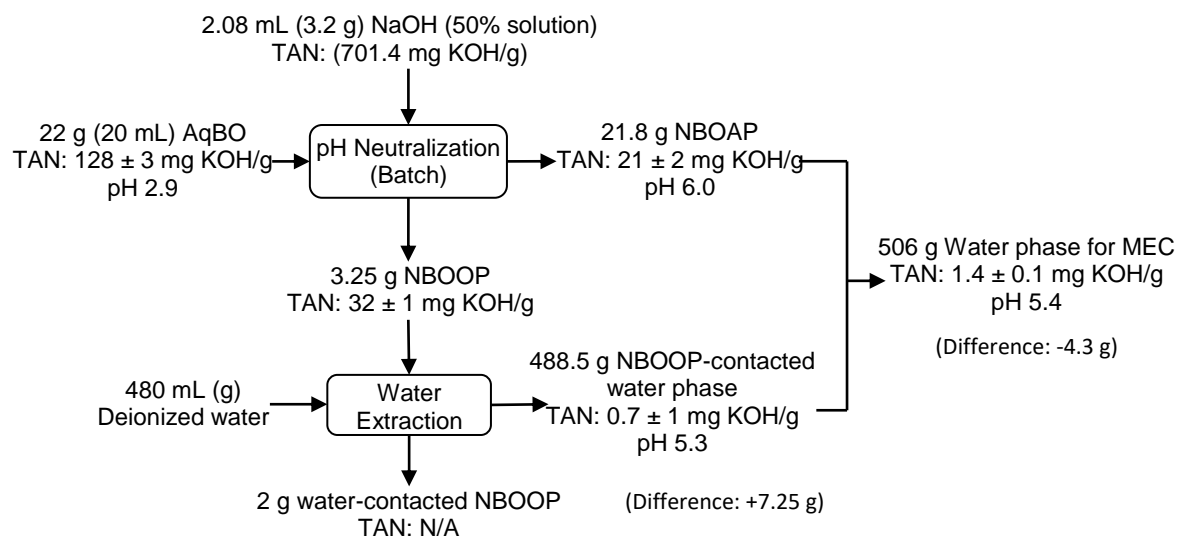
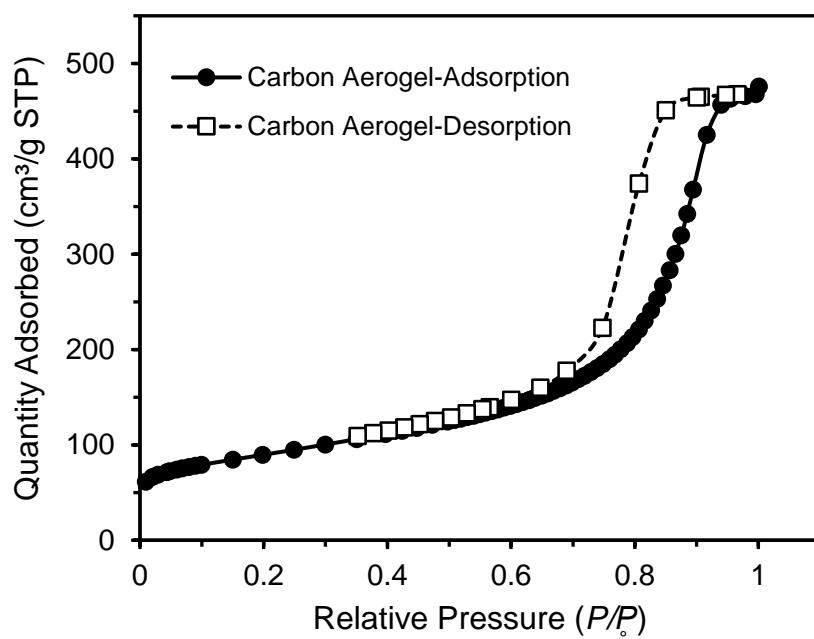


Figure 6.2. Flow chart of pH neutralization of AqBO followed by water extraction of NBOOP.

6.3.2 *Characteristics of Carbon Aerogels*

The nitrogen adsorption and desorption isotherms for the carbon aerogel sheets used as electrodes in this study are presented in **Figure 6.3 (A)**. In addition, the BJH pore size distribution of the carbon aerogel used in this study is shown in **Figure 6.3 (B)**. The specific surface area of the carbon aerogel used in this study is 316 m²/g. The carbon aerogel has a broad pore size distribution with the pore diameters of the carbon aerogel ranging from 2 to 50 nm (20 Å to 500 Å). Thus, the carbon aerogel can be categorized as mesoporous nanostructured material.

(A)



(B)

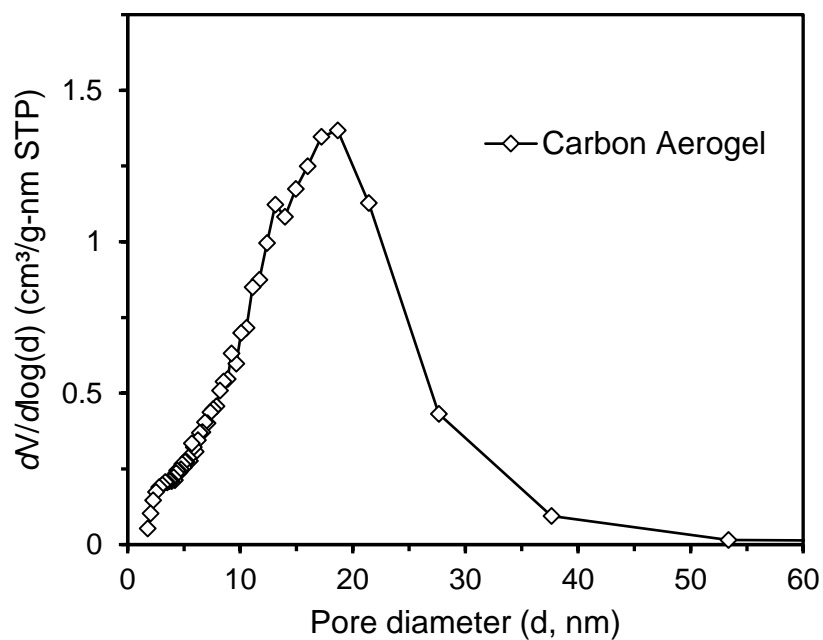


Figure 6.3. (A) Nitrogen sorption isotherms of the carbon aerogel material used in this study. (B) The BJH pore size distribution for carbon aerogel used in this study.

6.3.3 CDI Results

The pH, conductivity, COD, and concentrations of acetate and propionate ions of all samples obtained from the CDI experiments are summarized in **Table 6.2**. In general, when NBOOP-contacted water phases with a high dilution factor were used (Experiments 1, 2, and 9), the CDI-treated water phase had lower pH and conductivity values than the initial solution. The pH and conductivity values of the rinsing water phase were higher than those of the CDI-treated phase but lower than those of the initial solution. These trends indicated that CDI worked as expected, and ions were removed from the initial solutions used.

Figure 6.4 and **Figure 6.5** show relative concentrations of acetate and propionate ions in initial, CDI-treated, and rinsing water phases from Experiments 1, 3, and 8. The relative concentrations were calculated by dividing the concentrations of acetate and propionate ions in the CDI-treated and rinsing water phases by those in the initial phases. In the ideal CDI treatment, the CDI-treated phases would contain 0% ions, while the rinsing stream would contain all the ions present in the initial solution. This ideal situation, however, cannot be reached in CDI experiments because there is always an equilibrium between the ion concentration in the EDL and the bulk concentration. As the ionic strength of the initial solution increases, the EDL thickness decreases to allow more ions to accumulate in the EDL.

The concentration of acetate ions was the highest in the initial solution and the lowest in the CDI-treated solution for Experiment 1, as demonstrated in **Figure 6.4**. This result from Experiment 1 indicates that the CDI treatment was effective with acetate ions when an initial solution with a dilution factor of 25 was used. On the other hand, the

concentration of propionate ions was the highest in the initial water phase and the lowest in the rinsing water phase, as found in **Figure 6.5**. Thus, the CDI treatment in Experiment 1 was more effective for acetate ions than for propionate ions.

Though the COD levels do not specifically reflect the concentration of ions, they indicate the total organic compounds in each of the phases. The relative COD levels of the different phases from CDI experiments 1, 3, and 8 are presented in **Figure 6.6**. As demonstrated in **Figure 6.6**, organic compounds including acetate and propionate ions in the initial phases were transferred to the rinsing water after CDI treatment.

When high-conductivity solutions from less diluted initial solutions were used in CDI, no significant differences were observed between the initial and CDI-treated solutions. For example, the mixture of NBOAP and the NBOOP-contacted water phase (Experiment 8) had a high conductivity value, indicating that it contained a relatively high concentration of ions. The concentrations of acetate and propionate ions in the CDI-treated phase was not much different from that in the initial phase. Moreover, the concentrations of acetate and propionate ions in the rinsing water phase were lower than those in the initial and CDI-treated phase. The reason for this ineffective CDI treatment was the limited volume capacity and low ion capacity of the carbon aerogel electrodes used in the CDI cell. The CDI cell used in this study could hold only 11–14 mL of solution at a time, and all CDI experiments in this study were performed in a batch system.

Even though the CDI treatment was not significantly effective for highly concentrated or high-conductivity solutions, it is still promising that acetate and propionate ions could be recovered through CDI treatment from the NBOOP-contacted

water phase with dilution factors on the order of 25. To increase the capacity of the CDI cell, carbon electrodes with the higher specific area, electrical conductivity, and stability can be used in a larger cell with a continuous-flow system (e.g., flow-through mode). Obtained from the effective CDI treatment, the rinsing water phases with acetate and propionate ions can be useful for the MEC application because they contain acids and much fewer phenolics, which are known to inhibit the MEC application.

Table 6.2. Summary of results from CDI experiments.

Exp. #	Initial Water Phase Used	Overall dilution factor	Initial water phase					CDI-treated phase					Rinsing water phase				
			pH	Conductivity (mS/cm)	Acetate (mM)	Propionate (mM)	COD (g/L)	pH	Conductivity (mS/cm)	Acetate (mM)	Propionate (mM)	COD (g/L)	pH	Conductivity (mS/cm)	Acetate (mM)	Propionate (mM)	COD (g/L)
1	NBOOP-contacted water phase	25	5.5	0.414	3.5	0.44	1.53	4.6	0.0964	1.5	0.35	0.93	6.1	0.329	2.7	0.10	0.57
2	NBOOP-contacted water phase	25	5.2	0.348	3.2	0.66	N/A	4.5	0.1017	1.7	0.62	N/A	5.4	0.357	3.7	0.17	N/A
3	NBOOP-contacted water phase	2	5.2	6.79	433.5	36.5	98.77	5.1	3.01	118.1	34.8	77.63	5.0	1.6	46.8	13.7	27.77
4	NBOAP	15	5.4	6.15	88.0	18.4	N/A	5.2	5.71	80.9	16.3	N/A	5.3	3.64	36.2	7.6	N/A
5	NBOAP	5	5.4	14.6	257	54.8	N/A	5.4	13.27	236.2	53.0	N/A	5.4	6.89	88.6	18.7	N/A
6	NBOOP-contacted water phase	20	5.4	0.86	7.9	2.86	N/A	4.7	0.72	8.7	3.67	N/A	N/A	N/A	5.9	2.46	N/A
7	NBOOP-contacted water phase	20	5.2	0.5	4.6	1.85	N/A	4.3	0.26	4.2	2.17	N/A	5.6	0.32	1.8	0.76	N/A
8	NBOAP & NBOOP-contacted water	50	5.6	2.42	26.37	5.69	12.55	5.0	1.736	21.21	4.35	8.33	5.7	1.275	9.09	0.65	3.16
9	NBOOP-contacted water	25	5.2	0.42	3.71	1.08	N/A	4.4	0.158	2.69	0.72	N/A	5.6	0.382	2.38	0.41	N/A

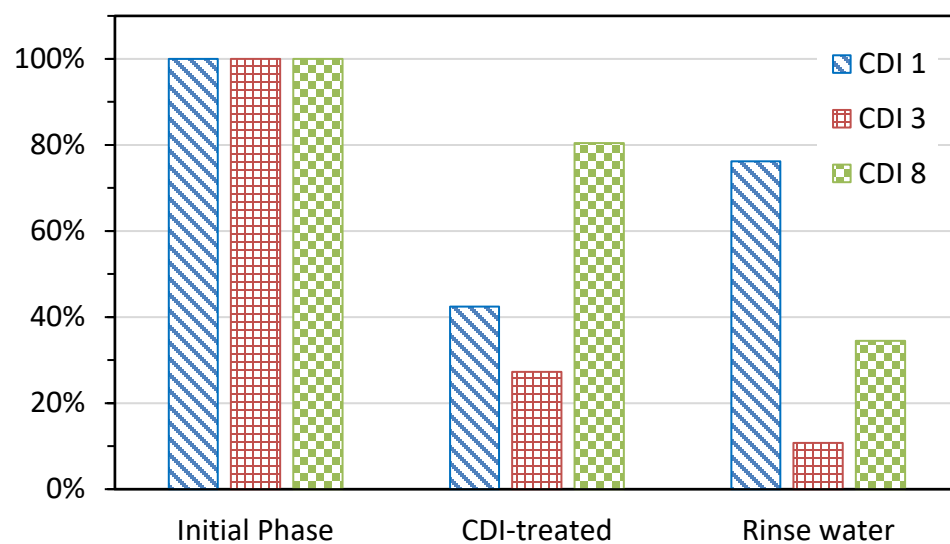


Figure 6.4. Relative concentrations of acetate ions in the initial phase, CDI-treated phase, and rinsing water phase for the CDI experiments 1, 3, and 8.

Note: The experiment numbers correspond to the numbers found in **Table 6.2**.

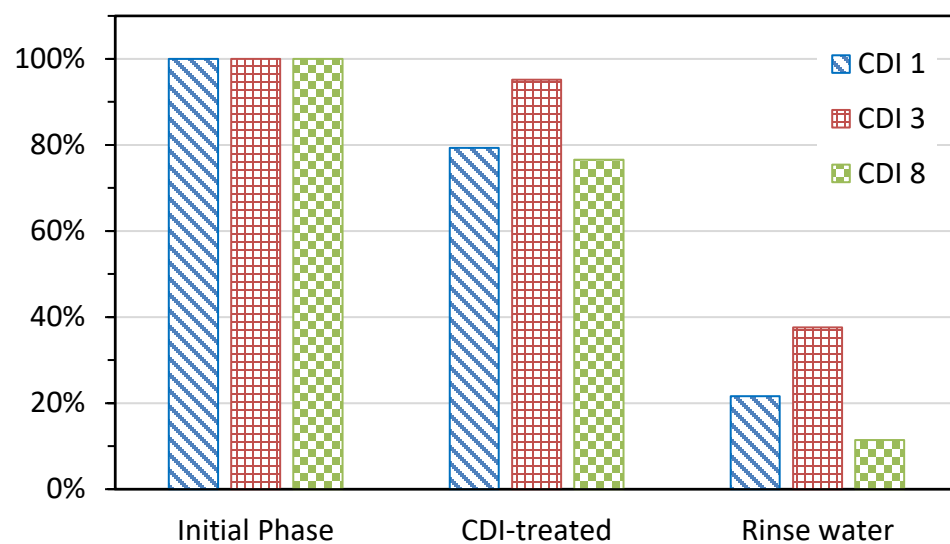


Figure 6.5. Relative concentrations of propionate ions in the initial phase, CDI-treated phase, and rinsing water phase for the CDI experiments 1, 3, and 8.

Note: The experiment numbers correspond to the numbers found in **Table 6.2**.

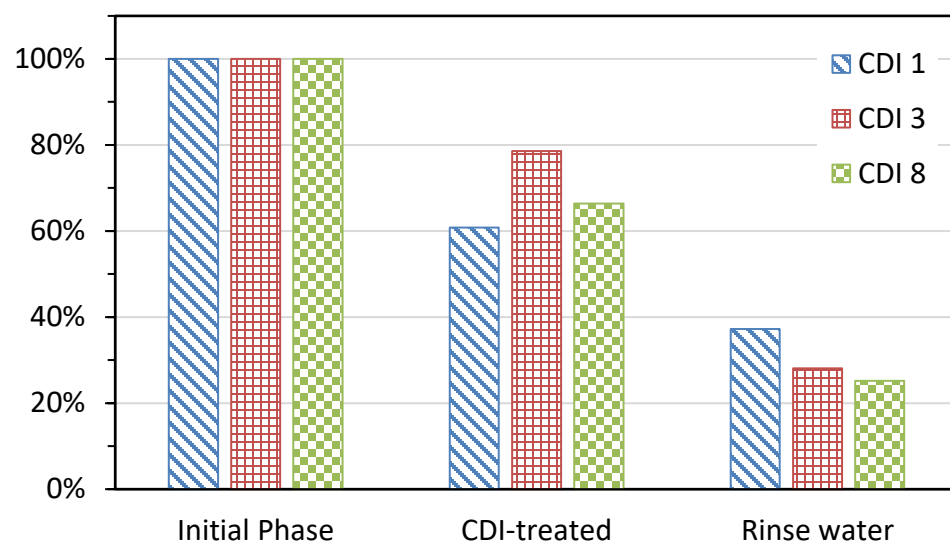


Figure 6.6. Relative percent of chemical oxygen demand (COD) levels in the initial phase, CDI-treated phase, and rinsing water phase for Experiments 1, 3, and 8.

6.4 Conclusions

After pH neutralization of AqBO, the precipitated NBOOP contains some acidic components that would be valuable to recover for other applications. Hence, water was used in this part of the work to extract hydrophilic compounds, including acetate and propionate ions from the NBOOP. The NBOOP-contacted water phase was then used in CDI for the recovery of acids. The CDI treatment was noticeably effective with the NBOOP-contacted water phase of relatively high dilution factors due to the limited capacity of the CDI cell used in this study. The rinsing water phase with regenerated ions can be used in MEC applications for renewable hydrogen production.

CHAPTER 7. CONCLUSIONS AND RECOMMENDATIONS

The work presented in this dissertation was performed to separate components of switchgrass intermediate pyrolysis bio-oil through solvent extraction, water addition, alkali addition, and capacitive deionization (CDI) in order to improve its utilization. A summary of the results and conclusions of this research are as follows:

- The combined extraction of bio-oil, adding water and organic solvents together, effectively extracts more bio-oil components than the sequential extraction in which water and organic solvents are added sequentially. Partitioned organic solvent into the aqueous phase during the combined extraction, however, may not be preferable for further utilization of the aqueous phase [e.g., microbial electrolysis cell (MEC) application].
- The addition of alkali separates aqueous bio-oil (AqBo) into aqueous and organic phases. The amount of precipitated organic phase increases as pH increases. The optimal pH value for phase separation is 6.0. The quality of bio-oil significantly improves through pH neutralization. The neutralized bio-oil contains approximately 37% less oxygen, and its heating value increases by 100% compared with the initial AqBO. The separated aqueous phase, which contains acidic and other hydrophilic components, may be used as a source of acids for the MEC application.
- The results of pH neutralization using various alkalis indicate that sodium hydroxide and potassium hydroxide are more appropriate for pH neutralization of

bio-oil than calcium hydroxide due to the limited solubility of calcium hydroxide in AqBO.

- The same linear relationship is found between the total acid number (TAN) and the molar concentrations of formic, acetic, propionic, and hydroxybenzoic acids that act as monoprotic acids during TAN analysis. A different linear relationship with a doubled slope applies for vanillic acid, however, due to the presence of multiple functional groups that can contribute to the TAN value. The results demonstrate that the TAN value of a sample with acids acting as monoprotic acids can be converted to the molar concentration of total acids. But for a sample containing a mixture of different acids that act as monoprotic and polyprotic acids, its TAN value cannot be simply converted to the molar concentration of total acids because these acids have different influences on the TAN values. Thus, the TAN analysis should be used with caution when comparing different bio-oils.
- The effect of different titration solvents on the TAN values can be investigated by employing the MINEQL+ model and experimental aqueous TAN analysis. The pK_a values included in the MINEQL+ model represent the aqueous system. Thus, the results from the aqueous TAN analysis are in agreement with those from the MINEQL+ model. On the other hand, the TAN values and titration curves obtained from the American Society for Testing and Materials (ASTM) standard method are significantly different from the results of the TAN analysis in the aqueous environment and the chemical equilibrium modeling. The major differences among the standard method, the aqueous TAN analysis, and the modeling are due to the different titration solvents used: a mixture of toluene, 2-

propanol, and water for the ASTM method and water for the modeling and aqueous system. The results indicate that the pK_a values or dissociation properties of acids vary when different solvents are used in the TAN analysis.

- The overall TAN values of the system increase after pH neutralization of aqueous bio-oil. The bio-oil heating experiment indicates that the heat generated during pH neutralization does not cause an increase in the acidity of bio-oil. After pH neutralization, the formation of phenolic compounds was initially suspected of increasing the overall TAN value of the system because acids that act as polyprotic acids (e.g., vanillic acid) have a stronger influence on the TAN values than acids acting as monoprotic acids (e.g., acetic acid). The mass balance of chemicals after pH neutralization, however, reveals that phenolic formation may have not caused the increase in the overall TAN values of the system because the mass of phenolics did not change significantly after the neutralization.
- The results from the continuous-flow systems of pH neutralization using the static mixer and centrifugal contactor are comparable with those from batch systems. The process intensification experiments using the static mixer and centrifugal contactor demonstrate a potential to scale up pH neutralization of bio-oil.
- After pH neutralization, acids are present as ions in the aqueous phase, and some acids are still present in the organic phase. By adding water to the neutralized organic phase, some acidic and hydrophilic components remaining in the neutralized organic phase are enriched in the water phase.
- The water phase from the water addition experiment with neutralized organic phase can be treated by CDI. The CDI treatment is effective with the diluted

solutions. The enrichment of acids through CDI would allow the MEC application to effectively produce hydrogen that is essential in the hydrodeoxygenation (HDO) of bio-oil and would lead the entire pyrolysis process to become a carbon-neutral process.

- The overall flow diagram from pyrolysis of switchgrass to hydrogen production via microbial electrolysis is found in **Figure 7.1**. The weights and organic contents are calculated on the basis of 100 g initial weight of switchgrass. The organic content of each stream is presented in parentheses. After separations, organic bio-oil and water-contacted NBOOP presented in orange boxes can be utilized in hydrocarbon fuel production or other chemical applications. The amount of organics in bio-oil for these applications is approximately 11.36 g assuming that the water contacted NBOOP contained mostly organics. The aqueous phases, indicated as blue boxes in **Figure 7.1**, contain a total of 18.95 g of organics in bio-oil and can be directed to capacitive deionization and microbial electrolysis for hydrogen production. The mass balance in the flow diagram of **Figure 7.1** is not completely closed. Slight deviations are observed because the weight values and water contents were obtained from several independent experiments.

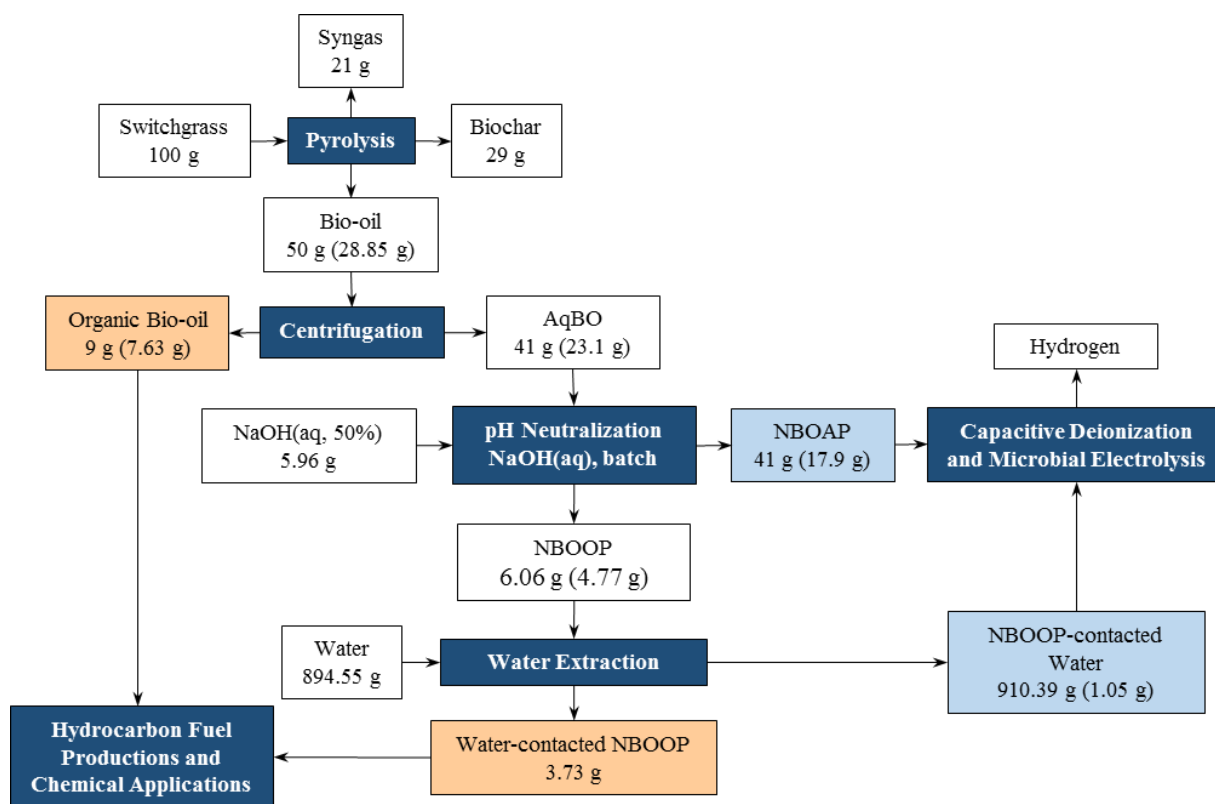


Figure 7.1. Overall flow diagram from pyrolysis to hydrogen production with weights and organic contents of phases.

Note: The numbers in parentheses represent weights of organics.

The findings from this work suggest that the bio-oil components can be separated through various processes, including solvent extraction, water addition, alkali addition, and CDI. Based on the results presented in this dissertation, recommendations are provided as follows to improve the separation of bio-oil components further.

- This research was limited to the use of aqueous bio-oil after centrifuging crude bio-oil due to the heterogeneity of the system. Further investigations are needed to maximize the use of organic bio-oil and better understand its properties.
- The MINEQL+ model used in this research is suitable for aqueous systems. Modeling for the ASTM standard TAN solvent may be beneficial to better understand the interactions among titrants, acids, and solvent molecules during TAN analysis.
- Using a glass pH electrode in an organic solvent is not ideal because the pH electrode is calibrated with aqueous buffer solutions. The behavior of the electrode in organic solvents and the effect of dehydration of the electrode on the TAN analysis need to be investigated.
- The currently available ASTM standard is more appropriate for analyzing petroleum products and biodiesel than bio-oil. Not all components of bio-oil can be dissolved in the standard titration solvent. Currently available modifications of the standard method suggest using various solvents for titration (e.g., methanol,¹²² ethylene glycol,¹²³ and acetone²). The titration solvent should be standardized for the bio-oil TAN analysis. Moreover, pK_a values of chemical components in bio-oil in such titration solvent need to be investigated to fully understand the relationship between the TAN values and concentrations of acids in bio-oil.

- Further optimization studies are needed to improve the use of the centrifugal contactor for the pH-neutralization treatment of AqBO. The accumulation of NBOOP inside the centrifugal contactor indicates that phase separation occurred in the centrifugal contactor. However, the neutralized bio-oil exited from only one of the two outlets during the experiment. A larger amount of initial AqBO is needed to increase the amount of organic phase formed. Attempts to increase further the retention time and lower the temperature of the neutralized bio-oil inside the centrifugal contactor may be beneficial to have two separate streams from the centrifugal contactor.
- A thorough chemical analysis is needed to investigate the changes in the acidity after pH neutralization. Further investigations are needed to fully understand why the overall TAN values of the system increase after neutralization and why NBOOP has higher TAN values than NBOAP.
- Due to the complex chemical composition of bio-oil, it may be worth studying a model bio-oil containing only major species of bio-oil to evaluate various separation processes.
- The enrichment of acids in the neutralized bio-oil can be further improved using a continuous-flow CDI system with carbon electrodes of the larger surface area and operated under different conditions (e.g., temperature and voltage). A CDI cell with larger capacity would maximize the CDI efficiency and remove more acidic ions from the neutralized bio-oil.
- The resulting solutions with enriched acids from the CDI experiments need to be tested for their applicability as a feedstock for the MEC application.

- The overall mass or TAN balance from the production of bio-oil to the end use of bio-oil needs to be performed to evaluate the applicability of bio-oil as a biorenewable energy.
- Real-world applications and alternative uses of the resulting aqueous and organic phases are required to maximize the utilization of switchgrass bio-oil. Some examples may include research related to the production of phenolic resin, fuel additives, and adhesives from the organic phase.

APPENDIX A. SUPPORTING INFORMATION

For Chapter 3

Table A1. Water addition ratio used in experiments and the amount of each phase after contacting aqueous bio-oil with water.

Type of Bio-oil	Weight ratio of aqueous bio-oil to water (AqBO:water, g:g)	Organic bio-oil phase (Boop) precipitated (g)	Water phase (Boap) after water addition (g)
Aqueous	1:2 (7:14)	0.78 ± 0.09	20.23 ± 0.09
Aqueous	1:4 (7:28)	1.155 ± 0.34	33.85 ± 0.34

Table A2. Chemical species identified in GC-MS analysis.

Peak Number	Average Retention Time	Name of Chemical	Peak Number	Average Retention Time	Name of Chemical
1	1.94	2,3-Butanedione	27	4.69	2-propanone, 1-acetyloxy-
2	2.00	2-Butanone	28	4.87	Furan, tetrahydro-2,5-dimethoxy-
3	2.11	Acetic Acid	29	5.07	1,3-Dioxepane, 2-methyl-2-propyl-
4	2.15	Furan, tetrahydro-	30	5.18	2-Cyclopenten-1-one, 2-methyl-
5	2.17	Furan	31	5.33	Ethanone, 1-(2-furanyl)-
6	2.41	Butanal, 3-methyl-	32	5.39	1,3-Dioxepane, 2-methyl-2-propyl-
7	2.43	2-Butenal, (E)-	33	5.40	2(5H)-Furanone
8	2.47	2-Propanone, 1-hydroxy-	34	5.49	2-Cyclopenten-1-one, 3,4-dimethyl-
9	2.51	3-Penten-2-one	35	5.64	2-Furanethanol, β -methoxy-(S)-4,5-Dihydro- $\beta,\beta,4,4$ -tetramethyl-1H-pyrazole-1-propanol
10	2.56	Acetic acid, hydrazide	36	5.65	2-Butyne-1,4-diol
11	2.58	Hexane, 2,2-dimethyl-	37	5.79	N-Ethyl-n-butan-4-ol-nitrosamine
12	2.67	2-Pentanone	38	5.79	Spiro[2.4]heptan-4-one
13	2.69	Heptane	39	5.93	2-Furancarboxaldehyde, 5-methyl-
14	2.73	2,3-Pentanedione	40	5.97	2(5H)-Furanone, 3-methyl-
15	3.28	2-Methoxytetrahydrofuran	41	6.06	Phenol
16	3.47	Heptane, 3-methyl-	42	6.09	Bicyclo[3.1.1]heptan-2-one
17	3.61	1-Hydroxy-2-butanone	43	6.21	2-Cyclopenten-1-one, 2-hydroxy-3-methyl-
18	3.62	Acetic acid, (acetyloxy)-	44	6.57	6-Hydroxymethyl-5-methyl-bicyclo[3.1.0]hexan-2-one
19	3.75	Cyclopentanone	45	6.61	2-Cyclopenten-1-one, 2-hydroxy-3-methyl-
20	3.73	Methyl 2-methoxypropenoate	46	6.67	Phenol, 2-methyl-
21	3.78	Octane	47	6.88	Phenol, 4-methyl-
22	4.10	Hexane, 2,4-dimethyl-	48	7.07	Phenol, 2-methoxy-
23	4.34	Furfural	49	7.21	Phenol, 2,4-dimethyl-
24	4.15	Cyclopentane, 1-ethyl-2-methyl-, cis-	50	7.83	Phenol, 4-ethyl-
25	4.23	Cyclopentane, propyl-	51	7.95	Phenol, 2-methoxy-4-methyl-
26	4.53	3-Furaldehyde	52	8.22	
53	8.52	1,4:3,6-Dianhydro- α -d-glucopyranose	77	10.97	Pentadecane
54	8.53	Benzofuran, 2,3-dihydro-	78	11.05	D-Allose

55	8.63	Benzenamine, N,4-dimethyl-	79	11.17	Trimethoxyamphetamine, 2,3,5-
56	8.64	2,3-Anhydro-d-galactosan	80	11.25	Benzene, 1,2,3-trimethoxy-5-methyl-
57	8.67	Phenol, 2-ethyl-5-methyl-	81	11.29	2-Propanone, 1-(4-hydroxy-3-methoxyphenyl)-
58	8.85	Phenol, 3-ethyl-5-methyl-	82	11.43	β -D-Glucopyranose, 1,6-anhydro-
59	8.87	d-Mannose	83	11.53	Pentadecane, 2-methyl-
60	9.07	Phenol, 4-ethyl-2-methoxy-	84	11.54	Ethanone, 1-(2,5-dimethoxyphenyl)-
61	9.48	Ethanone, 1-(2-hydroxy-5-methylphenyl)-	85	11.74	Hexadecane
62	9.40	2-Methoxy-4-vinylphenol	86	11.79	Phenol, 2,6-dimethoxy-4-(2-propenyl)-
63	9.72	Phenol, 2,6-dimethoxy-	87	12.14	Hexadecane
64	9.75	Phenol, 2-methoxy-4-(1-propenyl)-	88	12.29	Phenol, 2,6-dimethoxy-4-(2-propenyl)-
65	9.81	Phenol, 2-methoxy-5-(1-propenyl)-, (E)-	89	12.33	Hexadecane, 2-methyl-
66	9.82	3-Allyl-6-methoxyphenol	90	12.35	Benzaldehyde, 4-hydroxy-3,5-dimethoxy-
67	9.85	Phenol, 2-methoxy-4-propyl-	91	12.57	Heptadecane
68	10.24	Phenol, 2-methoxy-4-(1-propenyl)-	92	12.59	Phenol, 2,6-dimethoxy-4-(2-propenyl)-
69	10.25	5-Methyl-2-allylphenol	93	12.85	Ethanone, 1-(4-hydroxy-3,5-dimethoxyphenyl)-
70	10.31	Phenol, 2-methoxy-4-(1-propenyl)-	94	12.97	4-Hydroxy-2-methoxycinnamaldehyde
71	10.53	1,2,4-Trimethoxybenzene	95	13.08	Thiazolidine-4-carboxylic acid, 2-(2-isopropoxyphenyl)-
72	10.58	Phenol, 4-methoxy-3-(methoxymethyl)-	96	13.25	cis-2-Methoxycinnamic acid
73	10.58	1,2,4-Trimethoxybenzene	97	13.26	Octadecane
74	10.61	Phenol, 2-methoxy-4-(1-propenyl)-	98	13.32	3-Hexadecanol
75	10.76	phenol, 4-methoxy-3-(methoxymethyl)-	99	13.84	Hexadecen-1-ol, trans-9-
76	10.96	Ethanone, 1-(4-hydroxy-3-methoxyphenyl)-	100	14.64	3,5-Dimethoxy-4-hydroxycinnamaldehyde

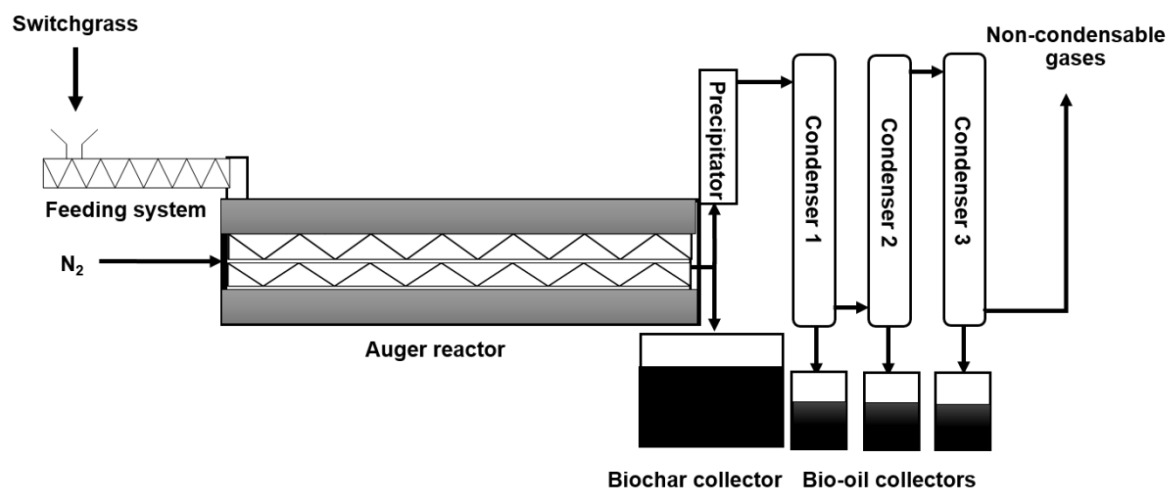


Figure A1. Schematic of an auger pyrolysis system using switchgrass to produce bio-oil.

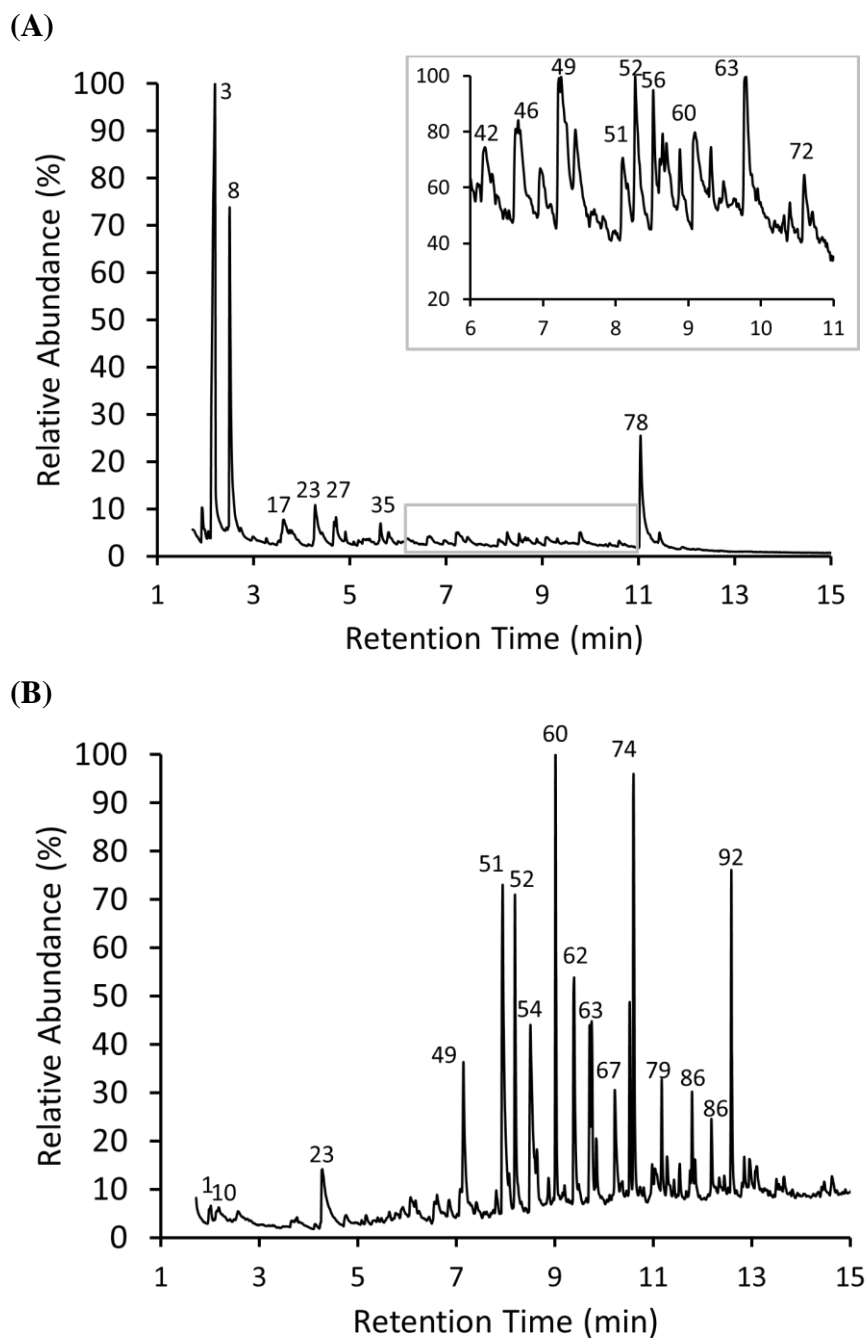
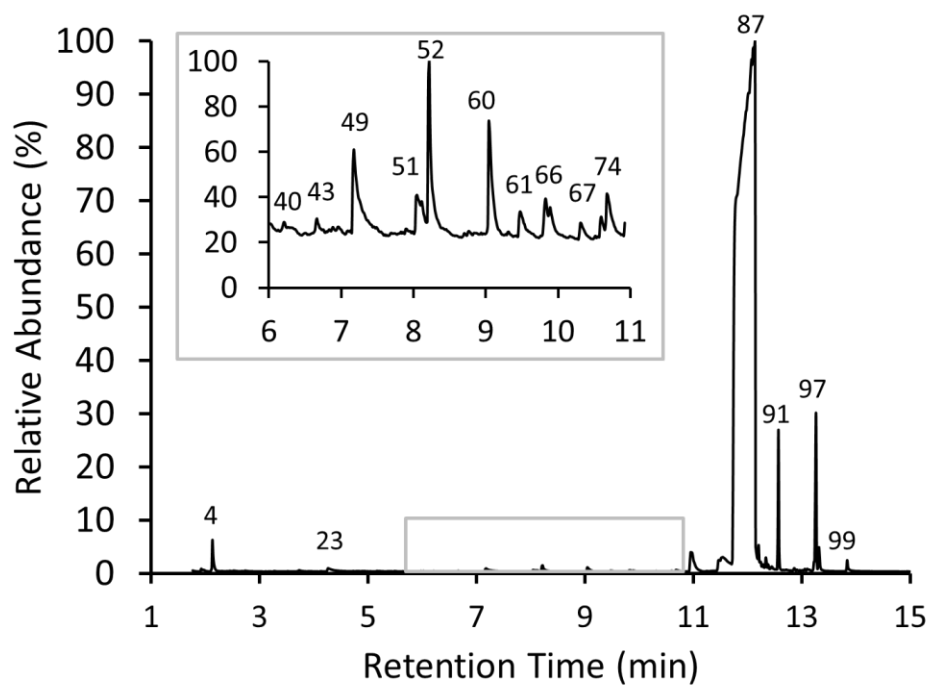


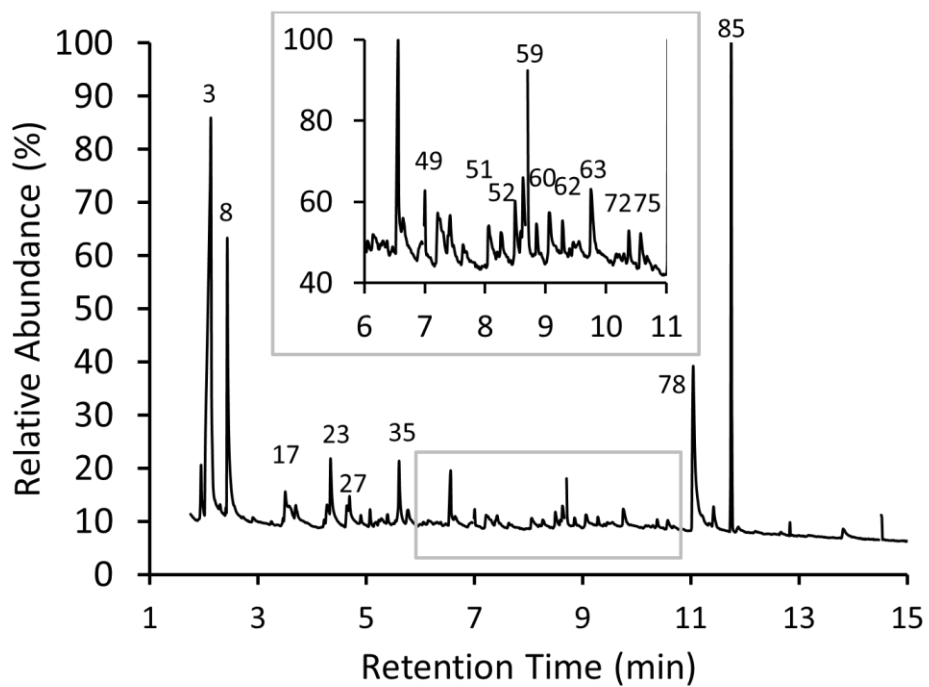
Figure A2. (A) Chromatogram of aqueous phase (Boap) from a water addition experiment. (B) Chromatogram of organic phase (Boop) from a water-addition experiment.

Note: Chemicals corresponding to the peak numbers (**Figure A2 – A4**) are summarized in **Table A2**.

(A)



(B)



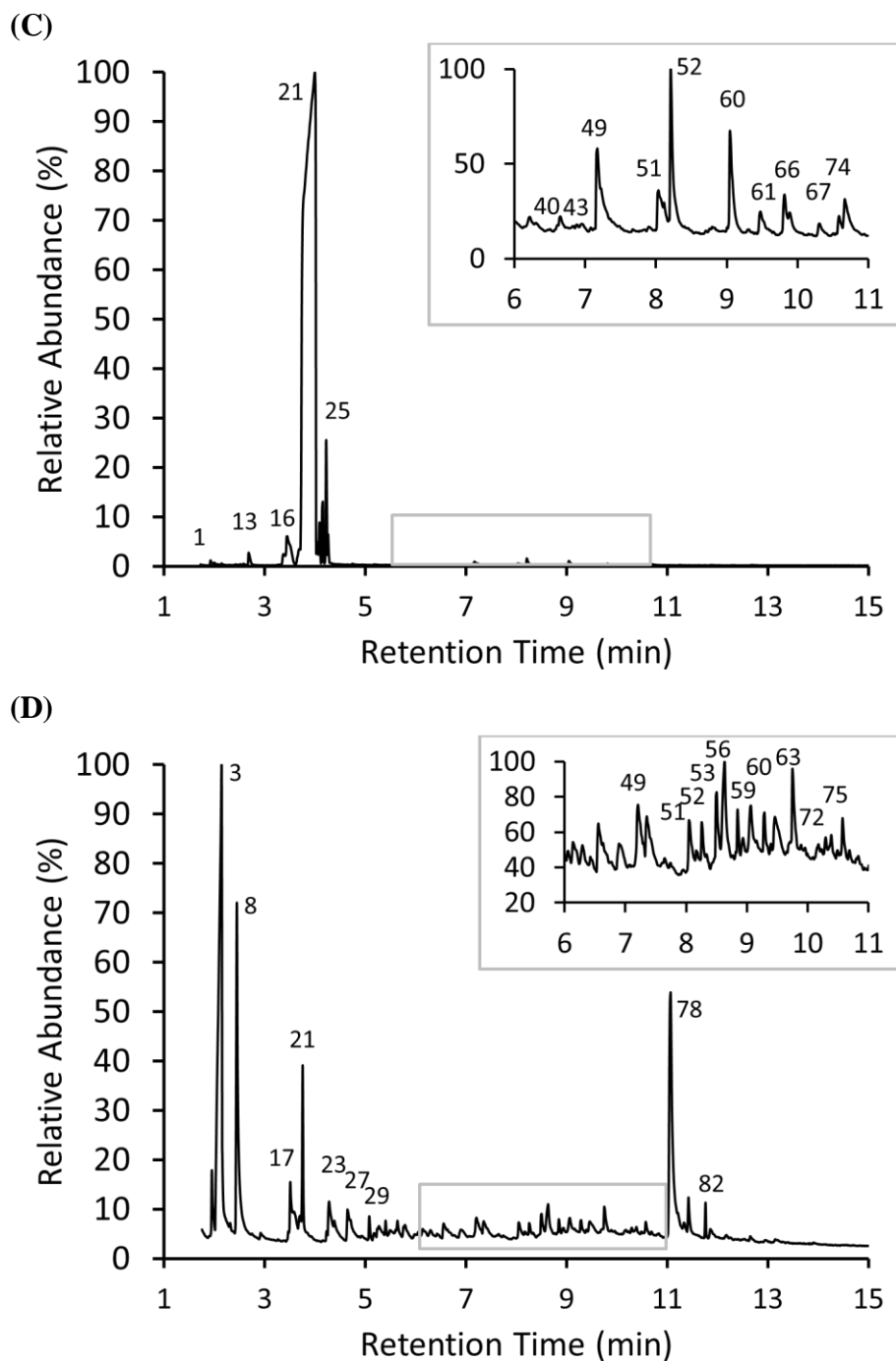
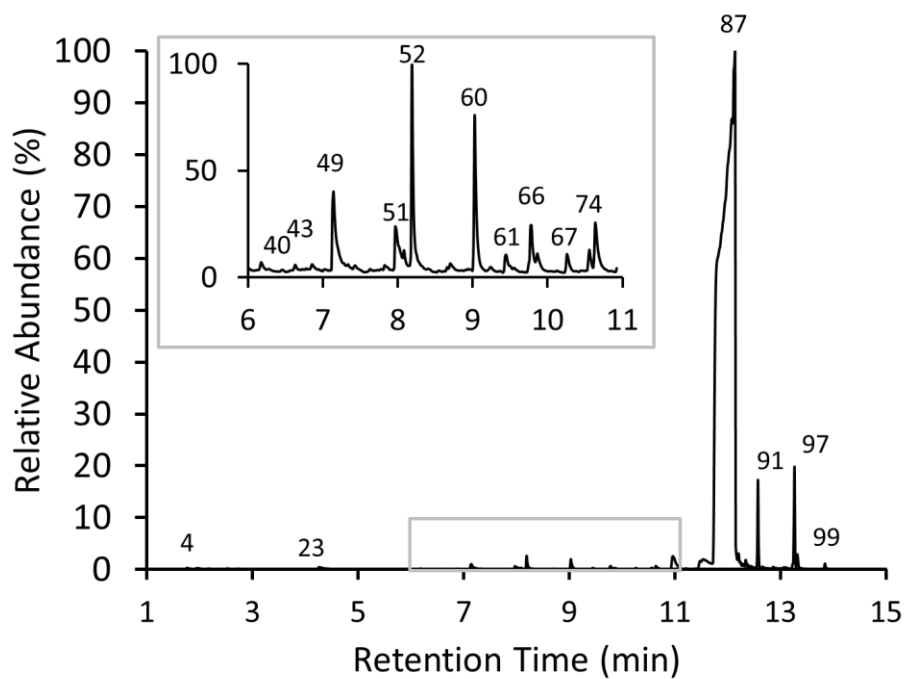
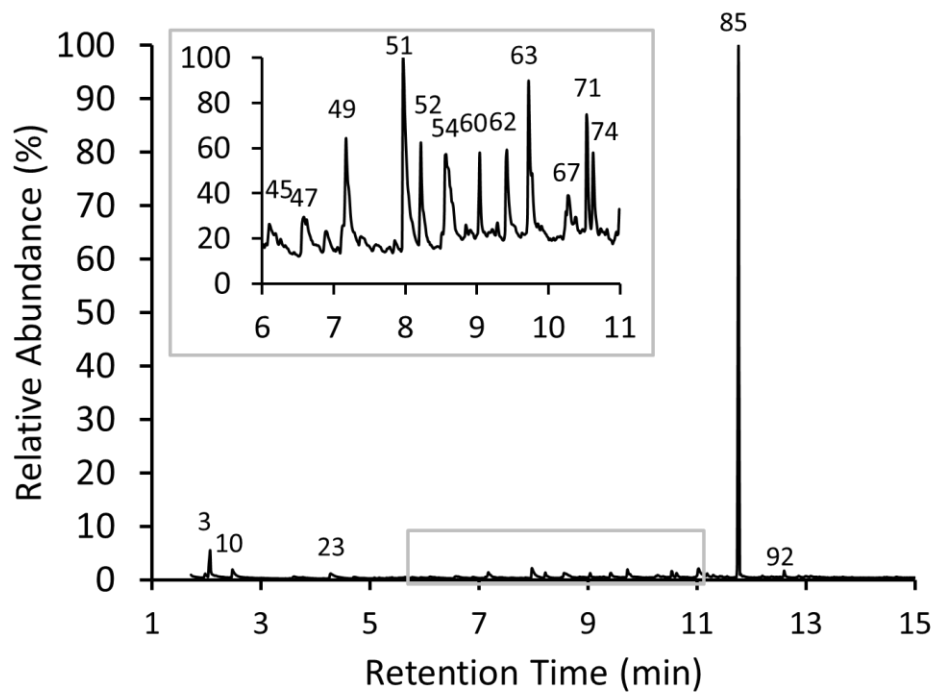


Figure A3. (A) Chromatogram of the hexadecane phase (SolvB-C16) after organic solvent extraction of AqBO. (B) Chromatogram of bio-oil phase (SBoap) after contact with hexadecane. (C) Chromatogram of octane phase (SolvB-C8) after solvent extraction of aqueous bio-oil. (D) Chromatogram of bio-oil phase (SBoap) after contact with octane.

(A)



(B)



(C)

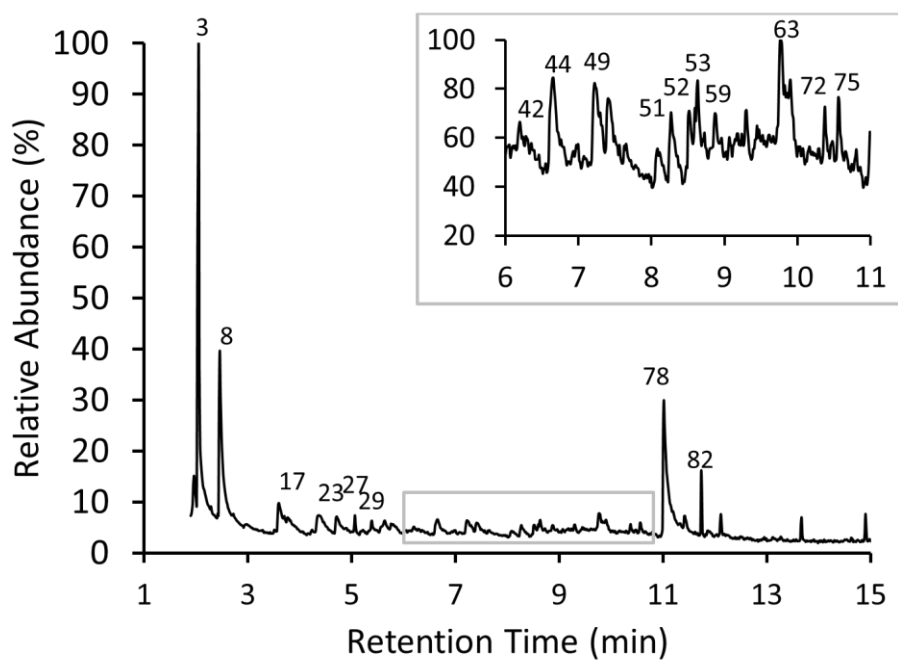


Figure A4. Chromatograms of (A) hexadecane (SolvB-C16) phase, (B) organic bio-oil phase (SBoop), and (C) water phase (SBoap) from combined extraction.

For Chapter 5

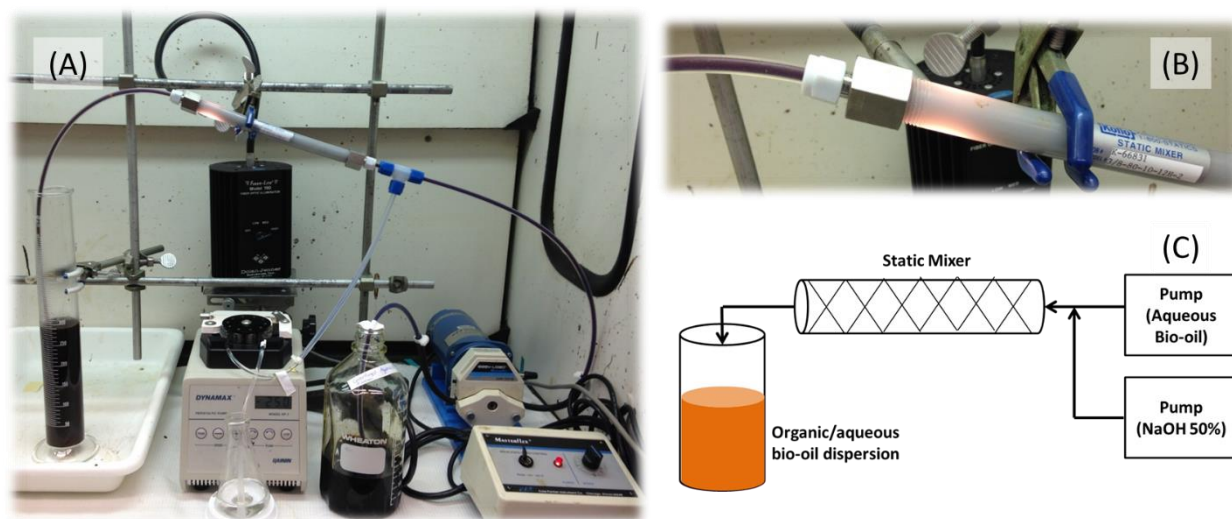


Figure A5. (A) Experimental arrangement for neutralization of bio-oil using a static mixer from Koflo (shown in B). A diagram of the system is shown in (C).



Figure A6. Experimental arrangement for neutralization of bio-oil using a centrifugal contactor.

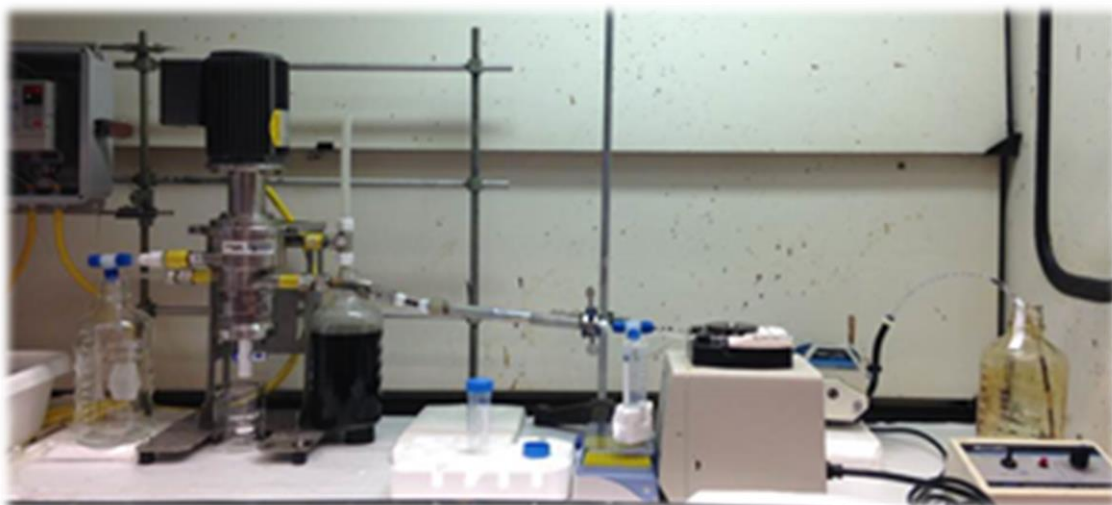


Figure A7. Experimental arrangement for neutralization of bio-oil using a static mixer followed by a centrifugal contactor.

REFERENCES

1. Conti, J. H., Paul; Diefenderfer, Jim; Rose, Angelina L.; Turnure, James T.; Westfall, Lynn, International Energy Outlook 2016. United State Energy Information Administration (EIA), United States Department of Energy: Washington D.C., 2016.
2. Shao, J.; Agblevor, F., New Rapid Method for the Determination of Total Acid Number (Tan) of Bio-Oils. *American Journal of Biomass and Bioenergy* **2015**, 4 (1), 1-9.
3. Colgan, J. D., Oil, Conflict, and U.S. National Interests. *Policy Brief, Belfer Center for Science and International Affairs* October 2013, 2013.
4. Colgan, J. D., Oil, Domestic Politics, and International Conflict. *Energy Research & Social Science* **2014**, 1, 198-205.
5. Colgan, J., Oil, Revolution, and International Conflict: A Toxic Mix. *PS: Political Science & Politics* **2009**, 42 (3), 613.
6. Solomon, S. Q., D.; Manning, M.; Chen, Z.; Marquis, M.; Averyt, K.B.; Tignor, M.; Miller, H.L. (eds.) *IPCC, 2007: Climate Change 2007: The Physical Science Basis.*; Intergovernmental Panel on Climate Change (IPCC): Cambridge University Press, Cambridge, United Kingdom and New York, NY, USA.
7. Shafiee, S.; Topal, E., When will fossil fuel reserves be diminished? *Energy Policy* **2009**, 37 (1), 181-189.
8. McGlade, C.; Ekins, P., The geographical distribution of fossil fuels unused when limiting global warming to 2 [deg]C. *Nature* **2015**, 517 (7533), 187-190.

9. Rode, K. D.; Robbins, C. T.; Nelson, L.; Amstrup, S. C., Can polar bears use terrestrial foods to offset lost ice-based hunting opportunities? *Frontiers in Ecology and the Environment* **2015**, *13* (3), 138-145.
10. O'Neill, B. C.; Oppenheimer, M.; Warren, R.; Hallegatte, S.; Kopp, R. E.; Portner, H. O.; Scholes, R.; Birkmann, J.; Foden, W.; Licker, R.; Mach, K. J.; Marbaix, P.; Mastrandrea, M. D.; Price, J.; Takahashi, K.; van Ypersele, J.-P.; Yohe, G., IPCC reasons for concern regarding climate change risks. *Nature Clim. Change* **2017**, *7* (1), 28-37.
11. Dincer, I., Renewable energy and sustainable development: a crucial review. *Renewable and Sustainable Energy Reviews* **2000**, *4* (2), 157-175.
12. Amorim, H. V.; Lopes, M. L.; de Castro Oliveira, J. V.; Buckeridge, M. S.; Goldman, G. H., Scientific challenges of bioethanol production in Brazil. *Applied Microbiology and Biotechnology* **2011**, *91* (5), 1267.
13. Noguee, A. C., Steven; Paulos, Bentham; Haddad, Brent *Powerful Solutions: 7 Ways to Switch America to Renewable Electricity*; Union of Concerned Scientists: Cambridge, MA, 1999.
14. International Energy Agency, *Biofuels for Transport: An International Perspective*. International Energy Agency: Paris, France, 2004.
15. Mohan, D.; Pittman, C. U.; Steele, P. H., Pyrolysis of wood/biomass for bio-oil: a critical review. *Energy & Fuels* **2006**, *20* (3), 848-889.
16. Lewis, A. J.; Ren, S.; Ye, X.; Kim, P.; Labbe, N.; Borole, A. P., Hydrogen production from switchgrass via an integrated pyrolysis–microbial electrolysis process. *Bioresource technology* **2015**, *195*, 231-241.

17. He, P.; Song, H., Catalytic conversion of biomass by natural gas for oil quality upgrading. *Industrial & Engineering Chemistry Research* **2014**, 53 (41), 15862-15870.
18. Chan, J. K.; Duff, S. J., Methods for mitigation of bio-oil extract toxicity. *Bioresource technology* **2010**, 101 (10), 3755-3759.
19. Jacobson, K.; Maheria, K. C.; Dalai, A. K., Bio-oil valorization: a review. *Renewable and Sustainable Energy Reviews* **2013**, 23, 91-106.
20. Vitasari, C. R.; Meindersma, G.; De Haan, A. B., Water extraction of pyrolysis oil: The first step for the recovery of renewable chemicals. *Bioresource technology* **2011**, 102 (14), 7204-7210.
21. Xu, R.; Ferrante, L.; Briens, C.; Berruti, F., Bio-oil production by flash pyrolysis of sugarcane residues and post treatments of the aqueous phase. *Journal of Analytical and Applied Pyrolysis* **2011**, 91 (1), 263-272.
22. Wei, Y.; Lei, H.; Wang, L.; Zhu, L.; Zhang, X.; Liu, Y.; Chen, S.; Ahring, B., Liquid-liquid extraction of biomass pyrolysis bio-oil. *Energy & Fuels* **2014**, 28 (2), 1207-1212.
23. Rasrendra, C. B.; Girisuta, B.; van de Bovenkamp, H. H.; Winkelman, J. G. M.; Leijenhorst, E. J.; Venderbosch, R. H.; Windt, M.; Meier, D.; Heeres, H. J., Recovery of acetic acid from an aqueous pyrolysis oil phase by reactive extraction using tri-n-octylamine. *Chemical Engineering Journal* **2011**, 176-177, 244-252.
24. Park, L. K.-E.; Ren, S.; Yiacoumi, S.; Ye, X. P.; Borole, A. P.; Tsouris, C., Separation of Switchgrass Bio-Oil by Water/Organic Solvent Addition and pH Adjustment. *Energy & Fuels* **2016**, 30 (3), 2164-2173.

25. Ren, S.; Ye, X. P.; Borole, A. P., Separation of chemical groups from bio-oil water-extract via sequential organic solvent extraction. *Journal of Analytical and Applied Pyrolysis* **2017**, *123*, 30-39.
26. Song, Q.-H.; Nie, J.-Q.; Ren, M.-G.; Guo, Q.-X., Effective phase separation of biomass pyrolysis oils by adding aqueous salt solutions. *Energy & fuels* **2009**, *23* (6), 3307-3312.
27. Tian, Q. K.; He, L.; Zhang, H.; Lv, Z. L.; Li, R. In *Study on Solvent Extraction of Fast Pyrolysis Bio-Oil*, Advanced Materials Research, Trans Tech Publ: 2011; pp 1532-1536.
28. Ma, B.; Agblevor, F. A., Polarity-based separation and chemical characterization of fast pyrolysis bio-oil from poultry litter. *Biomass and Bioenergy* **2014**, *64*, 337-347.
29. Diebold, J.; Czernik, S.; Scahill, J.; Phillips, S.; Feik, C. In *Hot-gas filtration to remove char from pyrolysis vapors produced in the vortex reactor at NREL*, Proceedings of Biomass Pyrolysis Oil Properties and Combustion Meeting, 1994; pp 90-108.
30. Bridgwater, A. V., Review of fast pyrolysis of biomass and product upgrading. *Biomass and Bioenergy* **2012**, *38*, 68-94.
31. Shihadeh, A. L. Rural electrification from local resources: biomass pyrolysis oil combustion in a direct injection diesel engine. Massachusetts Institute of Technology, 1999.
32. Teella, A.; Huber, G. W.; Ford, D. M., Separation of acetic acid from the aqueous fraction of fast pyrolysis bio-oils using nanofiltration and reverse osmosis membranes. *Journal of Membrane Science* **2011**, *378* (1), 495-502.

33. Gollakota, A. R. K.; Reddy, M.; Subramanyam, M. D.; Kishore, N., A review on the upgradation techniques of pyrolysis oil. *Renewable and Sustainable Energy Reviews* **2016**, 58, 1543-1568.
34. Leng, S.; Wang, X.; He, X.; Liu, L.; Liu, Y. e.; Zhong, X.; Zhuang, G.; Wang, J.-g., NiFe/ γ -Al₂O₃: a universal catalyst for the hydrodeoxygenation of bio-oil and its model compounds. *Catalysis Communications* **2013**, 41, 34-37.
35. Sun, J.; Karim, A. M.; Zhang, H.; Kovarik, L.; Li, X. S.; Hensley, A. J.; McEwen, J.-S.; Wang, Y., Carbon-supported bimetallic Pd–Fe catalysts for vapor-phase hydrodeoxygenation of guaiacol. *Journal of Catalysis* **2013**, 306, 47-57.
36. Gandarias, I.; Requies, J.; Arias, P. L.; Armbruster, U.; Martin, A., Liquid-phase glycerol hydrogenolysis by formic acid over Ni–Cu/Al₂O₃ catalysts. *Journal of Catalysis* **2012**, 290, 79-89.
37. Bykova, M. V.; Ermakov, D. Y.; Kaichev, V. V.; Bulavchenko, O. A.; Saraev, A. A.; Lebedev, M. Y.; Yakovlev, V. A., Ni-based sol–gel catalysts as promising systems for crude bio-oil upgrading: Guaiacol hydrodeoxygenation study. *Applied Catalysis B: Environmental* **2012**, 113–114, 296-307.
38. Ardiyanti, A. R.; Khromova, S. A.; Venderbosch, R. H.; Yakovlev, V. A.; Heeres, H. J., Catalytic hydrotreatment of fast-pyrolysis oil using non-sulfided bimetallic Ni–Cu catalysts on a δ -Al₂O₃ support. *Applied Catalysis B: Environmental* **2012**, 117–118, 105-117.
39. Guo, Q.; Wu, M.; Wang, K.; Zhang, L.; Xu, X., Catalytic hydrodeoxygenation of algae bio-oil over bimetallic Ni–Cu/ZrO₂ catalysts. *Industrial & engineering chemistry research* **2015**, 54 (3), 890-899.

40. Junming, X.; Jianchun, J.; Yunjuan, S.; Yanju, L., Bio-oil upgrading by means of ethyl ester production in reactive distillation to remove water and to improve storage and fuel characteristics. *Biomass and Bioenergy* **2008**, 32 (11), 1056-1061.
41. Mahfud, F. H.; Melián-Cabrera, I.; Manurung, R.; Heeres, H. J., Biomass to Fuels: Upgrading of Flash Pyrolysis Oil by Reactive Distillation Using a High Boiling Alcohol and Acid Catalysts. *Process Safety and Environmental Protection* **2007**, 85 (5), 466-472.
42. Xiong, W.-M.; Zhu, M.-Z.; Deng, L.; Fu, Y.; Guo, Q.-X., Esterification of Organic Acid in Bio-Oil using Acidic Ionic Liquid Catalysts. *Energy & Fuels* **2009**, 23 (4), 2278-2283.
43. Wang, J.-J.; Chang, J.; Fan, J., Upgrading of bio-oil by catalytic esterification and determination of acid number for evaluating esterification degree. *Energy & Fuels* **2010**, 24 (5), 3251-3255.
44. Hilten, R. N.; Das, K.; Kastner, J. R.; Bibens, B. P., Production of higher quality bio-oils by in-line esterification of pyrolysis vapor. Google Patents: 2014.
45. Bridgwater, A. V.; Meier, D.; Radlein, D., An overview of fast pyrolysis of biomass. *Organic Geochemistry* **1999**, 30 (12), 1479-1493.
46. Oasmaa, A.; Elliott, D. C.; Korhonen, J., Acidity of Biomass Fast Pyrolysis Bio-oils. *Energy & Fuels* **2010**, 24 (12), 6548-6554.
47. Ren, S.; Ye, X. P.; Borole, A. P.; Kim, P.; Labbé, N., Analysis of switchgrass-derived bio-oil and associated aqueous phase generated in a semi-pilot scale auger pyrolyzer. *Journal of Analytical and Applied Pyrolysis* **2016**, 119, 97-103.

48. Mahfud, F.; Van Geel, F.; Venderbosch, R.; Heeres, H., Acetic acid recovery from fast pyrolysis oil. An exploratory study on liquid-liquid reactive extraction using aliphatic tertiary amines. *Separation Science and Technology* **2008**, *43* (11-12), 3056-3074.
49. Aricetti, J. A.; Tubino, M., A green and simple visual method for the determination of the acid-number of biodiesel. *Fuel* **2012**, *95*, 659-661.
50. Baig, A.; Ng, F. T., Determination of acid number of biodiesel and biodiesel blends. *Journal of the American Oil Chemists' Society* **2011**, *88* (2), 243-253.
51. Baig, A.; Paszti, M.; Ng, F. T. T., A simple and green analytical method for acid number analysis of biodiesel and biodiesel blends based on potentiometric technique. *Fuel* **2013**, *104*, 426-432.
52. Barbieri Gonzaga, F.; Pereira Sobral, S., A new method for determining the acid number of biodiesel based on coulometric titration. *Talanta* **2012**, *97*, 199-203.
53. del Río, V.; Larrechi, M. S.; Callao, M. P., Sequential injection titration method using second-order signals: Determination of acidity in plant oils and biodiesel samples. *Talanta* **2010**, *81* (4-5), 1572-1577.
54. Gonçalves, M.; Cunha, K.; Sobral, S.; Gonzaga, F.; Fraga, I.; Borges, P., Acid Number Determination of Biodiesel by Potentiometric Titration Using Different Methods. In *Biofuels*, ASTM International: 2011.
55. Knothe, G., Analyzing biodiesel: standards and other methods. *Journal of the American Oil Chemists' Society* **2006**, *83* (10), 823-833.
56. Komers, K.; Skopal, F.; Stloukal, R., Determination of the Neutralization Number for Biodiesel Fuel Production. *Lipid / Fett* **1997**, *99* (2), 52-54.

57. Mahajan, S.; Konar, S. K., Determining the acid number of biodiesel. *Journal of the American Oil Chemists' Society* **2006**, *83* (6), 567-570.
58. Tubino, M.; Aricetti, J. A., A green method for determination of acid number of biodiesel. *Journal of the Brazilian Chemical Society* **2011**, *22*, 1073-1081.
59. Chen, D.; Zhou, J.; Zhang, Q.; Zhu, X., Evaluation methods and research progresses in bio-oil storage stability. *Renewable and Sustainable Energy Reviews* **2014**, *40*, 69-79.
60. Oasmaa, A.; Meier, D., Norms and standards for fast pyrolysis liquids: 1. Round robin test. *Journal of Analytical and Applied Pyrolysis* **2005**, *73* (2), 323-334.
61. Wu, L.; Hu, X.; Mourant, D.; Wang, Y.; Kelly, C.; Garcia-Perez, M.; He, M.; Li, C.-Z., Quantification of strong and weak acidities in bio-oil via non-aqueous potentiometric titration. *Fuel* **2014**, *115*, 652-657.
62. ASTM D664. Standard Test Method for Acid Number of Petroleum Products by Potentiometric Titration. American Society for Testing Materials (ASTM) International: West Conshohocken, PA, 2011.
63. ASTM D974-14e2. Standard Test Method for Acid and Base Number by Color-Indicator Titration. American Society for Testing Materials (ASTM) International: West Conshohocken, PA, 2014.
64. ASTM D3339-12. Standard Test Method for Acid Number of Petroleum Products by Semi-Micro Color Indicator Titration. American Society for Testing Materials (ASTM) International: West Conshohocken, PA, 2012.
65. AOCS Cd 3d-63. Acid Value. The American Oil Chemists' Society: Urbana, IL 2009.

66. McFarlane, J.; Tsouris, C.; Birdwell Jr, J. F.; Schuh, D. L.; Jennings, H. L.; Palmer Boitrage, A. M.; Terpstra, S. M., Production of biodiesel at the kinetic limit in a centrifugal reactor/separator. *Industrial & engineering chemistry research* **2010**, *49* (7), 3160-3169.
67. Qiu, Z.; Zhao, L.; Weatherley, L., Process intensification technologies in continuous biodiesel production. *Chemical Engineering and Processing: Process Intensification* **2010**, *49* (4), 323-330.
68. Qiu, Z.; Petera, J.; Weatherley, L., Biodiesel synthesis in an intensified spinning disk reactor. *Chemical Engineering Journal* **2012**, *210*, 597-609.
69. Van Gerven, T.; Stankiewicz, A., Structure, energy, synergy, time—The fundamentals of process intensification. *Industrial & engineering chemistry research* **2009**, *48* (5), 2465-2474.
70. Stankiewicz, A., Reactive separations for process intensification: an industrial perspective. *Chemical Engineering and Processing: Process Intensification* **2003**, *42* (3), 137-144.
71. Yildirim, Ö.; Kiss, A. A.; Kenig, E. Y., Dividing wall columns in chemical process industry: a review on current activities. *Separation and Purification Technology* **2011**, *80* (3), 403-417.
72. Ramshaw, C., Hige'e distillation-an example of process intensification. *Chemical Engineer* **1983**, 13-14.
73. Cross, W.; Ramshaw, C., Process intensification: laminar flow heat transfer. *Chemical engineering research & design* **1986**, *64* (4), 293-301.

74. Stankiewicz, A. I.; Moulijn, J. A., Process intensification: transforming chemical engineering. *Chemical Engineering Progress* **2000**, 96 (1), 22-34.
75. Tsouris, C. P., Joseph V, Process intensification-Has its time finally come? *Chemical Engineering Progress* **2003**, 99 (10), 50-55.
76. Reay, D., The role of process intensification in cutting greenhouse gas emissions. *Applied Thermal Engineering* **2008**, 28 (16), 2011-2019.
77. Portha, J.-F.; Falk, L.; Commenge, J.-M., Local and global process intensification. *Chemical Engineering and Processing: Process Intensification* **2014**, 84, 1-13.
78. Ponce-Ortega, J. M.; Al-Thubaiti, M. M.; El-Halwagi, M. M., Process intensification: new understanding and systematic approach. *Chemical Engineering and Processing: Process Intensification* **2012**, 53, 63-75.
79. Thakur, R.; Vial, C.; Nigam, K.; Nauman, E.; Djelveh, G., Static mixers in the process industries—a review. *Chemical Engineering Research and Design* **2003**, 81 (7), 787-826.
80. Kandhai, D.; Vidal, D.; Hoekstra, A.; Hoefsloot, H.; Iedema, P.; Slood, P., Lattice-Boltzmann and finite element simulations of fluid flow in a SMRX Static Mixer Reactor. *International Journal for Numerical Methods in Fluids* **1999**, 31 (6), 1019-1033.
81. Birdwell Jr, J. F.; McFarlane, J.; Hunt, R. D.; Luo, H.; DePaoli, D. W.; Schuh, D. L.; Dai, S., Separation of ionic liquid dispersions in centrifugal solvent extraction contactors. *Separation Science and Technology* **2006**, 41 (10), 2205-2223.
82. Birdwell Jr, J. F.; Jennings, H. L.; McFarlane, J.; Tsouris, C., Integrated reactor and centrifugal separator and uses thereof. Google Patents: 2012.

83. Tsouris, C.; McFarlane, J.; Birdwell Jr, J.; Jennings, H.; Moyer, B., Continuous Production of Biodiesel via an Intensified Reactive/Extraction Process. *SolVent Extraction. Fundamentals to Industrial Applications* **2008**, 923-930.
84. Tsouris, C.; Mayes, R.; Kiggans, J.; Sharma, K.; Yiacoumi, S.; DePaoli, D.; Dai, S., Mesoporous Carbon for Capacitive Deionization of Saline Water. *Environmental Science & Technology* **2011**, 45 (23), 10243-10249.
85. Jeon, S.-i.; Park, H.-r.; Yeo, J.-g.; Yang, S.; Cho, C. H.; Han, M. H.; Kim, D. K., Desalination via a new membrane capacitive deionization process utilizing flow-electrodes. *Energy & Environmental Science* **2013**, 6 (5), 1471-1475.
86. Kim, Y.-H. P., Lydia Kyoung-Eun; Yiacoumi, Sotira; Tsouris, Costas, Modular Chemical Process Intensification: a Review. *Annual review of chemical and biomolecular engineering* **2017**, 8.
87. Conti, J. J.; Holtberg, P. D.; Beamon, J. A.; Napolitano, S. A.; Schaal, A. M.; Turnure, J. T. *International Energy Outlook 2013*; United States Energy Information Administration: Washington, DC, 2013.
88. Ragauskas, A. J.; Williams, C. K.; Davison, B. H.; Britovsek, G.; Cairney, J.; Eckert, C. A.; Frederick, W. J.; Hallett, J. P.; Leak, D. J.; Liotta, C. L., The path forward for biofuels and biomaterials. *science* **2006**, 311 (5760), 484-489.
89. Perlack, R. D.; Wright, L. L.; Turhollow, A. F.; Graham, R. L.; Stokes, B. J.; Erbach, D. C. *Biomass as feedstock for a bioenergy and bioproducts industry: the technical feasibility of a billion-ton annual supply*; DTIC Document: 2005.

90. Rout, P.; Naik, M.; Naik, S.; Goud, V. V.; Das, L.; Dalai, A. K., Supercritical CO₂ fractionation of bio-oil produced from mixed biomass of wheat and wood sawdust. *Energy & Fuels* **2009**, *23* (12), 6181-6188.
91. Mahfud, F.; Melin-Cabrera, I.; Manurung, R.; Heeres, H., Biomass to fuels: upgrading of flash pyrolysis oil by reactive distillation using a high boiling alcohol and acid catalysts. *Process Safety and Environmental Protection* **2007**, *85* (5), 466-472.
92. Kim, J.-S., Production, separation and applications of phenolic-rich bio-oil—A review. *Bioresource technology* **2015**, *178*, 90-98.
93. Effendi, A.; Gerhauser, H.; Bridgwater, A. V., Production of renewable phenolic resins by thermochemical conversion of biomass: a review. *Renewable and Sustainable Energy Reviews* **2008**, *12* (8), 2092-2116.
94. Zhao, C.; He, J.; Lemonidou, A. A.; Li, X.; Lercher, J. A., Aqueous-phase hydrodeoxygenation of bio-derived phenols to cycloalkanes. *Journal of Catalysis* **2011**, *280* (1), 8-16.
95. Guo, J.; Ruan, R.; Zhang, Y., Hydrotreating of phenolic compounds separated from bio-oil to alcohols. *Industrial & Engineering Chemistry Research* **2012**, *51* (19), 6599-6604.
96. Žilnik, L. F.; Jazbinšek, A., Recovery of renewable phenolic fraction from pyrolysis oil. *Separation and Purification Technology* **2012**, *86*, 157-170.
97. Wang, S.; Wang, Y.; Cai, Q.; Wang, X.; Jin, H.; Luo, Z., Multi-step separation of monophenols and pyrolytic lignins from the water-insoluble phase of bio-oil. *Separation and Purification Technology* **2014**, *122*, 248-255.

98. Kim, P.; Johnson, A.; Edmunds, C. W.; Radosevich, M.; Vogt, F.; Rials, T. G.; Labbé, N., Surface functionality and carbon structures in lignocellulosic-derived biochars produced by fast pyrolysis. *Energy & fuels* **2011**, 25 (10), 4693-4703.
99. ASTM D1217. Standard Test Method for Density and Relative Density (Specific Gravity) of Liquids by Bingham Pycnometer. In *Annual Book of ASTM Standards*, vol. 11.05., American Society for Testing Materials (ASTM) International: West Conshohocken, PA, 2002.
100. ASTM D4377. Standard Test Method for Water in Crude Oils by Potentiometric Karl Fischer Titration. In *Annual Book of ASTM Standards*, vol. 11.05., American Society for Testing Materials (ASTM) International: West Conshohocken, PA, 2002.
101. ASTM D445-15. Standard Test Method for Kinematic Viscosity of Transparent and Opaque Liquids (and Calculation of Dynamic Viscosity). In *Annual Book of ASTM Standards*, vol. 05.01., American Society for Testing Materials (ASTM) International: West Conshohocken, PA, 2015.
102. ASTM D482-13. Standard Test Method for Ash from Petroleum Products. In *Annual Book of ASTM Standards*, vol. 05.01, American Society for Testing Materials (ASTM) International: West Conshohocken, PA, 2013.
103. Boucher, M.; Chaala, A.; Roy, C., Bio-oils obtained by vacuum pyrolysis of softwood bark as a liquid fuel for gas turbines. Part I: Properties of bio-oil and its blends with methanol and a pyrolytic aqueous phase. *Biomass and Bioenergy* **2000**, 19 (5), 337-350.

104. Garcia-Perez, M.; Adams, T. T.; Goodrum, J. W.; Geller, D. P.; Das, K., Production and fuel properties of pine chip bio-oil/biodiesel blends. *Energy & Fuels* **2007**, *21* (4), 2363-2372.
105. Chiaramonti, D.; Oasmaa, A.; Solantausta, Y., Power generation using fast pyrolysis liquids from biomass. *Renewable & Sustainable Energy Reviews* **2007**, *11* (6), 1056-1086.
106. Moens, L.; Black, S. K.; Myers, M. D.; Czernik, S., Study of the neutralization and stabilization of a mixed hardwood bio-oil. *Energy & Fuels* **2009**, *23* (5), 2695-2699.
107. Rover, M. R.; Johnston, P. A.; Lamsal, B. P.; Brown, R. C., Total water-soluble sugars quantification in bio-oil using the phenol–sulfuric acid assay. *Journal of Analytical and Applied Pyrolysis* **2013**, *104*, 194-201.
108. Ion Exchange Chromatography. <http://www.bio-rad.com/en-us/applications-technologies/liquid-chromatography-principles/ion-exchange-chromatography> (accessed 08. 11.).
109. Altria, K. D., Overview of capillary electrophoresis and capillary electrochromatography. *Journal of Chromatography A* **1999**, *856* (1), 443-463.
110. Tubino, M.; Aricetti, J. A., A green potentiometric method for determination of the acid number of oils and fats. *Journal of the Brazilian Chemical Society* **2013**, *24*, 1691-1696.
111. Kauffman, R., Rapid, portable voltammetric techniques for performing antioxidant, total acid number (TAN) and total base number (TBN) measurements. *Tribology & Lubrication Technology* **1998**, *54* (1), 39.

112. Fuhr, B.; Banjac, B.; Blackmore, T.; Rahimi, P., Applicability of Total Acid Number Analysis to Heavy Oils and Bitumens. *Energy & Fuels* **2007**, *21* (3), 1322-1324.
113. EN140104. Fat and oil derivatives - Fatty Acid Methyl Esters (FAME) - Determination of acid value European Standard: 2003.
114. *The Theory of pH Measurement*; ADS 43-002/rev.C; Emerson Process Management: Irvine, CA, November, 2010; pp 1-7.
115. Wang, J.; Xu, C.; Song, Q., Rapid and Environmentally Friendly Three-Dimensional-Printed Flow Injection Analysis System for the Determination of the Acid Number in Thermal Conductive Oil. *Energy & Fuels* **2015**, *29* (2), 1040-1044.
116. ASTM D4377-00, Standard test method for water in crude oils by potentiometric Karl Fischer titration. West Conshohocken, PA, 2011.
117. Zhang, Y.; Guo, F.; Cui, Q.; Lu, M.; Song, X.; Tang, H.; Li, Q., Measurement and Correlation of the Solubility of Vanillic Acid in Eight Pure and Water + Ethanol Mixed Solvents at Temperatures from (293.15 to 323.15) K. *Journal of Chemical & Engineering Data* **2016**, *61* (1), 420-429.
118. Wang, H.; Tang, H.; Wilson, J.; Salley, S. O.; Ng, K. Y. S., Total Acid Number Determination of Biodiesel and Biodiesel Blends. *Journal of the American Oil Chemists' Society* **2008**, *85* (11), 1083-1086.
119. Calculation, Chemicalize - Instant Cheminformatics Solutions. ChemAxon, Ltd: 2016. (<http://www.chemicalize.com/>).
120. Liu, F.; Sivoththaman, S.; Tan, Z., Solvent extraction of 5-HMF from simulated hydrothermal conversion product. *Sustainable Environment Research* **2014**, *24* (2).

121. Rossini, E.; Netz, R. R.; Knapp, E.-W., Computing pKa Values in Different Solvents by Electrostatic Transformation. *Journal of Chemical Theory and Computation* **2016**, *12* (7), 3360-3369.
122. Pollard, A.; Rover, M.; Brown, R., Characterization of bio-oil recovered as stage fractions with unique chemical and physical properties. *Journal of Analytical and Applied Pyrolysis* **2012**, *93*, 129-138.
123. Roby, S. H.; Dutta, M.; Zhu, Y.; Pathiparampil, A., Development of an Acid Titration for Fast Pyrolysis Oil. *Energy & Fuels* **2015**, *29* (2), 858-862.
124. Park, L. K.-E.; Liu, J.; Yiacoumi, S.; Borole, A. P.; Tsouris, C., Contribution of acidic components to the total acid number (TAN) of bio-oil. *Fuel* **2017**, *200*, 171-181.
125. Song, Q. H.; Nie, J. Q.; Ren, M. G.; Guo, Q. X., *Energy Fuels* **2009**, *23* (6), 3307.
126. Chen, H.-W.; Song, Q.-H.; Liao, B.; Guo, Q.-X., Further Separation, Characterization, and Upgrading for Upper and Bottom Layers from Phase Separation of Biomass Pyrolysis Oils. *Energy & Fuels* **2011**, *25* (10), 4655-4661.
127. Ren, S.; Ye, X. P.; Borole, A. P., Separation of chemical groups from bio-oil aqueous phase via sequential organic solvent extraction *Journal of Analytical and Applied Pyrolysis* **2017**, *123*, 30-39.
128. Fu, D.; Farag, S.; Chaouki, J.; Jessop, P. G., Extraction of phenols from lignin microwave-pyrolysis oil using a switchable hydrophilicity solvent. *Bioresource technology* **2014**, *154*, 101-108.
129. Patel, R. N.; Bandyopadhyay, S.; Ganesh, A., Extraction of cardanol and phenol from bio-oils obtained through vacuum pyrolysis of biomass using supercritical fluid extraction. *Energy* **2011**, *36* (3), 1535-1542.

130. Reverchon, E.; De Marco, I., Supercritical fluid extraction and fractionation of natural matter. *The Journal of Supercritical Fluids* **2006**, *38* (2), 146-166.
131. Amen-Chen, C.; Pakdel, H.; Roy, C., Separation of phenols from Eucalyptus wood tar. *Biomass and Bioenergy* **1997**, *13* (1–2), 25-37.
132. Kiss, A. A., *Process Intensification Technologies for Biodiesel Production: Reactive Separation Processes*. Springer Science & Business Media: 2014.
133. Diebold, J. P.; Czernik, S., Additives To Lower and Stabilize the Viscosity of Pyrolysis Oils during Storage. *Energy & Fuels* **1997**, *11* (5), 1081-1091.
134. Elliott, D. C.; Oasmaa, A.; Preto, F.; Meier, D.; Bridgwater, A. V., Results of the IEA Round Robin on Viscosity and Stability of Fast Pyrolysis Bio-oils. *Energy & Fuels* **2012**, *26* (6), 3769-3776.
135. Hilten, R. N.; Das, K. C., Comparison of three accelerated aging procedures to assess bio-oil stability. *Fuel* **2010**, *89* (10), 2741-2749.
136. Meng, J.; Moore, A.; Tilotta, D. C.; Kelley, S. S.; Adhikari, S.; Park, S., Thermal and Storage Stability of Bio-Oil from Pyrolysis of Torrefied Wood. *Energy & Fuels* **2015**, *29* (8), 5117-5126.
137. Oasmaa, A.; Kuoppala, E., Fast Pyrolysis of Forestry Residue. 3. Storage Stability of Liquid Fuel. *Energy & Fuels* **2003**, *17* (4), 1075-1084.
138. Zhang, L.; Yin, R.; Mei, Y.; Liu, R.; Yu, W., Characterization of crude and ethanol-stabilized bio-oils before and after accelerated aging treatment by comprehensive two-dimensional gas-chromatography with time-of-flight mass spectrometry. *Journal of the Energy Institute* **2016**.

139. Rasrendra, C.; Girisuta, B.; Van de Bovenkamp, H.; Winkelman, J.; Leijenhorst, E.; Venderbosch, R.; Windt, M.; Meier, D.; Heeres, H., Recovery of acetic acid from an aqueous pyrolysis oil phase by reactive extraction using tri-n-octylamine. *Chemical engineering journal* **2011**, *176*, 244-252.
140. Diebold, J. P., *A review of the chemical and physical mechanisms of the storage stability of fast pyrolysis bio-oils*. Citeseer: 2000.
141. Zeng, X.; Borole, A. P.; Pavlostathis, S. G., Performance evaluation of a continuous-flow bioanode microbial electrolysis cell fed with furanic and phenolic compounds. *RSC Advances* **2016**, *6* (70), 65563-65571.
142. Zeng, X.; Borole, A. P.; Pavlostathis, S. G., Inhibitory Effect of Furanic and Phenolic Compounds on Exoelectrogenesis in a Microbial Electrolysis Cell Bioanode. *Environmental Science & Technology* **2016**, *50* (20), 11357-11365.
143. Zeng, X.; Borole, A. P.; Pavlostathis, S. G., Biotransformation of Furanic and Phenolic Compounds with Hydrogen Gas Production in a Microbial Electrolysis Cell. *Environmental Science & Technology* **2015**, *49* (22), 13667-13675.
144. Ying, T.-Y.; Yang, K.-L.; Yiacoumi, S.; Tsouris, C., Electrosorption of ions from aqueous solutions by nanostructured carbon aerogel. *Journal of colloid and interface science* **2002**, *250* (1), 18-27.
145. Wang, J.; Angnes, L.; Tobias, H.; Roesner, R. A.; Hong, K. C.; Glass, R. S.; Kong, F. M.; Pekala, R. W., Carbon aerogel composite electrodes. *Analytical Chemistry* **1993**, *65* (17), 2300-2303.

146. Pekala, R. W.; Farmer, J. C.; Alviso, C. T.; Tran, T. D.; Mayer, S. T.; Miller, J. M.; Dunn, B., Carbon aerogels for electrochemical applications. *Journal of Non-Crystalline Solids* **1998**, 225, 74-80.
147. Zhang, S. Q.; Wang, J.; Shen, J.; Deng, Z. S.; Lai, Z. Q.; Zhou, B.; Attia, S. M.; Chen, L. Y., The investigation of the adsorption character of carbon aerogels. *Nanostructured Materials* **1999**, 11 (3), 375-381.
148. Kruk, M.; Jaroniec, M., Gas Adsorption Characterization of Ordered Organic-Inorganic Nanocomposite Materials. *Chemistry of Materials* **2001**, 13 (10), 3169-3183.
149. Barrett, E. P.; Joyner, L. G.; Halenda, P. P., The Determination of Pore Volume and Area Distributions in Porous Substances. I. Computations from Nitrogen Isotherms. *Journal of the American Chemical Society* **1951**, 73 (1), 373-380.

VITA

Lydia Kyoung-Eun Park was born in Seoul, the Republic of Korea, and she immigrated to the United States in 2003. She attended high school in Ridgefield, New Jersey. She came to the Georgia Institute of Technology in 2007 from where she received a Bachelor of Science in Environmental Engineering in 2011. She also received a Master of Science in Environmental Engineering from the Georgia Institute of Technology in 2013. Her M.S. research was on chemical and photochemical inactivation of pathogenic microorganisms, advised by Dr. Jaehong Kim. She joined Dr. Sotira Yiacoumi's group in January 2014 as a Ph.D. student. Her Ph.D. thesis is on separation processes to improve utilization of bio-oil from switchgrass pyrolysis. During her graduate studies, she mentored undergraduate and graduate students in their research. She also worked as a teaching assistant in undergraduate courses including Water Quality Engineering. In addition, she worked as a resident advisor in the Georgia Tech Family Housing. She received the Community Builder of the year award in 2015. She is a mother of two boys (two-year-old Isaac and eight-week-old David) who were born during her Ph.D. studies.